

USING STRONTIUM ISOTOPES TO TRACK PACIFIC SALMON MIGRATIONS IN

ALASKA

By

Sean Reiss Brennan

RECOMMENDED:



Dr. Diego Fernandez



Dr. Thure Cerling



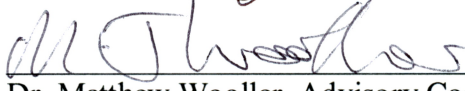
Dr. Christian Zimmerman



Dr. Megan McPhee



Dr. Thomas Weingartner



Dr. Matthew Wooller, Advisory Committee Chair



Dr. Brenda Konar

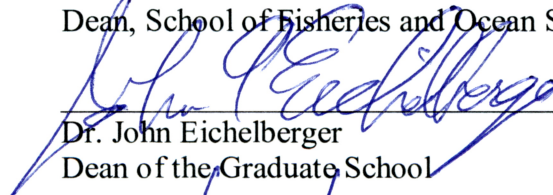
Head, Program, Marine Sciences and Limnology

APPROVED:



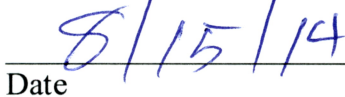
Dr. Michael Castellini

Dean, School of Fisheries and Ocean Sciences



Dr. John Eichelberger

Dean of the Graduate School



Date

USING STRONTIUM ISOTOPES TO TRACK PACIFIC SALMON MIGRATIONS IN
ALASKA

A
DISSERTATION

Presented to the Faculty
of the University of Alaska Fairbanks

in Partial Fulfillment of the Requirements
for the Degree of

DOCTOR OF PHILOSOPHY

By

Sean Reiss Brennan, B.S.

Fairbanks, Alaska

August 2014

ABSTRACT

Pacific salmon (*Oncorhynchus* spp.) are an important cultural, ecological, and economic natural resource in Alaska. Not only do salmon maintain an important mechanism of nutrient transport between marine, aquatic, and terrestrial ecosystems, but they also provide a sustainable food and economic resource for human communities. A challenging issue in the management, conservation, and research of Pacific salmon is tracking their responses to perturbations across the multiple scales of population structure that characterize these species. Research has shown how the inherent biodiversity of Pacific salmon imparts resiliency to environmental change, and temporal stability to their overall productivity and the human systems dependent upon such productivity (e.g., fisheries). The vast biodiversity of salmon arises primarily via precise natal homing of adults to their rivers of origin, resulting in locally adapted populations. Thus, there have been considerable efforts to develop methods to effectively manage and monitor Pacific salmon biodiversity. One important example is using genetic differentiation among populations to discern the relative contributions of genetically distinct stocks in mixed stock fishery harvests. In the Bristol Bay region, sockeye salmon (*O. nerka*) harvests can be discerned at the watershed level (i.e., the nine major watersheds contributing to the fishery). However, tens to hundreds of locally adapted populations exist within each of these watersheds and methods to apportion fishery harvests to this finer scale population structure are lacking. This dissertation presents a new method in Alaska to discern fine-scale population structure (i.e., within watersheds) of Chinook salmon (*O. tshawytscha*) harvests using a naturally occurring geochemical tracer in rivers, strontium (Sr) isotopes ($^{87}\text{Sr}/^{86}\text{Sr}$). To this end, in Chapter 1, I characterize the statewide geographic variation on multiple spatial scales in $^{87}\text{Sr}/^{86}\text{Sr}$ ratios of Alaska's rivers and discuss the geochemical and geological controls of observed $^{87}\text{Sr}/^{86}\text{Sr}$ ratios. In Chapter 2, I approach the

persistent problem of evaluating site-specific temporal variation, especially in remote Subarctic and Arctic regions, by employing the non-migratory behavioral ecology of slimy sculpin (*Cottus cognatus*). Finally, in Chapter 3, I demonstrate how the development of temporally and spatially robust $^{87}\text{Sr}/^{86}\text{Sr}$ baseline datasets within the Nushagak River was able to apportion a mixed stock fishery harvest of Chinook salmon conducted in Nushagak Bay back to natal sources at the sub-basin watershed level. Because of the conservative nature of the $^{87}\text{Sr}/^{86}\text{Sr}$ ratio during physical and biological processes, the development of this method is applicable not only to Chinook salmon, but also to other salmon species (e.g., sockeye and coho salmon, *O. kisutch*). Additionally, the development of baseline $^{87}\text{Sr}/^{86}\text{Sr}$ information (e.g., waters) and an overall research framework to employ this tracer in provenance studies, have statewide implications for the research and management of other migratory animals.

TABLE OF CONTENTS

	Page
Signature Page	i
Title Page	iii
Abstract.....	v
Table of Contents	vii
List of Figures.....	xiii
List of Tables	xv
Acknowledgements	xvii
GENERAL INTRODUCTION.....	1
CHAPTER 1: Strontium isotope variation and carbonate versus silicate weathering in rivers from across Alaska: implications for provenance studies.....	5
ABSTRACT.....	5
INTRODUCTION.....	6
Geological Setting of AK	8
METHODS	9
Field Collection Methods.....	10
⁸⁷ Sr/ ⁸⁶ Sr analyses.....	10
Elemental analyses	12
Calculation of idealized hyperbolic mixing lines between ⁸⁷ Sr/ ⁸⁶ Sr and X/Na ratios.....	12
RESULTS	14

$^{87}\text{Sr}/^{86}\text{Sr}$ ratios	14
North-South of Denali Fault	14
Intra-watershed variation and intra-regional comparisons	15
Elemental concentrations and molar ratios.....	17
$^{87}\text{Sr}/^{86}\text{Sr}$ ratios as a function of X/Na ratios.....	19
DISCUSSION	21
Regional patterns	22
North-South of Denali Fault	22
AK's east-west Sr isotopic gradient.....	25
Northern lowland vs. highland basins.....	26
Non-radiogenic silicate weathering of southwest AK	27
A radiogenic calcareous source in metamorphic regions of YTT and Brooks	
Range?.....	28
Consideration of temporal and spatial uncertainties	30
CONCLUSIONS AND IMPLICATIONS	31
FIGURES.....	33
TABLES.....	39
REFERENCES.....	42
APPENDIX 1.1	51
$^{87}\text{Sr}/^{86}\text{Sr}$ ratio analyses.....	51
Hyperbolic mixing line carbonate and silicate end-members (EMs)	53
CHAPTER 2: Strontium isotopes in otoliths of a non-migratory fish (slimy sculpin):	
implications for aquatic provenance studies	57

ABSTRACT	57
INTRODUCTION	58
Study area	60
METHODS	61
Otolith and water collection and preparation	61
Water and otolith ⁸⁷ Sr/ ⁸⁶ Sr ratio analyses	63
Statistical analyses	64
RESULTS	66
Spatially explicit water ⁸⁷ Sr/ ⁸⁶ Sr ratios	66
GAMs and ⁸⁷ Sr/ ⁸⁶ Sr ratio otolith profiles	67
Tributaries and main-stem river channels upstream of Mulchatna River confluence	68
Lower Nushagak River.....	70
Individuals with marine influence in their otolith core.....	70
Autumn water versus overall life-long otolith ⁸⁷ Sr/ ⁸⁶ Sr ratios.....	71
DISCUSSION	71
Elucidating hydrogeochemical temporal variability and micro-movements .	72
Upstream watershed area and geochemical heterogeneity as drivers of temporal variability ⁸⁷ Sr/ ⁸⁶ Sr ratios in river water	74
Autumn water ⁸⁷ Sr/ ⁸⁶ Sr ratios as a predictor of life-long values observed in otoliths.....	75
Implications for natal origins and movement pattern studies	76
Marine-derived Sr in the core of four individuals	77

CONCLUSION	79
FIGURES.....	81
TABLES.....	89
REFERENCES.....	95
CHAPTER 3: Strontium isotopes provide new tool for fine-scale biodiversity conservation of Pacific salmon	103
ABSTRACT.....	103
INTRODUCTION.....	104
RESULTS	108
Training the baseline DFA model.....	108
⁸⁷ Sr/ ⁸⁶ Sr life history profiles of juvenile Chinook salmon	109
Validating baseline DFA model	109
Mixed Stock Analysis (MSA)	110
Movement patterns	111
DISCUSSION	112
Building baseline ⁸⁷Sr/⁸⁶Sr datasets using water data	113
Insights from misclassifications of known origin fish.....	114
Movement patterns elucidated via otolith microchemistry	114
MSA using Strontium Isotopic Groups (SIGs)	116
Implications for biodiversity conservation	118
METHODS SUMMARY	120
FIGURES.....	121
REFERENCES.....	125

APPENDIX 3.1	129
METHODS	129
Otolith collections.....	129
⁸⁷ Sr/ ⁸⁶ Sr ratio analyses of otoliths.....	130
Classification statistics.....	133
RESULTS AND DISCUSSION	134
Mass-balance calculation of Sr sources within the otolith core	134
Additional discussion of a minor number of perplexing life history profiles.....	134
MSA results and potential habitat amount	135
FIGURES.....	137
TABLES.....	139
REFERENCES.....	143
GENERAL CONCLUSIONS	145
REFERENCES.....	148

List of Figures

	Page
Fig. 1.1. $^{87}\text{Sr}/^{86}\text{Sr}$ ratios of AK rivers	33
Fig. 1.2. Inter- and intra-watershed $^{87}\text{Sr}/^{86}\text{Sr}$ variation	34
Fig. 1.3. Elemental ratios of AK rivers.....	35
Fig. 1.4. Hyperbolic mixing plots.....	36
Fig. 1.5. PCA of $^{87}\text{Sr}/^{86}\text{Sr}$ and X/Na ratios.....	37
Fig. 1.6. $^{87}\text{Sr}/^{86}\text{Sr}$ patterns and tectonic realms of AK.....	38
Fig. 2.1. Slimy sculpin sampling sites and $^{87}\text{Sr}/^{86}\text{Sr}$ ratios of river waters	81
Fig. 2.2. An example of laser ablation transect	82
Fig. 2.3. An example of a frontal versus transverse section of a slimy sculpin otolith	83
Fig. 2.4. Examples of $^{87}\text{Sr}/^{86}\text{Sr}$ ratio profiles of slimy sculpin trapped in tributaries.....	84
Fig. 2.5. A logistic regression.....	85
Fig. 2.6. Examples of $^{87}\text{Sr}/^{86}\text{Sr}$ ratio profiles of slimy sculpin trapped in the lower river.....	86
Fig. 2.7. Autumn water values used to predict overall, long-term mean $^{87}\text{Sr}/^{86}\text{Sr}$ ratios	87
Fig. 2.8. $^{87}\text{Sr}/^{86}\text{Sr}$ ratio profiles of four individuals indicating marine Sr in otolith core.....	88
Fig. 3.1. Map of the Nushagak River's, Strontium Isotopic Groups (SIGs).....	121
Fig. 3.2. SIG $^{87}\text{Sr}/^{86}\text{Sr}$ ratios.....	122
Fig. 3.3. Mixed Stock Analysis (MSA).....	123
Fig. 3.4. $^{87}\text{Sr}/^{86}\text{Sr}$ life history profiles from each SIG of adult Chinook salmon	124
Fig. A3.1. Marine-derived Sr within the otolith cores	137
Fig. A3.2. SIG proportions and habitat quantity	138

List of Tables

	Page
Table 1.1. Summary of end-members used to calculate hyperbolic mixing lines	39
Table 1.2. Summary of all $^{87}\text{Sr}/^{86}\text{Sr}$, elemental, and molar ratio data	40
Table 2.1. Spatially explicit Nushagak River $^{87}\text{Sr}/^{86}\text{Sr}$ water data.....	89
Table 2.2. Slimy sculpin trapping site and otolith data	91
Table 2.3. Logistic regression results	93
Table 2.4. Linear regression results	94
Table A3.1. Classification tables for known origin otolith samples	139
Table A3.2. Posterior probability thresholds for SIG membership.....	140
Table A3.3. Movement patterns of adult Chinook salmon	141
Table A3.4. Summary of potential habitat amounts within each SIG	142

ACKNOWLEDGMENTS

Funding for this research was provided by Alaska Sea Grant, the National Institute of Water Resources, and the University of Alaska, Fairbanks Graduate School. I would like to express my sincere thank you to these institutions and agencies for their support. I thank my committee members, Matthew Wooller, Thure Cerling, Diego Fernandez, Christian Zimmerman, Thomas Weingartner, and Megan McPhee for their excellent support and guidance throughout all of this work. Each chapter of this dissertation was prepared as a manuscript for publication in a peer-reviewed journal. I wrote each manuscript, designed and performed all research, and conducted all data analysis and interpretation. Co-authors on each manuscript contributed to research design, data analysis, interpretation of data, and provided editorial advice. I thank all of my colleagues and friends who were integral during fieldwork and sampling campaigns. In particular, I thank Peter Christopher Sr. of New Stuyahok, Alaska for his invaluable knowledge of the Nushagak River region. Also, special thanks to Jesse Davis, Casey McConnell, Britt Retzlaff, Peter Barr, and Robert Kirchner for their help during field campaigns. This work could not have been achieved without your help. Thank you to Luki Akelkok Sr., Roger Skogen, Todd Radenbaugh, Dan Young, Mark Lisac, and Matt Johnson for logistical support while in the field. I also thank the teachers and students of the Kvichak School District for their outstanding help in collecting water samples from the Kvichak watershed. The design and implementation of Chapter 1 benefited significantly from the help of Thomas Douglas. Thank you to Peter Condon for providing a review and comments on an earlier version of Chapter 1. Special thanks to Glen Mackey for his excellent help and guidance during laboratory work. Thank you to Hannah Vander Zanden, Greg Stoddard and Arny Blanchard for their assistance with statistical analyses

used in this research. All experiments were conducted in compliance with Institutional Animal Care and Use Committee protocols (approved September 3, 2010, project: 178401-5).

GENERAL INTRODUCTION

Alaska is geographically vast, geologically diverse, and home to a large variety of migratory animals, including abundant runs of the five species of Pacific salmon (*Oncorhynchus* spp.). A challenging issue in the management, conservation, and research of Pacific salmon is tracking their responses to perturbations across the multiple scales of population structure that characterize these species. Three relevant perturbations to Pacific salmon populations in Alaska include climate change (Schindler et al. 2008), mineral development (EPA 2014), and commercial fisheries (Dann et al. 2009). These perturbations generally come in the form of changes to oceanic and freshwater habitat conditions (the former two), or over-fishing of distinct populations (the latter). Salmon population structure is hierarchical exhibiting a strong geographic component (Habicht et al. 2007) due to the precise homing of adults back to their natal sites resulting in locally adapted populations. Research has shown that this biodiversity imparts resiliency and temporal stability to the productivity of salmon regionally, and thus, also dependent human systems (e.g., fisheries) (Hilborn et al. 2003, Schindler et al. 2010). Thus, there have been large efforts to develop tools and management strategies to help conserve this biodiversity. One of the most useful tools has been using genetic methods to determine the composition of mixed stock harvests during fisheries (e.g., Bristol Bay commercial sockeye fishery) to determine accurate stock-specific total annual runs (Dann et al. 2009, Habicht et al. 2007). This information is integral when estimating escapement goals and managing a fishery sustainably. However, determining changes (i.e., inter-annual) in the relative proportions of productivity across the multiple levels of salmon biodiversity is often limited to the broad-scale level, which corresponds to that of an entire watershed (Dann et al. 2009, Habicht et al. 2007).

Tools are needed to be able to discern the role of fine-scale population structure in fisheries and how this level of biodiversity contributes to resiliency of salmon populations to perturbations.

One potential tool is strontium (Sr) isotope ($^{87}\text{Sr}/^{86}\text{Sr}$) ratios.

Heterogeneity in $^{87}\text{Sr}/^{86}\text{Sr}$ ratios throughout aquatic and terrestrial ecosystems has become an important tool in modern (Barnett-Johnson et al. 2008, Britton et al. 2009) and paleo ecology (Copeland et al. 2011, Koch et al. 1992), particularly in the realm of provenance research, which aims to track the movement patterns of organisms and materials. Its utility primarily stems from the conservative nature of a $^{87}\text{Sr}/^{86}\text{Sr}$ ratio during biological, chemical, and physical processes (i.e., there is no measureable mass-dependent fractionation) (Capo et al. 1998). Geographic variation in $^{87}\text{Sr}/^{86}\text{Sr}$ ratios scales with geologic diversity, and thus occurs at multiple spatial scales (e.g., regional and local) (Bataille and Bowen 2012, Bataille et al. 2013). Additionally, because Sr has the same charge and a similar ionic radius as calcium (Ca), it mimics Ca during physical, chemical, and biological processes (Capo et al. 1998). Thus, though Sr is a trace element in the Earth, it is easily measurable in Ca-rich biogenic tissues (e.g., teeth, bones, and otoliths) (Barnett-Johnson et al. 2005, Ehrlich et al. 2001, Woodhead et al. 2005).

The development of robust $^{87}\text{Sr}/^{86}\text{Sr}$ baseline datasets, and a reliable research framework to apply this tracer within provenance studies, has broad implications across multiple scientific and management disciplines. All provenance studies employing $^{87}\text{Sr}/^{86}\text{Sr}$ ratios depend on baseline information, which characterizes the spatial and temporal variability in the regions encompassing movement patterns of interest (Elsdon et al. 2008, Hobson et al. 2010). Prior to starting this research in the autumn of 2009 very little $^{87}\text{Sr}/^{86}\text{Sr}$ data existed across Alaska, except for some statewide geological (i.e., rock measurements) (Arth 1994) and localized geochemical weathering studies (i.e., water measurements) (Goldfarb et al. 1997, Keller et al. 2007). Only one

animal provenance study has been published from Alaska, which employed the $^{87}\text{Sr}/^{86}\text{Sr}$ tracer recorded in the teeth of caribou to investigate their migration patterns (Britton et al. 2009).

This dissertation evaluated the utility of $^{87}\text{Sr}/^{86}\text{Sr}$ ratios for determining the movement patterns and natal origins of Pacific salmon in Alaska. It spans multiple spatial scales from the statewide level to the tributary level, and focuses primarily on a case study to track Chinook salmon migrations in the Nushagak River flowing into Bristol Bay. Overall, the following research encompasses: i) an analysis of the geographic variation of $^{87}\text{Sr}/^{86}\text{Sr}$ ratios at multiple spatial scales in Alaska and the regional geochemical weathering patterns influencing these ratios in rivers (Chapter 1); ii) an approach for determining site-specific temporal variation in river waters, especially the remote rivers of Alaska by using otoliths from non-migratory, slimy sculpin (*Cottus cognatus*) (Chapter 2); and iii) a case study that uses $^{87}\text{Sr}/^{86}\text{Sr}$ ratios in otoliths to determine the movement patterns and natal origins of a mixed stock harvest of Chinook salmon in the ocean (Chapter 3). The findings and overall research framework of this dissertation have demonstrated how useful the naturally occurring variation in $^{87}\text{Sr}/^{86}\text{Sr}$ ratios across Alaska will be for investigating, not only Pacific salmon, but a diverse variety of migratory organisms and materials.

CHAPTER 1:

Strontium isotope variation and carbonate versus silicate weathering in rivers from across Alaska: implications for provenance studies¹

ABSTRACT

Characterizing strontium (Sr) isotopic ($^{87}\text{Sr}/^{86}\text{Sr}$) variation in surface waters of Alaska (AK) has significant implications for provenance studies aiming to track movement patterns of animals and/or materials. This study reports $^{87}\text{Sr}/^{86}\text{Sr}$ ratios, concentrations of Sr, Ca, Mg, Na and K, and selected molar ratios (Sr/Na, Ca/Na, Mg/Na and Sr/Ca) from 61 rivers from across AK to characterize regional patterns in i) $^{87}\text{Sr}/^{86}\text{Sr}$ variation and ii) carbonate versus silicate weathering influencing $^{87}\text{Sr}/^{86}\text{Sr}$ ratios. $^{87}\text{Sr}/^{86}\text{Sr}$ ratios range from 0.70422–0.74041±0.00009. Rivers north of the Denali Fault exhibit more radiogenic and variable $^{87}\text{Sr}/^{86}\text{Sr}$ ratios (0.70763 to 0.74041) than rivers to the south (0.70422 to 0.70895), reflecting the tectonic growth of southern AK via accretion of exotic island arcs along North America's continental margin during the Mesozoic. Within interior AK, an east-west gradient exists. Radiogenic $^{87}\text{Sr}/^{86}\text{Sr}$ ratios (>0.725) in east-central AK and relatively low ratios (<0.709) in western AK reflect AK's progressive western growth along the ancestral North American miogeocline from the Precambrian to Mesozoic. High relief rivers draining north of the Brooks Range are more radiogenic (>0.711) than lowland rivers (<0.709). Elemental ratios indicate carbonate weathering has a greater influence on $^{87}\text{Sr}/^{86}\text{Sr}$ ratios in high relief watersheds north of the Denali Fault and in watersheds of south-central AK. Elemental and $^{87}\text{Sr}/^{86}\text{Sr}$ ratios indicate silicate weathering is important

¹ Brennan, S.R., Fernandez, D.P., Mackey, G., Cerling, T.E., Bataille, C.P., Bowen, G.J. in revision. Strontium isotope variation and carbonate versus silicate weathering in rivers from across Alaska: implications for provenance studies. *Chemical Geology*.

across AK, but is notably more influential in lowland basins north of the Denali Fault and in southwestern AK. This study illustrates Sr isotopic heterogeneity on multiple spatial scales and provides necessary baseline information for provenance studies in AK.

INTRODUCTION

In the last two decades strontium (Sr) isotope ($^{87}\text{Sr}/^{86}\text{Sr}$) ratios of mineralized tissues of animals, such as tooth enamel, bone apatite, and otolith aragonite (auditory structure of teleost fish) have been used to elucidate the modern and paleoecology of organisms, both in the terrestrial (Beard and Johnson, 2000; Britton et al., 2009; Britton et al., 2011; Hodell et al., 2004; Hoppe and Koch, 2007; Hoppe et al., 1999; Radloff et al., 2010; Sellick et al., 2009) and aquatic realms (Barnett-Johnson et al., 2008; Barnett-Johnson et al., 2010; Kennedy et al., 2000; Kennedy et al., 1997; Kennedy et al., 2002; Koch et al., 1992; Miller, 2011; Miller and Kent, 2009; Muhlfeld et al., 2012; Outridge et al., 2002; Walther et al., 2008). $^{87}\text{Sr}/^{86}\text{Sr}$ ratios are particularly well suited for provenance studies because: i) $^{87}\text{Sr}/^{86}\text{Sr}$ ratios of biogenic tissues directly reflect source materials (Barnett-Johnson et al., 2008; Bentley, 2006; Muhlfeld et al., 2012) with no measurable mass-dependent fractionation during biological, chemical and/or physical processes (Capo et al., 1998); ii) Sr is relatively abundant in Ca-bearing minerals and tissues (e.g. teeth and bones) (Bentley, 2006; Capo et al., 1998; Kennedy et al., 2000) and easily measureable by both laser ablation and solution methods (Barnett-Johnson et al., 2005; Ehrlich et al., 2001; Woodhead et al., 2005); and iii) $^{87}\text{Sr}/^{86}\text{Sr}$ ratios vary across landscapes both on regional and local scales (Bataille and Bowen, 2012; Hobson et al., 2010).

All provenance studies employing $^{87}\text{Sr}/^{86}\text{Sr}$ ratios depend on baseline estimates of the isotopic composition of Sr in regions encompassing movement patterns of interest (Hobson,

1999; Hobson et al., 2010). There are two general baseline-development approaches in use: i) detailed sampling campaigns aimed at characterizing all potential sources of Sr (Barnett-Johnson et al., 2008; Chesson et al., 2012; Frei and Frei, 2011; Hodell et al., 2004; Muhlfeld et al., 2012; Walther et al., 2008) and ii) modeling approaches (Bataille and Bowen, 2012; Bataille et al., 2013; Beard and Johnson, 2000). Large-scale sampling campaigns are expensive and inherently incomplete, especially in vast remote regions, such as Alaska (AK), USA. Coupling sample campaigns with model development is a promising approach for mapping Sr isotope variation over large areas (Bataille et al., in revision). Maps of modeled $^{87}\text{Sr}/^{86}\text{Sr}$ ratios in bedrock and water have been previously published for North America (Bataille and Bowen, 2012), and the circum-Caribbean region (Bataille et al., 2013). To date there is no documentation of large-scale spatial variability of $^{87}\text{Sr}/^{86}\text{Sr}$ for AK and only a few water, bedrock and soil weathering studies exist reporting $^{87}\text{Sr}/^{86}\text{Sr}$ ratios on relatively small spatial scales (Anderson et al., 2000; Douglas et al., 2013; Keller et al., 2007; Keller et al., 2010).

Constraining the relative influence of dominant weathering reactions, such as carbonate vs. silicate weathering, is important for understanding and predicting $^{87}\text{Sr}/^{86}\text{Sr}$ variations on regional and local scales. The ultimate source of Sr in watersheds, soils and the biosphere is bedrock geology and variation in $^{87}\text{Sr}/^{86}\text{Sr}$ is primarily driven by differences in the age and chemical composition of bedrock (Bataille and Bowen, 2012; Beard and Johnson, 2000; Capo et al., 1998). However, the isotopic composition of soils, rivers, plants, and animals inherited from bedrock is moderated by differential mineral weathering rates within rocks (Bentley, 2006; Blum and Erel, 2003; Capo et al., 1998) and atmospheric inputs (Stewart et al., 1998). For surface waters, Sr released into water from bulk rock is neither stoichiometrically nor isotopically identical to its source (Blum and Erel, 2003). As a result the more reactive minerals, such as

calcite, release Sr at faster rates and tend to dominate the isotopic signature of waters and the soil-exchange complex over more recalcitrant minerals, such as K-feldspar.

This study presents measured $^{87}\text{Sr}/^{86}\text{Sr}$ ratios of Sr dissolved in surface waters, reporting new measurements from 61 AK rivers. Our study aims to: i) characterize the geographic distribution of $^{87}\text{Sr}/^{86}\text{Sr}$ ratios across AK and ii) infer likely influence of dominant weathering reactions (e.g. silicate vs. carbonate weathering) on regional variation in sources of Sr to rivers using $^{87}\text{Sr}/^{86}\text{Sr}$ and concomitant molar ratios of Sr/Ca and Na-normalized ratios (X/Na: Ca/Na, Sr/Na and Mg/Na). Generally, high X/Na ratios are indicative of carbonate weathering, whereas low ratios are indicative of silicate weathering; the converse is generally true for Sr/Ca ratios (Douglas et al., 2013; Gaillardet et al., 1999; Meybeck, 1986; Millot et al., 2003; Wadleigh et al., 1985). Comparing isotope and molar ratios instead of only absolute elemental abundances allows for better comparisons between different watersheds, as ratios control for confounding factors associated with dilution and evaporation, which affect absolute elemental abundances (Gaillardet et al., 1999).

Geological Setting of AK

Sedimentary and meta-sedimentary rocks ranging in age from the Quaternary to the Precambrian dominate AK's land surface and bedrock geology, composing ~72.9% of the land surface area (Peucker-Ehrenbrink and Miller, 2003). The large majority of igneous and metamorphic rocks (composing ~18.4% and 3.4% of land surface area, respectively) (Peucker-Ehrenbrink and Miller, 2003) found in AK occur in high relief mountain ranges in the southern regions, associated with the convergent boundary of the Pacific and the North American plates (Trop and Ridgeway, 2007), such as the Alaska Range, the Wrangell-St. Elias Mountains, The

Coastal Range, and the Alaskan-Aleutian Arc. The remaining 5.3% land surface area is covered by water and ice (Peucker-Ehrenbrink and Miller, 2003). Interior AK, the expansive region stretching between the Alaska Range and the Brooks Range is composed of vast lowland basins and lower elevation rolling hills (Wahrhaftig, 1965), which are dominated by sedimentary and meta-sedimentary lithologies, and into which volumetrically small igneous rocks have intruded or extruded (Arth, 1994). Strata of far east-central AK are composed of and/or derived from the Precambrian to Triassic parautochthonous ancestral North American miogeocline, whereas progressively to the west strata are allochthonous, accreted in more recent times, e.g. Mesozoic to Cenozoic (Colpron et al., 2007; Nelson et al., 2006). Particularly expansive across AK in these lowland basins are Cretaceous flysch deposits (e.g. Koyukuk, Yukon and Kuskokwim basins) (Beikman, 1980).

A distinctive geologic feature we refer to throughout this report is the Denali-Farewell Fault system (referred to as Denali Fault hereafter) (Figure 1.1). This boundary reflects what is called the ‘mega-suture’ zone, the result of the accretion of exotic composite terranes, e.g. the Wrangellia Composite Terrane (WCT) (a collection of three Paleozoic island arcs: Wrangellia, Peninsular and Alexander terranes) onto the North American Continent in south-central AK during the Mesozoic (Trop and Ridgeway, 2007).

METHODS

This study incorporates: i) a field sampling campaign of surface waters from rivers across the geologically diverse and remote regions of AK, ii) geochemical analyses using Inductively Coupled Plasma Mass Spectrometry (ICPMS) (both multi-collector and single collector instruments), and iii) the use of molar ratios (Ca/Na, Sr/Na, Mg/Na and Sr/Ca) and concomitant

$^{87}\text{Sr}/^{86}\text{Sr}$ ratios measured in river waters to infer regional source patterns of Sr across AK between silicate and carbonate weathering.

Field Collection Methods

Water samples were collected from 61 rivers across AK in 2010, 2011 and 2012 (Figure 1.1). The majority of samples were collected in the autumn between mid-August and mid-October. At each sample site water was collected upstream of the collector in acid-washed 250 ml low-density polyethylene (LDPE) wide-mouth bottles, which were rinsed three times with sample water. Within 48 hours of collection, each sample was filtered through a 0.45 μm Luer-lock syringe filter (polypropylene membrane) using a 50 cm^3 polypropylene syringe into a clean acid-washed 125ml LDPE narrow-mouth bottle. Within a maximum of 16 days of collection, samples were acidified with 2 ml ultra pure concentrated HNO_3 (BDH Aristar Ultra). The sample from the Canning River (R.) was filtered using a PALL Acrodisc® syringe filter with a 0.45 μm Supor® membrane. To evaluate consistency in field collection methods 33 of these samples were collected as field triplicates. To evaluate any field-related contamination, regular blanks were collected in the field (n=12) using the same steps described above for samples, but by using NANOpure de-ionized water (type I, 18.0 $\text{M}\Omega$) (Barnstead, NANOpure Diamond).

$^{87}\text{Sr}/^{86}\text{Sr}$ analyses

All water samples were prepared and analyzed for $^{87}\text{Sr}/^{86}\text{Sr}$ ratios and elemental analyses in a clean-laboratory environment at the University of Utah Department of Geology and Geophysics ICPMS laboratory. $^{87}\text{Sr}/^{86}\text{Sr}$ ratios of waters were determined using multi-collector

(MC) ICPMS (Thermo Scientific, High Resolution NEPTUNE, Bremen, Germany). The University of Utah ICPMS laboratory has developed an introduction system to purify Sr for $^{87}\text{Sr}/^{86}\text{Sr}$ ratio analyses of aqueous solutions using an inline chromatographic column packed with a crown ether resin (Eichrom's Sr Resin ®) (Mackey and Fernandez, 2011) (see Supplementary material). This system provides large throughput of $^{87}\text{Sr}/^{86}\text{Sr}$ ratio measurements with high accuracy and precision. During analyses reported herein, we determined the $^{87}\text{Sr}/^{86}\text{Sr}$ ratio of the standard reference material SRM987 (NIST; www.nist.gov) ($n = 147$) to be 0.710280 ± 0.000048 (2σ standard error (SE)). Precision of field triplicates ($2\sigma\text{SE}$) ranges from $\pm 0.000011 - 0.000124$, whereas the majority of triplicates (29 of 33) are $< \pm 0.000089$. Analytical precision ($2\sigma\text{SE}$) of all water samples (including samples making up triplicates) ranges from $\pm 0.000012 - 0.000090$, whereas the majority of analyses (126 of 127) are $< \pm 0.000069$.

All $^{87}\text{Sr}/^{86}\text{Sr}$ ratios of river waters have been corrected for mass bias and isobaric interference. The $^{87}\text{Sr}/^{86}\text{Sr}$ ratios were corrected for mass bias using an exponential law by simultaneous measurements of the internal $^{88}\text{Sr}/^{86}\text{Sr}$ ratio (i.e. that of the same sample), which is invariant in nature ($^{88}\text{Sr}/^{86}\text{Sr} = 8.375209$) (Steiger and Jager, 1977). Isobaric interferences on the $^{87}\text{Sr}/^{86}\text{Sr}$ ratios, such as from ^{87}Rb and ^{86}Kr , were corrected by simultaneous monitoring of ^{85}Rb and ^{83}Kr and the corresponding invariant ratios $^{87}\text{Rb}/^{85}\text{Rb} = 0.385706$ and $^{86}\text{Kr}/^{83}\text{Kr} = 1.502522$ (Steiger and Jager, 1977). The mass bias correction used for these reported data is an iterative process.

Elemental analyses

Major and trace element concentration analyses were conducted on an Agilent 7500ce ICPMS (Agilent Technologies, Santa Clara, CA, USA). Samples were diluted 4:1 with 2.4% ultra pure HNO₃ (BDH Aristar Ultra); Indium (In) at a concentration of 25 ng mL⁻¹ was added as an internal standard. Concentrations of Sr, Ca, Mg, Na and K were calculated using a six-point calibration curve. The USGS standard reference sample T-205 was analyzed after every fifth sample as an external consistency standard. During the analyses reported herein we determined the Sr, Ca, Mg, Na and K concentrations (mean of weighted means of each analysis run) in USGS T-205 to be 0.00067 mmol/L, 0.211 mmol/L, 0.091 mmol/L, 0.374 mmol/L and 0.019 mmol/L, respectively, which are all within 5% of mean reported values. Total analytical errors (2 σ) in mmol L⁻¹ of each element measured in AK waters were Sr < ± 0.00015 , Ca < ± 0.12 , Mg < ± 0.04 , Na < ± 0.04 and K < ± 0.04 .

In field blanks, concentrations of Ca, Na and K were all below limits of detection (LoD) (maximum LoDs of all runs were 0.004 mmol/L, 0.009 mmol/L and 0.004 mmol/L, respectively). In most, but not all, field blanks, concentrations of Sr and Mg were below LoDs (n=3 and n=5, respectively); these concentrations are negligible compared to concentrations in water samples (< 0.2 nmol/L and < 0.03 μ mol/L, respectively).

Calculation of idealized hyperbolic mixing lines between ⁸⁷Sr/⁸⁶Sr and X/Na ratios

We compare ⁸⁷Sr/⁸⁶Sr and X/Na ratios (Ca/Na, Sr/Na and Mg/Na) to infer regional patterns in the relative contribution of carbonate versus silicate sources to Sr measured in AK rivers. Our inferences were based on comparing observed patterns of these tracers to idealized

mixing curves between monolithic end-member (EM) sources that have been characterized in the literature (Table 1.1) (for description of EMs see Supplementary Information). We calculated idealized mixing between the conventional carbonate end-member (Carb EM), estimated from Phanerozoic marine carbonates (Gaillardet et al., 1999), and one of five hypothesized silicate end-members (Sil EM1-EM5) encompassing basaltic to granitoid silicates with varying $^{87}\text{Sr}/^{86}\text{Sr}$ ratios, which have been derived from previous studies in AK (Douglas et al., 2013; Goldfarb et al., 1997; Keller et al., 2007) or similar geologic settings, such as the Eastern (Millot et al., 2003) and Western Canadian Cordillera (Gaillardet et al., 2003) and Sierra Nevada Batholith (Ingram and Weber, 1999) (Table 1.1). EM values correspond to ratios of the respective constituents dissolved in water, not the parent lithology. The Na-normalized molar ratios (X/Na) of any given river are described by:

$$(\text{X/Na})_{\text{river}} = \sum[(\text{X/Na})_i \square_i (\text{Na})] \quad (1)$$

where, $\text{X/Na}_{\text{river}} = \text{Ca/Na}$, Mg/Na or Sr/Na ratios of river waters, $(\text{X/Na})_i$ indicates X/Na ratio of each individual EM_i , and $\square_i(\text{Na})$ is the proportion of each EM_i . The $^{87}\text{Sr}/^{86}\text{Sr}$ composition of a river is described by:

$$(^{87}\text{Sr}/^{86}\text{Sr})_{\text{river}} (\text{Sr/Na})_{\text{river}} = \sum[(^{87}\text{Sr}/^{86}\text{Sr})_i (\text{Sr/Na})_i \square_i(\text{Na})] \quad (2)$$

where $(^{87}\text{Sr}/^{86}\text{Sr})_i$ and $(\text{Sr/Na})_i$ are the $^{87}\text{Sr}/^{86}\text{Sr}$ and Sr/Na ratios of each EM_i , and $\square_i(\text{Na})$ is the proportion of each EM_i contributing to each measured sample.

To summarize regional patterns across AK and elucidate geographic groupings in $^{87}\text{Sr}/^{86}\text{Sr}$ and X/Na ratios, we performed a Principle Component Analysis (PCA) in R (<http://cran.r-project.org/>) using a correlation matrix to reduce the multivariate relationships between these four tracers down to two axes. Since distributions of $^{87}\text{Sr}/^{86}\text{Sr}$ and X/Na ratios were right skewed, each tracer was log-transformed prior to the PCA.

RESULTS

$^{87}\text{Sr}/^{86}\text{Sr}$ ratios

$^{87}\text{Sr}/^{86}\text{Sr}$ ratios of 61 rivers from across AK were heterogeneous, both on regional and local scales, ranging from 0.70422 to 0.74041 (Figure 1.1 and Table 1.2). The most radiogenic values we observed were from rivers draining the Yukon-Tanana Uplands (YTU) (e.g. the Chatanika R., Chena R. and Salcha R.), which is the northern part of the polygenetic Yukon-Tanana Terrane (YTT) bounded by the Tintina Fault to the north and the Denali Fault to the south (as in Figure 1.1). The lowest values we observed were in the southwest AK region from watersheds of the Ahklun Mountains Province (AMP) (e.g. lakes of the Wood River Mountains draining directly into Bristol Bay) and the Alaskan-Aleutian Range (AAR) (e.g. tributaries of the Kvichak R.), rivers that also drain into Bristol Bay (Figure 1.1).

North-South of Denali Fault

There was an abrupt Sr isotopic transition north and south of the Denali Fault system (Figure 1.1 and 1.2a). Rivers draining north of the Denali Fault were more radiogenic and encompassed a larger range in $^{87}\text{Sr}/^{86}\text{Sr}$ than rivers south of this tectonic boundary (Welch's t-

test, $p < 0.001$) (Figure 1.2a). Rivers to the south had a median $^{87}\text{Sr}/^{86}\text{Sr}$ ratio of 0.70573 and ranged from 0.70422 to 0.70895 ($n = 38$), whereas rivers to the north had a median ratio of 0.71263 and ranged from 0.70763 to 0.74041 ($n = 23$) (Figure 1.2a). The overlap we observed in $^{87}\text{Sr}/^{86}\text{Sr}$ between rivers north and south of the Denali Fault, 0.70763 - 0.70895 ($n = 9$), consisted of rivers draining four geographically distinct regions: foothills of the Eastern Brooks Range (Kuparuk R.), lowland tributaries of Yukon and Koyukuk basins (Innoko R., Hogatza R. and Dulbi R.), portions of the upper Kuskokwim (Tokatna R., George R. and Holitina R.) and Nushagak basins (above Mulchatna R. confluence), and Susitna basin (see Figures 1 and 2a).

The isotopic transition north and south of the Denali Fault was less distinct in western and southwestern AK than it was in south-central AK (Figure 1.1), where the fault system extends west of the central Alaska Range, cuts through the upper Kuskokwim basin, and approaches the northeast extent of the AMP (as mapped by Beikman 1980, and indicated in Figure 1.1). Tributaries of the Kuskokwim R. and Nushagak R., both north and south of Denali Fault, had similar isotope ratios, which fell within the north-south overlapping range.

Intra-watershed variation and intra-regional comparisons

Intra-watershed and intra-regional variation in $^{87}\text{Sr}/^{86}\text{Sr}$ ratios was significant (i.e. $>> \pm 0.00009$, the field triplicate $2\sigma\text{SE}$) (Figure 1.2b). In south-central AK, including data from Kenai Peninsula rivers, Susitna R. and Copper R., $^{87}\text{Sr}/^{86}\text{Sr}$ ratios ranged from 0.70540 to 0.70895 ($n = 17$). The most radiogenic values were of rivers draining the central Alaska Range (Susitna R. and Chulitna R.) and Wrangell-St. Elias Mountains (Chitina R.), whereas rivers with significant inputs from, or solely draining, the Chugach Mountains (Kenai R., Resurrection R.,

Matanuska R., Knik R., Tonsina R., Klutina R. and Tazlina R.) or draining south of the eastern Alaska Range (Gulkana R.), were less radiogenic.

In southwestern AK, $^{87}\text{Sr}/^{86}\text{Sr}$ ratios of rivers draining into Bristol Bay varied from 0.70422 to 0.70778 with low ratios from AAR and AMP and high ratios from Nushagak Hills. Variation within the Kuskokwim R. basin ($^{87}\text{Sr}/^{86}\text{Sr} = 0.70498 - 0.70932$, $n=12$) exhibited a strong east-west gradient, where lower-river, western tributaries draining the AMP were much less radiogenic than upper-river, eastern tributaries draining the Kuskokwim Mountains and central Alaska Range (Figure 1.1).

$^{87}\text{Sr}/^{86}\text{Sr}$ ratios within the entire Yukon R. basin ranged from 0.70763 to 0.74041 ($n = 14$). Within the Yukon basin, high ratios were observed in the eastern and higher elevation tributaries, i.e. the Brooks Range (tributaries of the Koyukuk R.), YTU (northern tributaries of the Tanana R.), and the northern Alaska Range (southern tributaries of Tanana R.). Relatively high ratios pervaded throughout the volumetrically large Yukon R. (sampled above the confluence with Tanana R.), Tanana R. (sampled at the town of Nenana, AK), and Koyukuk R. (sampled at the village of Huslia, AK) (see Figure 1.1). Contrastingly, the western and lower-river tributaries, such as the Innoko R., Hogatza R., and Dulbi R., were much less radiogenic.

Samples from rivers draining north of the continental divide of the Brooks Range came from four distinct watersheds, the Sagavanirktok R., Kuparuk R., Colville R., and Canning R., which span a large majority of the east-west extent of this northern region. These data indicated that ratios of rivers deriving in part, or predominantly, from the Brooks Range were more radiogenic than rivers of the lowlands (Inigok Cr.) or foothills (Kuparuk R.).

Elemental concentrations and molar ratios

We also reported Ca, Mg, Na, K, and Sr concentrations and molar ratios (Sr/Ca and X/Na ratios) of AK rivers (Table 1.2). Sr concentrations ranged from 0.314 $\mu\text{mol/L}$ to 6.502 $\mu\text{mol/L}$ and Ca concentrations ranged from 0.12 mmol/L to 2.27 mmol/L (Table 1.2). Concentrations of Sr and Ca were log-normally distributed, where the majority of rivers were relatively dilute (i.e., $< 2 \mu\text{mol/L}$ and 0.5 mmol/L, respectively). Generally, north of the Denali Fault, lowland rivers were more dilute in Sr and Ca than the high relief watersheds (Table 1.2). For example, the mountainous tributaries in the Yukon basin (Dietrich R., Middle and South Fork Koyukuk R., and Nenana R.) had relatively high concentrations (Sr $> 2.0 \mu\text{mol/L}$; Ca $> 0.6 \text{ mmol/L}$), whereas the lowland tributaries (Dulbi R., Hogatza R., and Innoko R.) were relatively dilute (Sr $< 2.0 \mu\text{mol/L}$; Ca $< 0.6 \text{ mmol/L}$), and tributaries originating from the Y TU (Chatanika R., Salcha R., and Chena R.) had intermediate values. Interestingly, with the exception of the South Fork of the Kuskokwim (Sr = 6 $\mu\text{mol/L}$; Ca = 1.6 mmol/L), we observed relatively low Sr and Ca concentrations (Sr $< 1.7 \mu\text{mol/L}$; Ca $< 0.42 \text{ mmol/L}$) in rivers of the mountainous southwest AK region (tributaries of Kvichak, Nushagak, and lower Kuskokwim basins), relative to rivers of the mountainous south-central region (e.g. Susitna and Copper basins).

Sr/Ca ratios varied by almost one order of magnitude (0.91 and 5.54 mmol/mol). Concentrations of Sr and Ca in AK rivers measured in this study exhibited a strong positive correlation ($r = 0.94$) (Figure 1.3a), with data plotting in between Sr/Ca lines observed from catchments of pure carbonates (and/or marble) and mixed silicates (plutonic and volcanic, including sedimentary and metamorphic derivatives) (Meybeck, 1986). Rivers exhibited less variation at low Sr and Ca concentrations and greater variation at higher concentrations. In contrast to our data, previously published measurements for small catchments in the Eastern

Foothills of the Brooks Range (red triangles, Figure 1.3a) fall primarily along the carbonate Sr/Ca line, consistent with the fact that the sampled catchments drain carbonate bedrock lithologies (Keller et al., 2007).

X/Na ratios (mol/mol) of Ca, Sr and Mg each varied over one order of magnitude (i.e. Ca/Na: 1.79 - 20.16, $< \pm 8.8\%$; Sr/Na: 0.004 - 0.053, $< \pm 7.2\%$; and Mg/Na: 0.44 - 9.32, $< \pm 7.2\%$). Na concentrations ranged from 0.046 mmol/L to 0.77 mmol/L and were log-normally distributed, where the majority of rivers were relatively dilute (Na < 0.15 mmol/L). Na concentrations in rivers north and south of the Denali Fault showed similar distributions (0.06 - 0.77 mmol/L and 0.04 - 0.40 mmol/L, respectively), whereas Mg (0.06 - 2.45 mmol/L and 0.03 - 0.24 mmol/L, respectively), Ca (0.15 - 2.27 mmol/L and 0.12 - 0.96 mmol/L, respectively), and Sr concentrations (0.3 - 6.5 $\mu\text{mol/L}$ and 0.3 - 2.8 $\mu\text{mol/L}$, respectively) did not. Thus, the majority of variation in X/Na ratios observed with respect to rivers north or south of the Denali Fault was driven by changes in Mg, Sr, or Ca, not Na. The respective distributions of X/Na ratios were all log-normally distributed. Log-log plots of Sr/Na and Mg/Na ratios versus Ca/Na ratios indicated strong positive relationships ($r = 0.89$ and $r = 0.79$, respectively) between these tracers (Figure 1.3c and d), which approximated a linear trend with the data plotting between published silicate and carbonate end-member values (listed in Table 1.1) (Gaillardet et al., 1999). Southern rivers exhibited lower Mg/Na ratios relative to northern rivers, indicating a difference in proportions of Mg derived from silicate versus carbonate weathering in these regions. Namely, Mg in southern rivers was derived from silicate sources in greater proportion than northern rivers. The cation ternary diagram (Figure 1.3b) corroborated this result, whereby southern rivers plotted closer to the Na+K apex (indicative of silicate weathering) and northern rivers plotted closer to the Ca-Mg line (indicative of carbonate weathering).

$^{87}\text{Sr}/^{86}\text{Sr}$ ratios as a function of X/Na ratios

AK rivers appeared to derive Sr from at least three general EMs, depending on region: Phanerozoic carbonates (e.g., Carb EM), non-radiogenic silicates (e.g. Sil EM1 and EM2) and radiogenic silicates (e.g., Sil EM3-EM5) (Figure 1.4a-c). Increases in all X/Na ratios were associated with $^{87}\text{Sr}/^{86}\text{Sr}$ ratios converging towards intermediate values, approximating the conventional $^{87}\text{Sr}/^{86}\text{Sr}$ ratio of Phanerozoic marine carbonates (Figure 1.4a-c). Before $^{87}\text{Sr}/^{86}\text{Sr}$ ratios converge, when X/Na ratios were low ($\text{Ca}/\text{Na} < 10$, $\text{Sr}/\text{Ca} < 0.026$, $\text{Mg}/\text{Na} < 2.5$), the data bifurcated towards radiogenic and non-radiogenic values (Figure 1.4a-c).

In each $^{87}\text{Sr}/^{86}\text{Sr}$ -X/Na comparison, southern rivers scattered along or between the mixing lines of the less radiogenic Sil EM1 and EM2, whereas northern rivers scattered along mixing lines of the more radiogenic Sil EM3-EM5 (Figure 1.4a-c). Overall clustering of data was much tighter in southern rivers than it was for northern rivers, indicating greater geochemical heterogeneity in northern regions of AK. In the northern regions, different radiogenic end-members contributed to rivers draining the YTU (Chatanika R., Salcha R., and Chena R.), the Brooks Range (Atigan R., Sag R., Canning R. and Etivluk R.), and the north-draining Alaska Range (Nenana R. and Tanana R.). Rivers originating in the Brooks Range, both in our data set and data from Keller et al. (2007) (red triangles in Figure 1.4a-c), plotted along mixing lines characterized by Sil EM3 ($^{87}\text{Sr}/^{86}\text{Sr} = 0.719$) and Sil EM4 ($^{87}\text{Sr}/^{86}\text{Sr} = 0.732$). The main stem Tanana R. and Nenana R. also plotted along these mixing lines. In contrast, YTU rivers plotted away from these mixing lines, indicating a much more radiogenic silicate EM (Sil EM5, $^{87}\text{Sr}/^{86}\text{Sr} = 0.78$) may contribute Sr to these rivers. Some northern rivers, i.e. the lowland rivers (Innoko R., Hogatza R., Dulbi R. and Kuparuk R.), plotted closer to the mixing line of Sil EM2 and Carb

EM (Figure 1.4a-c), suggesting a less radiogenic silicate source of Sr for these four lowland northern rivers.

South-central and southwestern rivers showed distinct patterns in all $^{87}\text{Sr}/^{86}\text{Sr}$ -X/Na plots (Figure 1.4a-c). Watersheds of south-central AK (Copper, Susitna, and Kenai Peninsula watersheds), with the exceptions of the Copper R. upstream of the Chitina R. confluence, Gulkana R. and the Matanuska R., had higher Ca/Na and Sr/Na ratios ($\text{Ca}/\text{Na} > 3.0$, $\text{Sr}/\text{Ca} > 0.01$) and higher $^{87}\text{Sr}/^{86}\text{Sr}$ ratios (> 0.70540), than rivers of the southwest region draining into Bristol Bay ($\text{Ca}/\text{Na} < 3.5$, $\text{Sr}/\text{Ca} < 0.008$, $^{87}\text{Sr}/^{86}\text{Sr}$ ratios < 0.70518), with the exception of the Nushagak and Kuskokwim watersheds (Figure 1.4a,b). This resulted in a pattern where south-central rivers plotted closer to the Carb EM than southwestern rivers. This pattern was not as distinct in the plot of $^{87}\text{Sr}/^{86}\text{Sr}$ and Mg/Na ratios (Figure 1.4c). We include all Kuskokwim R. tributaries in the category of southern rivers (denoted with black-filled circles) in Figure 1.4a-c, because the isotopic distinction between north and south of the Denali Fault was more arbitrary in western AK (Figure 1.1). The Nushagak R. and upper Kuskokwim R. tributaries (except for the South Fork) had relatively radiogenic $^{87}\text{Sr}/^{86}\text{Sr}$ ratios (> 0.70572 and > 0.70752 , respectively) with concomitant low X/Na ratios ($\text{Ca}/\text{Na} < 4$, $\text{Sr}/\text{Ca} < 0.014$, $\text{Mg}/\text{Na} < 2.5$) (Figure 1.4a-c).

The PCA indicated that 90.5% of the variation observed in $^{87}\text{Sr}/^{86}\text{Sr}$ and X/Na ratios was explained by PC1 and PC2 axes (Figure 1.5) and corroborated results of hyperbolic mixing plots (Figure 1.4a-c). Variation along PC1 was predominantly driven by X/Na ratios, indicated by the direction and magnitude of X/Na ordination vectors (Figure 1.5). Variation along PC2 was primarily driven by $^{87}\text{Sr}/^{86}\text{Sr}$ ratios. All southern rivers except the south-central rivers (Kenai Peninsula and Copper R.) and Chulitna R. formed a distinct group with low PC1 scores (< 0) and PC2 scores (ranging from -0.5 to 0.5) (Figure 1.5). Lowland northern rivers also clustered with

southern rivers at low PC1 and PC2 scores. Kenai Peninsula rivers and tributaries of the Copper R. had low PC2 scores, (< -0.5) but notably higher PC1 scores (ranging from 0 to 0.5). Northern rivers plotted at higher PC1 and PC2 scores and exhibited a marked increase in variability. While northern rivers indicated an overall more radiogenic $^{87}\text{Sr}/^{86}\text{Sr}$ composition compared to southern rivers, they showed a gradation of influence from carbonate weathering and their radiogenic nature, indicated by the spread along both PC1 and PC2 in the positive direction in which northern data plot.

DISCUSSION

This study documents geochemical heterogeneity in rivers across AK and illustrates regional patterns in the dominant weathering reactions (carbonate versus silicate) influencing the $^{87}\text{Sr}/^{86}\text{Sr}$ ratios of Sr dissolved in AK rivers. By comparing conservative tracers of $^{87}\text{Sr}/^{86}\text{Sr}$ and molar ratios we have illustrated regional patterns in the relative contribution of radiogenic silicate, non-radiogenic silicate and carbonate weathering (Figure 1.4a-c and Figure 1.5). Compared to southern regions, $^{87}\text{Sr}/^{86}\text{Sr}$ ratios are more radiogenic, molar ratios are generally higher, and both tracers exhibit increased geochemical heterogeneity north of the Denali Fault. In northern regions we also observe a general increase in influence from carbonate weathering associated primarily with the high relief watersheds, not lowland basins. South of the Denali Fault, carbonate weathering is more influential in watersheds of south-central AK (e.g. Copper R.) than those of southwestern AK (e.g. Kvichak R.) where mafic silicate weathering is dominant. These regional geochemical patterns (Figures 4a-c and 5) correspond well with the broad-scale geologic and tectonic setting of AK (Figure 1.6). The geologic terranes of southern AK (i.e. south of Denali Fault) are a collection of exotic island arcs, which collided with, and

were accreted onto, the North American continent during the Mesozoic (Trop and Ridgeway, 2007). Thus, materials of southern AK have a strong mantle affinity, reflected in the low $^{87}\text{Sr}/^{86}\text{Sr}$ ratios of this region's rivers. Much older terranes associated with, and/or derived from, the North American craton lie north of the Denali Fault (Colpron et al., 2007; Trop and Ridgeway, 2007) and exhibit a continental crustal affinity as reflected in their more radiogenic $^{87}\text{Sr}/^{86}\text{Sr}$ ratios. Rivers of lowland basins of AK (e.g. those of western AK and those north of the Brooks Range) influenced by expansive Cretaceous flysch deposits (Beikman, 1980) exhibit intermediate $^{87}\text{Sr}/^{86}\text{Sr}$ ratios (0.707 - 0.709) and low X/Na ratios (Table 1.2). An east-west gradient exists within interior AK, evident within the Yukon, Koyukuk and Kuskokwim basins. Radiogenic $^{87}\text{Sr}/^{86}\text{Sr}$ ratios (> 0.725) in far east-central AK and relatively low ratios (< 0.709) in western AK reflect AK's progressive western growth along the ancestral North American miogeocline from the Precambrian to Mesozoic (Figure 1.6) (Colpron et al., 2007; Nelson et al., 2006; Till et al., 2007; Trop and Ridgeway, 2007).

Regional patterns

North-South of Denali Fault

The abrupt transition of $^{87}\text{Sr}/^{86}\text{Sr}$ north and south of the Denali fault in central AK (Figure 1.1 and 1.2a) reflects the tectonic growth of North America's continental margin in the Mesozoic. In south-central AK the Denali fault bisects what is referred to as the mega-suture zone defining the geologic boundary between the WCT and Northern Kahlitna Terrane (NKT) to the south and YTT to the north (Fisher et al., 2007; Trop and Ridgeway, 2007). The NKT is the remnants of a Cretaceous flysch basin that extended along the North American continental

margin both prior to and during final emplacement of WCT (Trop and Ridgeway, 2007). Rocks of the Kahiltna flysch are thus derived from both North American continental sources (i.e., YTT) and WCT. WCT is generally composed of island-arc related volcanic, plutonic, and sedimentary rocks ranging from the late Paleozoic to mid Mesozoic (Trop and Ridgeway, 2007). The Susitna R. basin ($^{87}\text{Sr}/^{86}\text{Sr} = 0.708 - 0.709$) is the major drainage of NKT, whereas the Copper R. basin ($^{87}\text{Sr}/^{86}\text{Sr} = 0.705 - 0.707$) is the major drainage of WCT. Additionally, the Chugach Mountains represent the accretionary complex related to the collision of WCT and the Yakutat Terrane (YA) with North America (Trop and Ridgeway, 2007) and the rivers of this region (e.g., Kenai, Resurrection, Matanuska, Knik, Tonsina, Klutina, and Tazlina) reflect influence from mantle derived volcanoclastic rocks ($^{87}\text{Sr}/^{86}\text{Sr} = 0.705 - 0.706$) (Cowan, 2003; Harris et al., 1996).

South of the Denali Fault, rivers of south-central AK exhibit influence from carbonate weathering (elevated X/Na ratios) (Figure 1.4a-c and 1.5), which may partly explain relatively high $^{87}\text{Sr}/^{86}\text{Sr}$ ratios (compared to southwestern AK) in this region that approach the Phanerozoic carbonate window (0.707 - 0.709) (Shields and Veizer, 2002). Carbonate weathering is particularly evident in rivers of the Chugach Mountains and Susitna basin, but is not as evident in tributaries receiving input from the Wrangell-St. Elias (e.g., Chitina R.), draining the eastern Alaska Range (e.g., Gulkana R.), or the Matanuska R. The latter drainages appear to be influenced by silicate plutonic and volcanic rocks associated with the Mesozoic collision of WCT and concomitant growth of the North American continent (Trop and Ridgeway, 2007) with reduced influence from carbonate weathering. Although molar ratios of these drainages do not indicate strong influence from carbonate weathering, overall elemental concentrations are quite high (e.g., Matanuska R., Sr = 0.003 and Ca = 0.963 mmol/L), indicating increased silicate weathering likely from loess and proglacial deposits prevalent in the Matanuska R. and Chitina

R. valleys (Anderson, 2007). In contrast, rivers of the Chugach Mountains and Susitna basin indicate influence from marine carbonates and/or trace calcite phases associated with the meta-sedimentary rocks of these regions (Wilson et al., 2008). For example, relatively high elemental concentrations (e.g., Sr = 0.001-0.003 mmol/L) and high molar ratios, but low $^{87}\text{Sr}/^{86}\text{Sr}$ ratios (~0.7055) in some rivers of eastern Chugach Mountains (e.g., Klutina R. and Tonsina R.) (Figure 1.4a-c) implicate influence from a calcareous weathering component with $^{87}\text{Sr}/^{86}\text{Sr}$ below the Phanerozoic marine carbonate window. Non-radiogenic trace calcite associated with young mafic siliciclastic and/or igneous rocks has been shown to be influential on river $^{87}\text{Sr}/^{86}\text{Sr}$ ratios in similar geologic regions (e.g., Stikine Province) (Gaillardet et al., 2003). Thus, tectonic, eolian and glacial processes and their influence on weathering appear to be important dynamics influencing $^{87}\text{Sr}/^{86}\text{Sr}$ ratios of south-central AK rivers.

Directly north of the Denali Fault resides the YTT, much of which is part of the parautochthonous ancestral (Precambrian to Paleozoic) North American miogeocline (Colpron et al., 2007). The Tanana River ($^{87}\text{Sr}/^{86}\text{Sr} = 0.7185$), an axial drainage flowing approximately parallel to the Alaska Range receives tributaries flowing directly north from the Alaska Range (e.g. Nenana R.) ($^{87}\text{Sr}/^{86}\text{Sr} = 0.7132$) and tributaries flowing south from the YTT (e.g., Chatanika R., Chena R., and Salcha R.) ($^{87}\text{Sr}/^{86}\text{Sr} = 0.72281 - 0.74041$). Both sets of tributaries are significantly more radiogenic than rivers south of Denali Fault. Precambrian and Paleozoic continentally derived metamorphic rocks, abundant throughout the YTT, are likely sources of radiogenic Sr (e.g., akin to Sil EM3-5) (Arth, 1994; Douglas et al., 2013; Goldfarb et al., 1997). Similar to south-central rivers, rivers of the YTT show elevated X/Na ratios (and lower Sr/Ca ratios) relative to pure silicate weathering (Figure 1.4a-c), indicating influence from carbonate weathering.

AK's east-west Sr isotopic gradient

$^{87}\text{Sr}/^{86}\text{Sr}$ ratios of the Kuskokwim basin exhibit an east-west gradient (Figure 1.1) reflecting western growth from the Precambrian to Mesozoic along the ancestral North American miogeocline (Figure 1.6) (Colpron et al., 2007; Nelson et al., 2006). The isotopic transition across the Denali Fault system is more abrupt in south-central AK than in western AK (Figure 1.1) due to the juxtaposition of WCT with the Mesozoic North American Continental margin (i.e. the YTT). Once the fault system extends west of, and away from, the central Alaska Range it cuts through the expansive meta-sedimentary rock units of the Paleozoic Farewell Terrane and the Cretaceous Kuskokwim Group, both of which overlap the fault (Bradley et al., 2007) (Figure 1.1). Rocks of the Farewell Terrane derive from a Paleozoic continental source, hypothesized to be the Siberian Craton (Bradley et al., 2007). The Kuskokwim Group is a large back-arc flysch basin deposited in the Late Cretaceous atop several basement terranes, which at that time had only recently amalgamated: the Farewell and Kilbuck (continental fragments), Innoko (obducted ocean floor), and Togiak (an island arc) (Bradley et al., 2007; Goldfarb et al., 2004; Miller et al., 2007). Thus, the Kuskokwim Group is compositionally intermediate between continental crustal sources and mantle sources (Goldfarb et al., 2004), as indicated by lithic and volcanoclastic grains in meta-sedimentary rocks common to Kuskokwim Group (Miller et al., 2007). Consequently, tributaries of the Kuskokwim R. (and Nushagak R.) do not exhibit an abrupt isotopic transition across the Denali Fault.

The Kuskokwim watershed (with the exception of the South Fork) indicates water compositions derived from two different silicate sources (EM1 and EM2) (Figure 1.4a-c) with small influence from carbonate weathering. $^{87}\text{Sr}/^{86}\text{Sr}$ and X/Na ratios of tributaries from the

northern AMP (those of the Kilbuck Mountains) suggest influence from the less radiogenic Sil EM1, whereas the upper river tributaries show influence from the relatively radiogenic Cretaceous meta-sedimentary rocks of the Kuskokwim Group (Goldfarb et al., 2004). The South Fork of the Kuskokwim R. (furthest east tributary measured) plots towards higher $^{87}\text{Sr}/^{86}\text{Sr}$ and X/Na ratios (Figure 1.4a-c), indicating influence from the Paleozoic meta-sedimentary rocks of the Farewell Terrane, which contain metamorphic rocks of an older, continental protolith as well as Paleozoic limestone (Bradley et al., 2007).

Northern lowland vs. highland basins

The lowlands of the Yukon-Koyukuk basin, a Cretaceous flysch deposit, are bordered to the north (Brooks Range), west (Seward Peninsula), and southeast (Ruby geanticline) by Precambrian and Paleozoic continental rocks (Arth, 1994; Arth et al., 1989a; Arth et al., 1989b). Lowland tributaries (Dulbi R. and Hogatza R.) have little to no weathering inputs originating from the Brooks Range and reflect the relatively un-radiogenic derived materials of the Cretaceous flysch (e.g. akin to Sil EM2) (also present in the Innoko basin). Whereas, the most radiogenic values in the Yukon-Koyukuk drainage occur in the upper-river tributaries (Dietrich R., North Fork of Koyukuk R., and South Fork of Koyukuk R.), which have significant inputs from the old metamorphic and meta-sedimentary rocks of the Brooks Range (e.g. akin to Sil EM3 and EM4). The Jim R., which has no water originating from the Brooks Range, but has strong influence from Cretaceous plutonic rocks of the northeast portions of Ruby batholith, has an intermediate $^{87}\text{Sr}/^{86}\text{Sr}$ value of 0.7100, consistent with the geology of this region (Arth et al., 1989b; Blum et al., 1987). Additionally, lower elevation tributaries do not exhibit elevated X/Na ratios, indicating a decreased influence of carbonate weathering relative to the high relief rivers

of the Brooks Range (Figure 1.4a-c, Table 1.2), where elevated X/Na ratios suggest the marked influence of carbonate weathering from Phanerozoic limestone sequences (Beikman, 1980; Wilson et al., 1998).

Similar to patterns of the Yukon-Koyukuk, rivers draining north of the continental divide with significant input from Precambrian and Paleozoic rocks of the Brooks Range (e.g. Atigan R. and Sagavanirktok R.) are more radiogenic than lowland rivers draining the Cretaceous flysch of the NSAK (Kuparuk R. and Inigok Cr.) (Figure 1.1). Aside from the Canning R., X/Na ratios are low to intermediate for both high relief and lowland rivers indicating less influence from carbonate weathering relative to high relief rivers draining south of the divide into the Yukon-Koyukuk. Both our data and some data from Keller et al. (2007) from this region of AK plot along/between Sil EM3 and EM4 mixing lines, indicating a less radiogenic silicate source than for rivers of the YTU.

Non-radiogenic silicate weathering of southwest AK

The low $^{87}\text{Sr}/^{86}\text{Sr}$ ratios in southwestern AK rivers, particularly those rivers from the AMP and AAR reflect a strong influence from mantle derived mafic silicate rocks. A large majority of the AMP is part of the Togiak Terrane, which represents a Mesozoic arc and is composed of volcanoclastic materials built on an ophiolitic basement (Miller et al., 2007). The AAR is a Cenozoic arc forming along the convergent boundary of the Pacific plate and the North American continental margin and is composed of mafic and intermediate plutonic and volcanic rocks (Trop and Ridgeway, 2007). As such, rivers of the Wood River Mountains (i.e. of the AMP) draining into Bristol Bay, the lower Kuskokwim tributaries (i.e. of the AMP), and tributaries of the Kvichak R. (i.e. of the AAR) reflect the influence from young mafic mantle

derived materials. The Kuskokwim Group extends into the Nushagak basin, which is situated between the AMP and AAR. The influence of the relatively radiogenic nature of the Kuskokwim group is evident in the elevated $^{87}\text{Sr}/^{86}\text{Sr}$ ratios of the Nushagak R. (particularly upstream of the Mulchatna R.) as compared to rivers of the AMP and AAR.

We observe the lowest $^{87}\text{Sr}/^{86}\text{Sr}$ ratios and concomitant lowest X/Na ratios in rivers of AMP and AAR, indicating very little influence from carbonate weathering and strong influence from the young mafic silicate materials prevalent in these geologic regions (Alaskan-Aleutian Arc and Togiak Terrane, respectively) (Wilson et al., 2006). The data from Nushagak River (the basin separating AMP from AAR) also exhibit low X/Na ratios, but relatively radiogenic $^{87}\text{Sr}/^{86}\text{Sr}$ ratios plotting towards Sil EM2. This indicates that relatively radiogenic continentally derived silicate materials of the Kuskokwim Group, the dominant lithology in the upper reaches of the Nushagak R., influence Nushagak R. geochemistry (Goldfarb et al., 2004; Wilson and Coonrad, 2005).

A radiogenic calcareous source in metamorphic regions of YTT and Brooks Range

Across the whole AK dataset, particularly from YTT and Brooks Range rivers, the PCA (Figure 1.5) and hyperbolic mixing plots (Figure 1.4a-c) indicate concomitant increases in $^{87}\text{Sr}/^{86}\text{Sr}$ and X/Na ratios (e.g., in PCA, $^{87}\text{Sr}/^{86}\text{Sr}$ and X/Na ordination vectors are all positively correlated). This ‘anomalous’ finding (Edmond, 1992), where $^{87}\text{Sr}/^{86}\text{Sr}$ ratios increase with indicators of carbonate weathering (e.g., high X/Na ratios), is opposite to what would be expected in the shield terranes, such as the Amazon (Edmond et al., 1995; Palmer and Edmond, 1992) and Canada (Wadleigh et al., 1985), in which the most radiogenic regions are composed of old felsic silicate materials from respective cratons, which impart concomitant low X/Na ratios.

However, one would expect a positive relationship between $^{87}\text{Sr}/^{86}\text{Sr}$ and X/Na in young mafic silicate terranes (e.g., AK's Cenozoic arc), juxtaposed with sedimentary sequences composed in part of marine carbonates, where the least radiogenic ratios derive from mafic silicate materials ($^{87}\text{Sr}/^{86}\text{Sr} = \sim 0.703$; low X/Na) and more radiogenic ratios derive from Phanerozoic carbonate weathering ($^{87}\text{Sr}/^{86}\text{Sr} = 0.707 - 0.709$; high X/Na). The latter example may in part explain the seemingly anomalous pattern in AK water data. However, in both the Brooks Range and the YTT (particularly the YTU), we observe elevated X/Na ratios (relative to pure silicate weathering) and radiogenic $^{87}\text{Sr}/^{86}\text{Sr}$ ratios (e.g. Brooks Range > 0.712 ; YTU > 0.722) falling far from the Phanerozoic carbonate window (0.707 - 0.709) (Figure 1.4a-c). This is also evident in Keller et al. (2007) (Figure 4a-c), and suggests that in these regions a reactive source of radiogenic Sr (e.g. calcareous) may be present.

Three well-documented examples where geochemical constituents of surface waters indicate influence from carbonate weathering, but have $^{87}\text{Sr}/^{86}\text{Sr}$ which fall far from the Phanerozoic marine carbonate window (0.707 - 0.709) are the Himalaya (Edmond, 1992; Quade et al., 2003), the Eastern Canadian Cordillera (Millot et al., 2003), and Siberia (Huh and Edmond, 1999). In all three examples, one hypothesis advanced is that during regional metamorphism in these areas Sr is exchanged between carbonates and the surrounding siliciclastic rock. Though our data do not indicate strong examples of the occurrence of these processes, the influence of this phenomenon may be an important and general influence on $^{87}\text{Sr}/^{86}\text{Sr}$ ratios of river dissolved Sr in metamorphic regions where deformed carbonate-bearing lithologies are common, such as the Brooks Range (Moore and Mull, 2013) and YTT (Newberry et al. 1996; Wilson et al., 1998). This phenomenon may also help explain why modeling approaches (Bataille et al., in revision) that assume all carbonate present in a watershed

contributes Sr with $^{87}\text{Sr}/^{86}\text{Sr}$ ratios falling within the Phanerozoic carbonate window (0.707-0.709) substantially under-predict the $^{87}\text{Sr}/^{86}\text{Sr}$ ratios of rivers draining the YTU.

Consideration of temporal and spatial uncertainties

AK data herein show distinct regional and local scale patterns in $^{87}\text{Sr}/^{86}\text{Sr}$ ratios, but the dataset is limited by two general uncertainties: i) the spatial resolution of sampling does not fully match the geologic heterogeneity of AK, as is evident in our companion paper (Bataille et al., in revision), and ii) these data are fall/summer time ‘snapshots’ of $^{87}\text{Sr}/^{86}\text{Sr}$ ratios of sampled rivers and the evaluation of temporal variability is not possible with this dataset. The former limitation is inherent to remote, expansive and geologically diverse regions such as AK. But the coupling of these data, which correspond to a wide spatial distribution and cover major geologic regions, with a modeling approach, which indicates the same regional patterns (Bataille et al., in revision), further validates the patterns found in these data. Additionally, the coupling of sampling campaigns with modeling approaches will afford better hypothesis development and study design of provenance investigations, and identifies regions where more data and resources are needed. Future work is needed to quantify and evaluate the latter limitation (temporal variability) including, i) which regions across AK are likely to exhibit time-dependent variations in $^{87}\text{Sr}/^{86}\text{Sr}$ ratios, ii) the magnitude and scale of temporal variation, and iii) what the primary controls are on these variations. For example, the distribution of permafrost across AK and its time-dependent (decadal, inter-annual and seasonal) influence on $^{87}\text{Sr}/^{86}\text{Sr}$ ratios of surface waters are important factors to consider when characterizing geographic variation of $^{87}\text{Sr}/^{86}\text{Sr}$ ratios in northern latitudes. In Arctic and Subarctic regions, the presence of permafrost in both continuous (Keller et al., 2007; Keller et al., 2010) and discontinuous permafrost regions

(Douglas et al., 2013) can play a significant role in influencing the $^{87}\text{Sr}/^{86}\text{Sr}$ ratios of surface waters on multiple time-scales. In addition to dictating water flow paths, the presence of permanently frozen ground essentially protects constituent rocks and minerals from interacting with liquid water, i.e. from chemical weathering (Douglas et al., 2013; Keller et al., 2007; Keller et al., 2010). Thus, variation in magnitude and duration of short-term (e.g. seasonal) and long-term (e.g. decadal) freeze-thaw cycles and how they influence rock-weathering are likely sources of $^{87}\text{Sr}/^{86}\text{Sr}$ time-dependent heterogeneity within Arctic and Subarctic watersheds. Other documented processes, which have time-dependent effects on $^{87}\text{Sr}/^{86}\text{Sr}$ ratios of surface waters include glacial retreat (Anderson et al., 2000).

CONCLUSIONS AND IMPLICATIONS

Data herein span the majority of geographic and geologic regions of AK illustrating significant heterogeneity of $^{87}\text{Sr}/^{86}\text{Sr}$ ratios of river-dissolved Sr on multiple spatial scales. Across AK we report the following conclusions based on isotopic and molar ratio analyses:

- 1) Rivers north of the Denali Fault exhibit higher and more variable ratios than rivers south, because they drain rocks i) spanning a larger age range and ii) are composed of a diverse mixture of continentally influenced materials. The isotopic end-members of AK are the AAR and AMP in southwestern AK ($^{87}\text{Sr}/^{86}\text{Sr} < 0.7045$) and YTU in far east-central, AK (> 0.74).
- 2) North of the Denali Fault high relief rivers are more radiogenic, whereas lowland rivers are less radiogenic, largely because the high relief areas are Precambrian and Paleozoic metamorphic terranes (e.g. the Brooks Range and YTT), whereas the lowland basins are

composed of Cretaceous flysch. Thus interior, AK exhibits an east-west gradient of high ratios in the east and low ratios further west.

3) Carbonate weathering is more influential in high relief basins north of the Denali Fault and in south-central AK than it is in lowland basins north of the fault and southwestern AK.

4) The silicate end-members contributing to dissolved loads differ north and south of the Denali Fault. Rivers north of the fault indicate more diverse silicate end-members, with $^{87}\text{Sr}/^{86}\text{Sr}$ ratios between 0.707 (Sil EM2) and 0.78 (Sil EM5), whereas rivers south of Denali Fault appear to derive Sr from silicate end members with a narrower $^{87}\text{Sr}/^{86}\text{Sr}$ range from 0.703 (Sil EM1) to 0.707 (Sil EM2).

Characterizing $^{87}\text{Sr}/^{86}\text{Sr}$ ratios and dominant weathering patterns across AK has implications for numerous modern and paleo ecological studies. AK is currently home to many migratory wild animal populations, including abundant runs of five species of Pacific salmon and several species of migratory ungulates (caribou, bison and musk ox). Additionally, AK was part of an ice-free corridor composing Beringia (the largely unglaciated region lying between the Lena River in the west and the McKenzie River in the east) during the last glaciation. As such, it provided habitat for Pleistocene megafauna, now extinct, and early populations of humans (Potter et al., 2011). Much of the habitat used by these past and present populations, is and has been, relatively undisturbed by large-scale human impact compared to other places in the world. Development of baseline datasets, such as the one presented here and the companion paper (Bataille, et al., in revision), provide necessary data and predictions that will inform study design and hypothesis development for future provenance investigations.

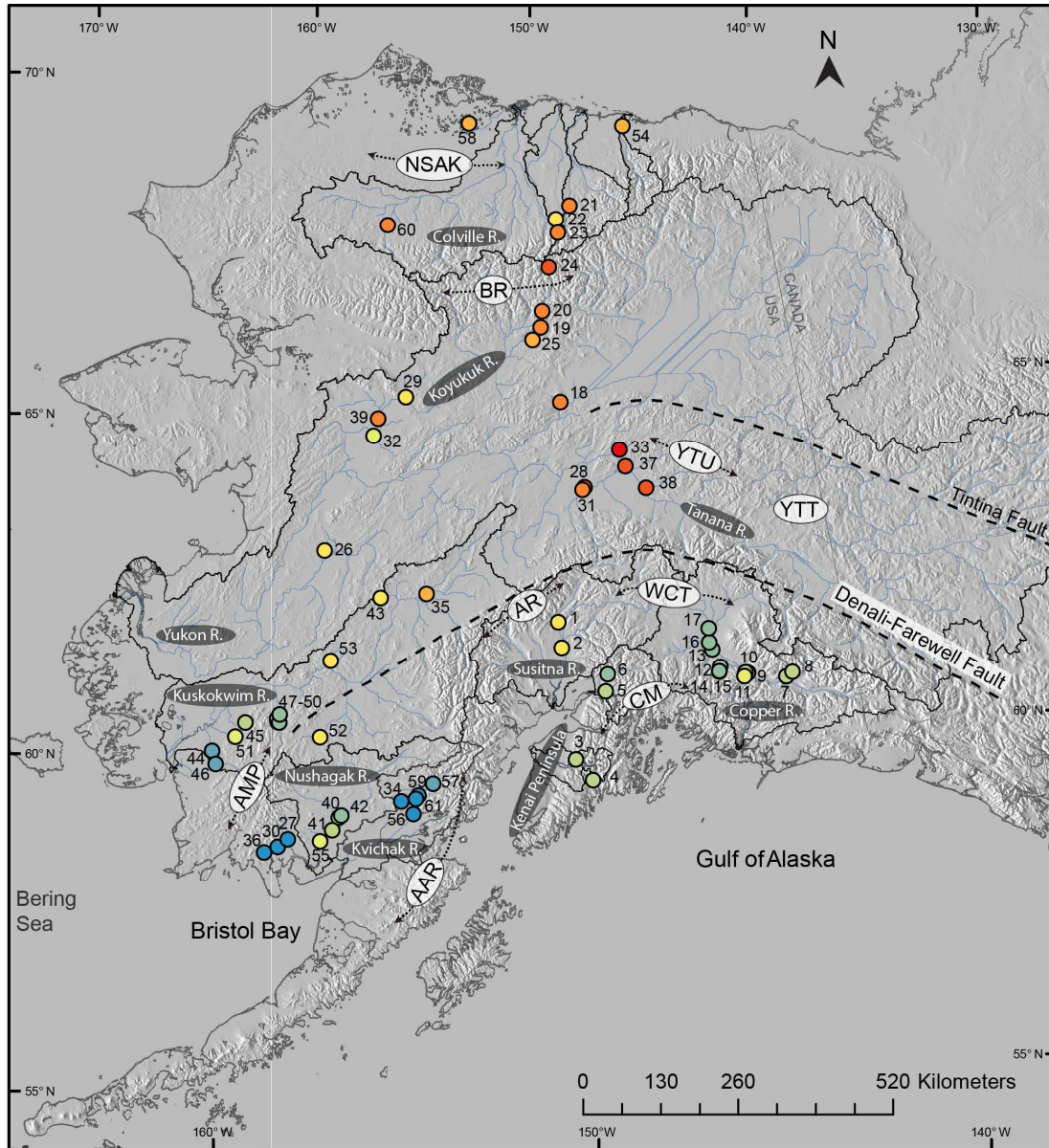


Figure 1.1. $^{87}\text{Sr}/^{86}\text{Sr}$ ratios of AK rivers. Locations of water samples analyzed from Alaska (AK), color-coded according to $^{87}\text{Sr}/^{86}\text{Sr}$ ratios and shown with sample ID numbers. AR=Alaska Range, BR=Brooks Range, NSAK=North Slope of AK, YTU=Yukon Tanana Uplands, AAR=Alaskan-Aleutian Range, AMP=Ahklun Mountain Province, CM=Chugach Mountains.

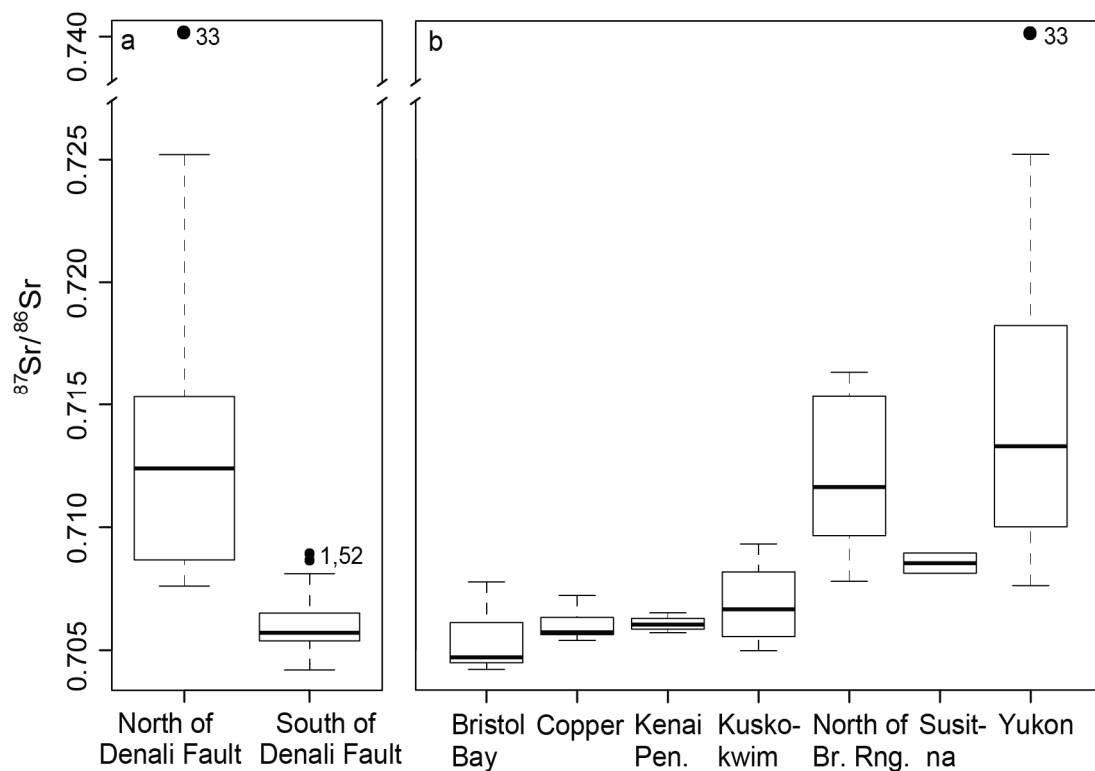


Figure 1.2. Inter- and intra-watershed $^{87}\text{Sr}/^{86}\text{Sr}$ variation. Box-plots illustrating distribution of $^{87}\text{Sr}/^{86}\text{Sr}$ ratios in AK rivers (bold horizontal line = median, box extent = quartiles 25% and 75%, dotted line = non-outlier range). A) Rivers north and south of the Denali-Farewell Fault system. Numbers next to black-filled circles indicate sample IDs as in Table 2 and Figure 1. B) Intra- and inter-watershed variation in $^{87}\text{Sr}/^{86}\text{Sr}$ ratios.

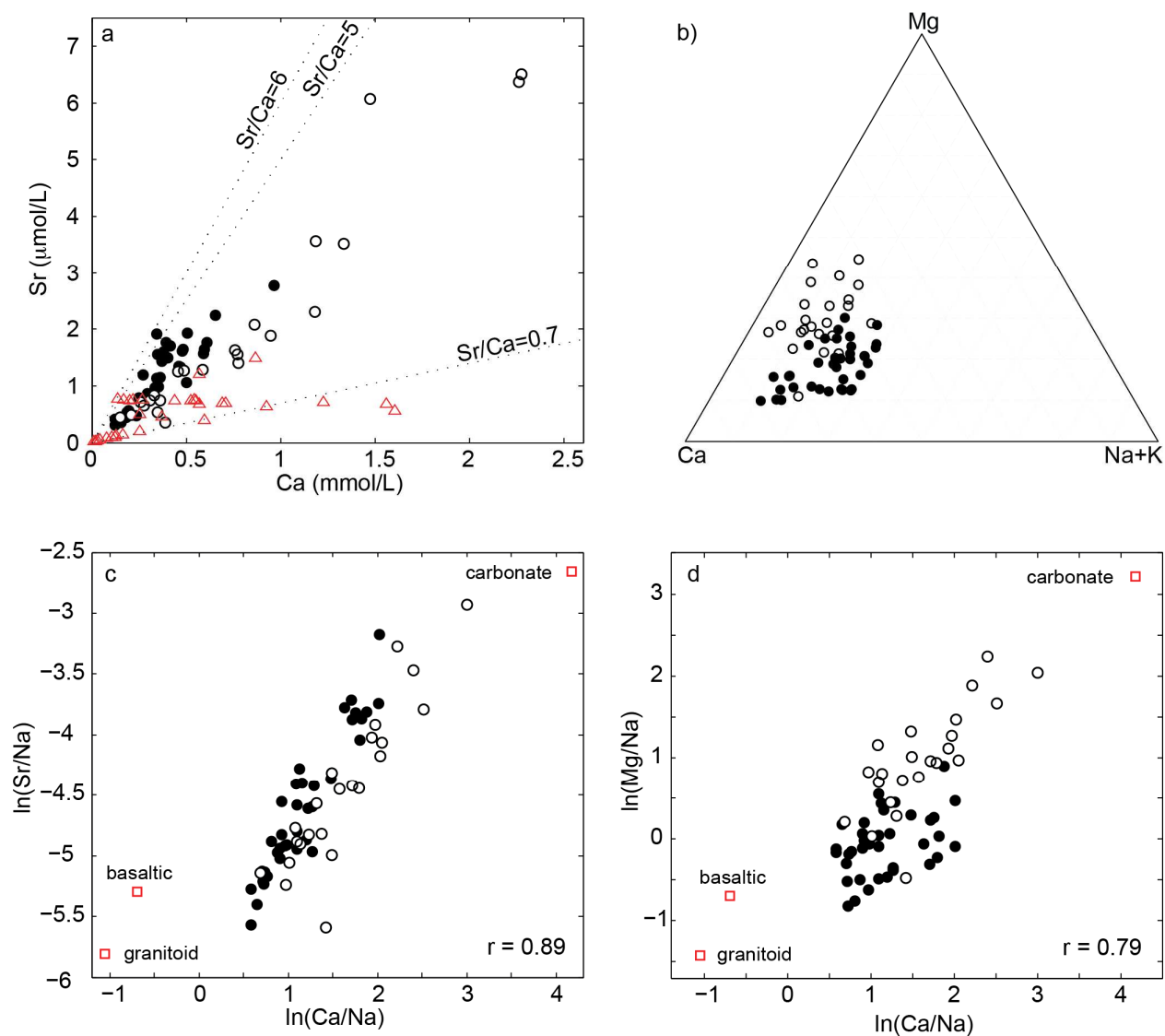


Figure 1.3. Elemental ratios of AK rivers. A) Sr versus Ca for northern (open circles) and southern (black-filled circles) AK rivers. Dotted lines indicate Sr/Ca ratios of monolithic catchments reported by Meybeck (1986): mafic silicates Sr/Ca=6mmol/mol, felsic silicates Sr/Ca=5mmol/mol, and pure carbonates Sr/Ca=0.7mmol/mol. Data from Keller et al., 2007 (open red triangles) also are plotted. B) Mg-Ca-Na+K ternary diagram of southern and northern AK rivers (axes are fractions (%) of molar concentrations (mmol/L)). C & D) X/Na log-log plots indicating mixing between carbonate (high X/Na values) and silicate (low X/Na values) weathering sources. Published felsic silicate, mafic silicate and carbonate end-members are also plotted (open red squares) (values from Gaillardet et al., 1999) (see Table 1).

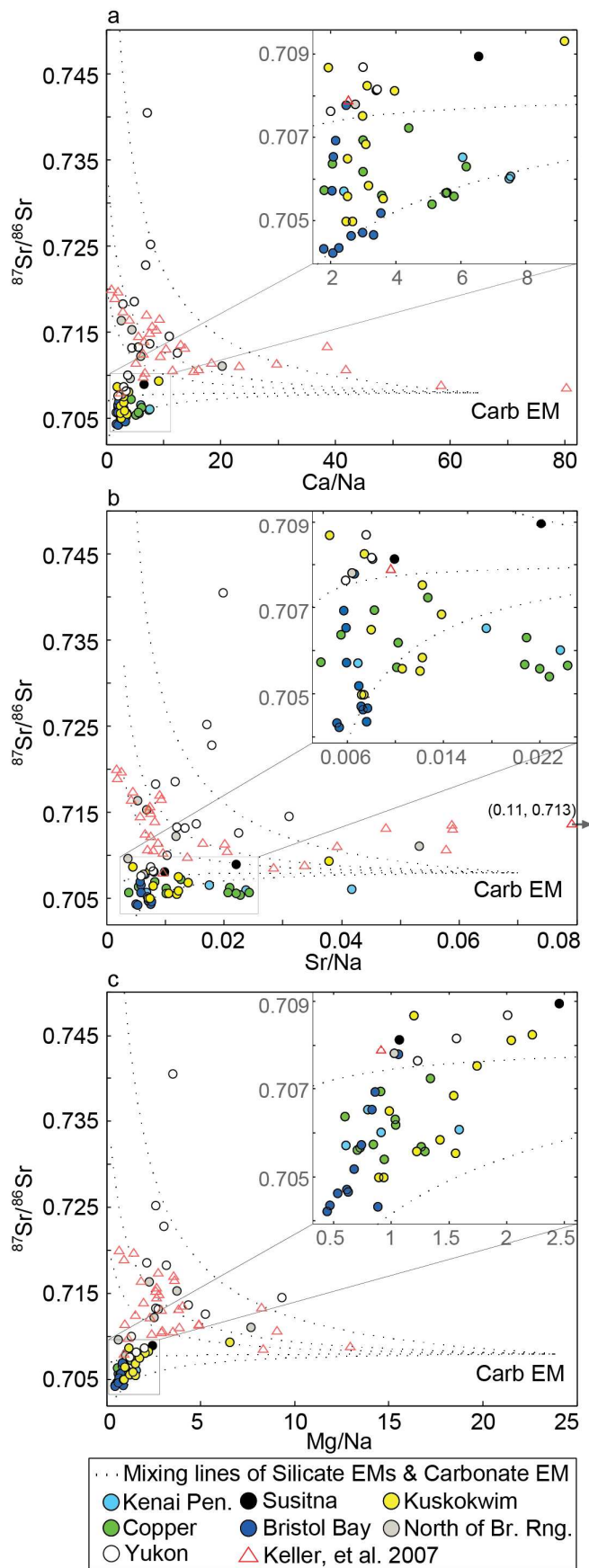


Figure 1.4. Hyperbolic mixing plots. Hyperbolic mixing plots of $^{87}\text{Sr}/^{86}\text{Sr}$ versus X/Na ratios of AK rivers. Open/gray-filled circles = northern rivers; color-filled circles = southern rivers (includes all Kuskokwim data); and red open triangles = Keller et al. (2007). Dotted lines are hyperbolic mixing lines between silicate EMs (Sil EM1 - Sil EM5) and carbonate EM (Carb EM), see Table 1 for EM values and discussion in text.

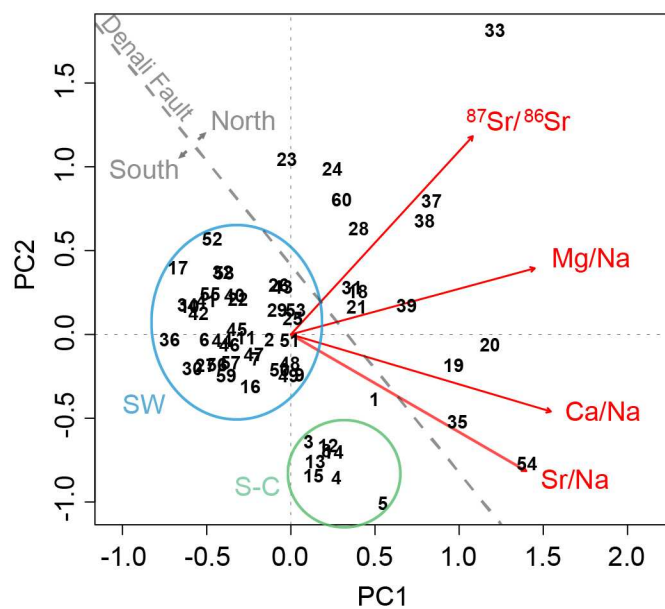


Figure 1.5. PCA of $^{87}\text{Sr}/^{86}\text{Sr}$ and X/Na ratios. PCA of log-transformed $^{87}\text{Sr}/^{86}\text{Sr}$ and X/Na ratios of all AK water data. Data are plotted as ID number as in Table 1.2 and Figure 1.1. Circled groups: SW =southwestern, AK rivers (incl. northern lowland and some south-central rivers, see text for discussion); S-C =south-central, AK rivers.

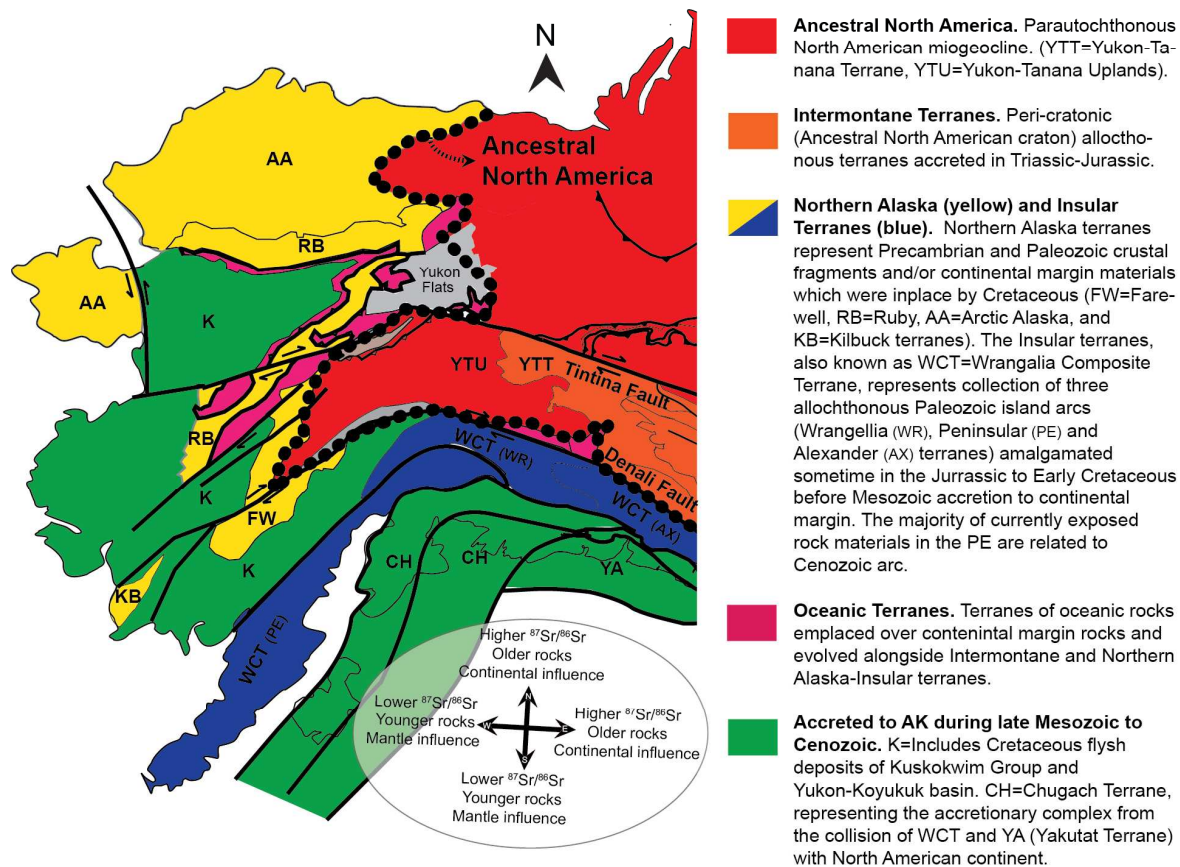


Figure 1.6. $^{87}\text{Sr}/^{86}\text{Sr}$ patterns and tectonic realms of AK. Tectonic realms of AK reflect gross geographic patterns observed in $^{87}\text{Sr}/^{86}\text{Sr}$ ratios in AK river waters (map modified from Colpron, et al., 2007). Choice of map color scheme approximately congruent with $^{87}\text{Sr}/^{86}\text{Sr}$ color scheme in Figure 1.1 (hot colors~higher ratios, cold colors~lower ratios).

Table 1.1. Summary of end-members used to calculate hyperbolic mixing lines. Refer to Supplementary Material in Appendix for description of each EM.

End Member	Ca/Na	Sr/Na	Mg/Na	⁸⁷Sr/⁸⁶Sr	Reference
Silicate EM1	0.5	0.005	0.5	0.703	Gaillardet et al., 1999; Ingram and Weber, 1999
Silicate EM2	0.35	0.003	0.24	0.707	Gaillardet et al., 1999; Ingram and Weber, 1999
Silicate EM3	0.35	0.003	0.24	0.719	Gaillardet et al., 1999; Keller et al., 2007
Silicate EM4	0.35	0.003	0.24	0.732	Gaillardet et al., 1999; Goldfarb et al., 1997; Douglas et al., 2013
Silicate EM5	0.35	0.003	0.24	0.78	Gaillardet et al., 1999; Millot et al., 2003
Carbonate EM	65	0.07	25	0.708	Gaillardet et al., 1999

Table 1.2. Summary of $^{87}\text{Sr}/^{86}\text{Sr}$, elemental, and molar ratio data from different rivers of AK determined in this study. All elemental concentration estimates are units of mmol/L. ID numbers correspond to Figure 1.1. Field triplicates are indicated by an *; the isotopic and concentration errors of rivers indicated as triplicates are $2\sigma\text{SE}$ of the three samples making up each triplicate.

ID	Date Collected	River	Denali Fault		Watershed	Latitude	Longitude	$^{87}\text{Sr}/^{86}\text{Sr}$	$\pm 2\sigma\text{SE}$	Sr	$\pm 2\sigma$ error	Ca	$\pm 2\sigma$ error	Mg	$\pm 2\sigma$ error	Na	$\pm 2\sigma$ error	K	$\pm 2\sigma$ error	Sr/Na	Ca/Na	Mg/Na	Sr/Ca	
			North(N)/South(S)																					
27	6/30/11	Lake Aleknagik	S		Bristol Bay	59.274	-158.599	0.704631	0.000059	0.00037	0.000015	0.135	0.005	0.027	0.0014	0.051	0.0056	0.006	0.0024	0.0073	2.6	0.54	0.0028	
30	6/30/11	Snake Lake	S		Bristol Bay	59.151	-158.887	0.704346	0.000055	0.00041	0.000011	0.123	0.006	0.026	0.0011	0.055	0.0056	0.004	0.0023	0.0076	2.3	0.47	0.0034	
34	6/17/11	Upper Talarik Cr.	S		Bristol Bay	59.917	-155.270	0.704324	0.000028	0.00076	0.000024	0.268	0.011	0.132	0.0030	0.149	0.0080	0.012	0.0024	0.0051	1.8	0.88	0.0028	
36	6/30/11	Lake Amanka*	S		Bristol Bay	59.048	-159.272	0.704217	0.000074	0.00031	0.000008	0.122	0.005	0.026	0.0008	0.059	0.0035	0.004	0.0009	0.0053	2.1	0.44	0.0026	
40	8/28/11	Nushagak upstr Mulchatna	S		Bristol Bay	59.642	-157.123	0.707779	0.000047	0.00048	0.000009	0.182	0.004	0.078	0.0009	0.074	0.0040	0.006	0.0034	0.0066	2.5	1.06	0.0027	
41	8/28/11	Nushagak downstr Mulchatna	S		Bristol Bay	59.447	-157.303	0.706531	0.000036	0.00053	0.000013	0.188	0.004	0.075	0.0010	0.090	0.0039	0.009	0.0034	0.0059	2.1	0.83	0.0028	
42	8/28/11	Mulchatna*	S		Bristol Bay	59.670	-157.053	0.705724	0.000029	0.00057	0.000002	0.197	0.005	0.072	0.0004	0.097	0.0029	0.012	0.0002	0.0059	2.0	0.74	0.0029	
55	9/13/12	Nushagak mouth	S		Bristol Bay	59.268	-157.649	0.706929	0.000034	0.00050	0.000021	0.189	0.011	0.075	0.0031	0.088	0.0051	0.007	0.0028	0.0057	2.2	0.86	0.0026	
56	9/27/12	Newhalen*	S		Bristol Bay	59.725	-154.901	0.704709	0.000124	0.00044	0.000006	0.183	0.012	0.038	0.0006	0.061	0.0084	0.016	0.0016	0.0071	3.0	0.62	0.0024	
57	4/24/12	Tanalian	S		Bristol Bay	60.189	-154.319	0.705185	0.000027	0.00047	0.000006	0.238	0.010	0.046	0.0011	0.067	0.0070	0.010	0.0019	0.0070	3.5	0.68	0.0020	
59	5/16/12	Lake Clark mouth	S		Bristol Bay	60.012	-154.761	0.704656	0.000028	0.00049	0.000027	0.211	0.024	0.040	0.0022	0.063	0.0084	0.021	0.0034	0.0077	3.3	0.62	0.0023	
61	10/26/12	Gibraltar	S		Bristol Bay	59.430	-154.832	0.704321	0.000090															
7	9/15/10	Nizina*	S		Copper	61.380	-143.154	0.706182	0.000019	0.00224	0.000037	0.653	0.026	0.227	0.0042	0.219	0.0071	0.018	0.0009	0.0102	3.0	1.04	0.0034	
8	9/16/10	Kennicott*	S		Copper	61.433	-142.944	0.706303	0.000011	0.00164	0.000033	0.485	0.023	0.081	0.0032	0.079	0.0034	0.014	0.0007	0.0209	6.2	1.04	0.0034	
9	9/17/10	Chitina*	S		Copper	61.518	-144.333	0.707227	0.000033	0.00176	0.000033	0.609	0.024	0.186	0.0042	0.139	0.0046	0.039	0.0014	0.0127	4.4	1.34	0.0029	
10	9/17/10	Copper upstr Chitina*	S		Copper	61.531	-144.408	0.706374	0.000036	0.00157	0.000030	0.589	0.024	0.172	0.0035	0.288	0.0075	0.022	0.0009	0.0055	2.0	0.60	0.0027	
11	9/17/10	Copper downstr Chitina*	S		Copper	61.475	-144.455	0.706939	0.000038	0.00164	0.000036	0.595	0.021	0.180	0.0035	0.199	0.0059	0.030	0.0012	0.0083	3.0	0.91	0.0028	
12	9/17/10	Tonsina downstr LT*	S		Copper	61.663	-145.182	0.705678	0.000017	0.00149	0.000033	0.401	0.022	0.091	0.0031	0.072	0.0037	0.010	0.0007	0.0207	5.6	1.26	0.0037	
13	9/17/10	Klutina*	S		Copper	61.947	-145.354	0.705397	0.000015	0.00176	0.000035	0.393	0.019	0.072	0.0032	0.077	0.0032	0.010	0.0007	0.0228	5.1	0.94	0.0045	
14	9/18/10	Little Tonsina (LT)*	S		Copper	61.595	-145.223	0.705579	0.000012	0.00193	0.000036	0.507	0.021	0.113	0.0035	0.088	0.0034	0.011	0.0007	0.0220	5.8	1.29	0.0038	
15	9/18/10	Tonsina upstr LT *	S		Copper	61.598	-145.225	0.705661	0.000062	0.00119	0.000029	0.270	0.019	0.036	0.0010	0.049	0.0031	0.006	0.0006	0.0243	5.5	0.73	0.0044	
16	9/19/10	Tazlina*	S		Copper	62.058	-145.431	0.705608	0.000036	0.00133	0.000033	0.469	0.025	0.093	0.0032	0.131	0.0056	0.012	0.0008	0.0101	3.6	0.71	0.0028	
17	9/19/10	Gulkana*	S		Copper	62.270	-145.385	0.705733	0.000028	0.00106	0.000029	0.504	0.022	0.236	0.0045	0.280	0.0077	0.024	0.0009	0.0038	1.8	0.85	0.0021	
3	9/12/10	Kenai*	S		Kenai Pen.	60.487	-149.935	0.706517	0.000012	0.00086	0.000028	0.296	0.019	0.039	0.0009	0.049	0.0032	0.014	0.0008	0.0175	6.1	0.80	0.0029	
4	9/13/10	Resurrection*	S		Kenai Pen.	60.163	-149.454	0.706014	0.000041	0.00115	0.000030	0.364	0.019	0.044	0.0010	0.049	0.0032	0.006	0.0006	0.0237	7.5	0.91	0.0032	
5	9/14/10	Knik*	S		Kenai Pen.	61.476	-148.876	0.706074	0.000075	0.00191	0.000030	0.345	0.021	0.073	0.0011	0.046	0.0031	0.008	0.0007	0.0417	7.5	1.59	0.0055	
6	9/14/10	Matanuska*	S		Kenai Pen.	61.734	-148.765	0.705711	0.000013	0.00277	0.000055	0.963	0.036	0.244	0.0039	0.401	0.0263	0.014	0.0009	0.0069	2.4	0.61	0.0029	
35	Oct_2011	South Fork Kuskokwim*	N		Kuskokwim	63.039	-154.573	0.709318	0.000012	0.00607	0.000058	1.472	0.015	1.051	0.0095	0.160	0.0027	0.031	0.0003	0.0379	9.2	6.56	0.0041	
43	9/13/12	Takotna	N		Kuskokwim	62.968	-156.092	0.708245	0.000023	0.00074	0.000026	0.310	0.010	0.221	0.0051	0.099	0.0047	0.007	0.0017	0.0074	3.1	2.22	0.0024	
44	9/21/12	Kwethuk old wier*	S		Kuskokwim	60.494	-161.100	0.704984	0.000024	0.00097	0.000034	0.334	0.001	0.120	0.0032	0.135	0.0039	0.013	0.0009	0.0072	2.5	0.89	0.0029	
45	9/21/12	Tulusak	S		Kuskokwim	60.965	-160.170	0.706492	0.000022	0.00079	0.000029	0.249	0.009	0.097	0.0027	0.099	0.0046	0.010	0.0017	0.0080	2.5	0.98	0.0032	
46	9/21/12	Kwethluk elbow	S		Kuskokwim	60.298	-160.960	0.704977	0.000025	0.00098	0.000039	0.353	0.011	0.124	0.0022	0.132	0.0057	0.012	0.0017	0.0074	2.7	0.94	0.0028	
47	9/21/12	Kipchuk (Kip)	S		Kuskokwim	61.012	-159.177	0.705579	0.000029	0.00160	0.000045	0.382	0.011	0.185	0.0030	0.152	0.0057	0.012	0.0017	0.0105	2.5	1.22	0.0042	
48	9/21/12	Salmon (Sal)	S		Kuskokwim	61.063	-159.195	0.706844	0.000030	0.00156	0.000037	0.348	0.008	0.174	0.0037	0.113	0.0044	0.009	0.0017	0.0139	3.1	1.54	0.0045	
49	9/21/12	Aniak upstr Kip and Sal	S		Kuskokwim	61.008	-159.117	0.705527	0.000030	0.00114	0.000027	0.343	0.008	0.147	0.0031	0.095	0.0046	0.006	0.0017	0.0120	3.6	1.56	0.0033	
50	9/21/12	Aniak downstr Timber	S		Kuskokwim	61.126	-159.121	0.705835	0.000025	0.00144	0.000031	0.372	0.007	0.167	0.0014	0.118	0.0045	0.009	0.0017	0.0123	3.2	1.42	0.0039	
51	9/21/12	Kisaralik	S		Kuskokwim	60.737	-160.447	0.707520	0.000028	0.00170	0.000040	0.414	0.017	0.242	0.0049	0.139	0.0071	0.009	0.0017	0.0122	3.0	1.74	0.0041	
52	9/22/12	Holitina upstr Kokcugluk wier*	S		Kuskokwim	60.829	-157.829	0.708675	0.000024	0.00036	0.000014	0.155	0.008	0.097	0.0034	0.081	0.0045	0.006	0.0011	0.0045	1.9	1.20	0.0023	
53	9/22/12	George	N		Kuskokwim	61.984	-157.628	0.708119	0.000024	0.00074	0.000031	0.363	0.015	0.187	0.0056	0.092	0.0097	0.008	0.0017	0.0081	4.0	2.04	0.0020	
21	9/23/10	Sagavanirktok*	N		N. of Br. Rng.	68.834	-148.821	0.712186	0.000040	0.00231	0.000052	1.180	0.043	0.499	0.0077	0.196	0.0078	0.011	0.0007	0.0118	6.0	2.54	0.0020	
22	9/23/10	Kuparuk*	N		N. of Br. Rng.	68.647	-149.411	0.707796	0.000088	0.00049	0.000028	0.211	0.019	0.078	0.0033	0.076	0.0033	0.006	0.0007	0.0064	2.8	1.03	0.0023	
23	9/23/10	Atigan*	N		N. of Br. Rng.	68.437	-149.368	0.716335	0.000112	0.00189	0.000031	0.946	0.037	0.810	0.0075	0.357	0.0253	0.017	0.0009	0.0053	2.7	2.27	0.0020	
54	9/1/12	Canning	N		N. of Br. Rng.	69.972	-146.276	0.711081	0.000022	0.00352	0.000149	1.335	0.117	0.509	0.0258	0.066	0.0052	0.009	0.0029	0.0532	20.2	7.68	0.0026	
58	7/3/12	Inigok	N		N. of Br. Rng.	70.162	-152.903	0.709660	0.000032	0.00035	0.000017	0.387	0.014	0.058	0.0026	0.094	0.0071	0.009	0.0019	0.0037	4.1	0.62	0.0009	
60	6/20/12	Etivluk	N		N. of Br. Rng.	68.601	-156.271	0.715329	0.000026	0.00053	0.000026	0.347	0.015	0.296	0.0154	0.079	0.0070	0.010	0.0019	0.0068	4.4	3.76	0.0015	
1	9/11/10	Chulitna*	S		Susitina	62.568	-150.236	0.708948	0.000042	0.00162	0.000034	0.481	0.024	0.180	0.0034	0.073	0.0038	0.034	0.0014	0.0221	6.6	2.46	0.0034	
2	9/11/10	Susitna*	S		Susitina	62.178	-150.172	0.708127	0.000057	0.00135	0.000035	0.463	0.021	0.146	0.0040	0.136	0.0042	0.037	0.0011	0.0099	3.4	1.07	0.0029	

Table 1.2. continued:

ID	Date Collected	River	Denali Fault North(N)/South(S)	Watershed	Latitude	Longitude	⁸⁷ Sr/ ⁸⁶ Sr	±2σSE	Sr	±2σ error	Ca	±2σ error	Mg	±2σ error	Na	±2σ error	K	±2σ error	Sr/Na	Ca/Na	Mg/Na	Sr/Ca
18	9/21/10	Yukon*	N	Yukon	65.877	-149.710	0.713285	0.000028	0.00163	0.000031	0.758	0.027	0.354	0.0050	0.136	0.0048	0.027	0.0010	0.0120	5.6	2.60	0.0022
19	9/21/10	South Fork Koyukuk*	N	Yukon	67.017	-150.286	0.712632	0.000043	0.00141	0.000029	0.777	0.029	0.331	0.0038	0.063	0.0035	0.011	0.0007	0.0225	12.4	5.27	0.0018
20	9/22/10	Middle Fork Koyukuk*	N	Yukon	67.258	-150.195	0.714574	0.000065	0.00637	0.000081	2.261	0.056	1.906	0.0220	0.205	0.0061	0.018	0.0008	0.0311	11.1	9.32	0.0028
24	9/23/10	Dietrich*	N	Yukon	67.916	-149.823	0.718241	0.000029	0.00650	0.000136	2.274	0.078	2.447	0.0393	0.771	0.0366	0.018	0.0009	0.0084	3.0	3.18	0.0029
25	9/24/10	Jim's*	N	Yukon	66.838	-150.607	0.710022	0.000111	0.00072	0.000027	0.261	0.020	0.093	0.0035	0.070	0.0038	0.012	0.0007	0.0103	3.7	1.33	0.0028
26	Oct_2011	Innoko	N	Yukon	63.638	-158.038	0.708691	0.000028	0.00083	0.000031	0.331	0.015	0.222	0.0062	0.110	0.0065	0.011	0.0024	0.0076	3.0	2.01	0.0025
28	9/25/11	Tanana	N	Yukon	64.559	-149.066	0.718543	0.000025	0.00208	0.000020	0.861	0.072	0.380	0.0109	0.178	0.0066	0.046	0.0027	0.0117	4.8	2.13	0.0024
29	6/16/11	Hogatza	N	Yukon	66.001	-155.397	0.708160	0.000029	0.00065	0.000027	0.279	0.009	0.127	0.0036	0.081	0.0060	0.009	0.0024	0.0080	3.4	1.57	0.0023
31	9/25/11	Nenana	N	Yukon	64.529	-149.131	0.713168	0.000019	0.00357	0.000100	1.185	0.080	0.734	0.0240	0.267	0.0107	0.043	0.0030	0.0134	4.4	2.75	0.0030
32	6/17/11	Dulbi	N	Yukon	65.399	-156.523	0.707628	0.000049	0.00044	0.000012	0.149	0.005	0.092	0.0015	0.075	0.0054	0.009	0.0024	0.0058	2.0	1.23	0.0029
33	9/25/11	Chatanika	N	Yukon	65.085	-147.724	0.740407	0.000029	0.00126	0.000039	0.457	0.015	0.225	0.0065	0.063	0.0057	0.020	0.0025	0.0199	7.2	3.54	0.0028
37	9/18/11	Chena	N	Yukon	64.830	-147.566	0.725196	0.000027	0.00129	0.000015	0.585	0.025	0.198	0.0017	0.075	0.0042	0.025	0.0036	0.0171	7.8	2.63	0.0022
38	9/18/11	Salcha*	N	Yukon	64.473	-146.917	0.722815	0.000114	0.00127	0.000004	0.488	0.010	0.215	0.0008	0.071	0.0010	0.021	0.0005	0.0179	6.9	3.03	0.0026
39	6/18/11	Koyukuk mainstem*	N	Yukon	65.665	-156.384	0.713651	0.000036	0.00155	0.000065	0.770	0.033	0.439	0.0193	0.101	0.0049	0.014	0.0004	0.0153	7.6	4.34	0.0020

*field triplicate

REFERENCES

- Anderson, S.P., 2007. Biogeochemistry of glacial landscape systems. *Annual Review of Earth and Planetary Sciences*, 35: 375-399.
- Anderson, S.P., Drever, J.I., Frost, C.D., Holden, P., 2000. Chemical weathering in the foreland of a retreating glacier. *Geochimica Et Cosmochimica Acta*, 64(7): 1173-1189.
- Arth, J.G., 1994. Isotopic composition of the igneous rocks of Alaska. In: Plafker, G., Berg, H.C. (Ed.), *The Geology of Alaska*. Geological Society of America, The Geology of North America, Boulder, Colorado.
- Arth, J.G. et al., 1989a. Remarkable Isotopic and Trace-Element Trends in Potassic through Sodic Cretaceous Plutons of the Yukon-Koyukuk Basin, Alaska, and the Nature of the Lithosphere beneath the Koyukuk Terrane. *Journal of Geophysical Research-Solid Earth and Planets*, 94(B11): 15957-15968.
- Arth, J.G., Zmuda, C.C., Foley, N.K., Criss, R.E., 1989b. Isotopic and Trace-Element Variations in the Ruby Batholith, Alaska, and the Nature of the Deep Crust beneath the Ruby and Angayucham Terranes. *Journal of Geophysical Research-Solid Earth and Planets*, 94(B11): 15941-15955.
- Barnett-Johnson, R., Pearson, T.E., Ramos, F.C., Grimes, C.B., MacFarlane, R.B., 2008. Tracking natal origins of salmon using isotopes, otoliths, and landscape geology. *Limnology and Oceanography*, 53(4): 1633-1642.
- Barnett-Johnson, R., Ramos, F.C., Grimes, C.B., MacFarlane, R.B., 2005. Validation of Sr isotopes in otoliths by laser ablation multicollector inductively coupled plasma mass spectrometry (LA-MC-ICPMS): opening avenues in fisheries science applications. *Canadian Journal of Fisheries and Aquatic Sciences*, 62(11): 2425-2430.

- Barnett-Johnson, R., Teel, D.J., Casillas, E., 2010. Genetic and otolith isotopic markers identify salmon populations in the Columbia River at broad and fine geographic scales. *Environmental Biology of Fishes*, 89(3-4): 533-546.
- Bataille, C.P., et al. in revision. A geostatistical framework to predict strontium isotope variations in Alaska Rivers. *Chemical Geology*.
- Bataille, C.P., Bowen, G.J., 2012. Mapping Sr-87/Sr-86 variations in bedrock and water for large scale provenance studies. *Chemical Geology*, 304: 39-52.
- Bataille, C.P., Laffoon, J., Bowen, G.J., 2013. Mapping multiple source effects on the strontium isotopic signatures of ecosystems from the circum-Caribbean region. *Ecosphere*, 3(12):118.
- Beard, B.L., Johnson, C.M., 2000. Strontium isotope composition of skeletal material can determine the birth place and geographic mobility of humans and animals. *Journal of Forensic Sciences*, 45(5): 1049-1061.
- Beikman, H.M., 1980. Geologic Map of Alaska. U.S. Geological Survey, 1 sheet, scale 1:2,500,000.
- Bentley, R.A., 2006. Strontium Isotopes from the Earth to the Archaeological Skeleton: A Review. *Journal of Archaeological Method and Theory*, 13(3): 135-187.
- Blum, J.D., Blum, A.E., Davis, T.E., Dillon, J.T., 1987. Petrology of Cogenetic Silica-Saturated and Silica-Oversaturated Plutonic Rocks in the Ruby Geanticline of North-Central Alaska. *Canadian Journal of Earth Sciences*, 24(1): 159-169.
- Blum, J.D., Erel, Y., 2003. Radiogenic Isotopes in Weathering and Hydrology. In: Drever, J.I., Executive Editors: Holland, H.D., Turekian, K.K. (Eds.), *Treatise on Geochemistry*. Elsevier, pp. 365-392.

- Bradley, D.C. et al., 2007. Detrital zircon geochronology of some Neoproterozoic to Triassic rocks in interior Alaska. In: Ridgeway, K.D., Trop, J.M., Glen, J.M.G., O'Neill, J.M. (Eds.), Tectonic Growth of a Collisional Continental Margin: Crustal Evolution of Southern Alaska. Geological Society of America, Boulder, CO, pp. 155-189.
- Britton, K., Grimes, V., Dau, J., Richards, M.P., 2009. Reconstructing faunal migrations using intra-tooth sampling and strontium and oxygen isotope analyses: a case study of modern caribou (*Rangifer tarandus granti*). *Journal of Archaeological Science*, 36(5): 1163-1172.
- Britton, K. et al., 2011. Strontium isotope evidence for migration in late Pleistocene Rangifer: Implications for Neanderthal hunting strategies at the Middle Palaeolithic site of Jonzac, France. *Journal of Human Evolution*, 61(2): 176-185.
- Capo, R.C., Stewart, B.W., Chadwick, O.A., 1998. Strontium isotopes as tracers of ecosystem processes: theory and methods. *Geoderma*, 82(1-3): 197-225.
- Chesson, L.A. et al., 2012. Strontium isotopes in tap water from the coterminous USA. *Ecosphere*, 3(7).
- Colpron, M., Nelson, J.L., Murphy, D.C., 2007. Northern Cordilleran terranes and their interactions through time. *GSA Today*, 17(4/5).
- Cowan, D.S., 2003. Revisiting the Baranof-Leech River hypothesis for early Tertiary coastwise transport of the Chugach-Prince William terrane. *Earth and Planetary Science Letters*, 213(3-4): 463-475.
- Douglas, T.A., Blum, J.D., Guo, L.D., Keller, K., Gleason, J.D., 2013. Hydrogeochemistry of seasonal flow regimes in the Chena River, a subarctic watershed draining discontinuous permafrost in interior Alaska (USA). *Chemical Geology*, 335: 48-62.

- Edmond, J.M., 1992. Himalayan Tectonics, Weathering Processes, and the Strontium Isotope Record in Marine Limestones. *Science*, 258(5088): 1594-1597.
- Edmond, J.M., Palmer, M.R., Measures, C.I., Grant, B., Stallard, R.F., 1995. The Fluvial Geochemistry and Denudation Rate of the Guayana Shield in Venezuela, Colombia, and Brazil. *Geochimica Et Cosmochimica Acta*, 59(16): 3301-3325.
- Ehrlich, S., Gavrieli, I., Dor, L.B., Halicz, L., 2001. Direct high-precision measurements of the Sr-87/Sr-86 isotope ratio in natural water, carbonates and related materials by multiple collector inductively coupled plasma mass spectrometry (MC-ICP-MS). *Journal of Analytical Atomic Spectrometry*, 16(12): 1389-1392.
- Fisher, M.A., Pellerin, L., Nokleberg, W.J., Ratchkovski, N.A., Glen, J.M.G., 2007. Crustal structure of the Alaska Range orogen and Denali fault along the Richardson Highway. In: Ridgeway, K.D., Trop, J.M., Glen, J.M.G., O'Neill, J.M. (Eds.), *Tectonic Growth of a Collisional Continental Margin: Crustal Evolution of Southern Alaska Geological Society of America*, Boulder, Colorado, pp. 43-53.
- Frei, K.M., Frei, R., 2011. The geographic distribution of strontium isotopes in Danish surface waters - A base for provenance studies in archaeology, hydrology and agriculture. *Applied Geochemistry*, 26(3): 325-340.
- Gaillardet, J., Dupre, B., Louvat, P., Allegre, C.J., 1999. Global silicate weathering and CO₂ consumption rates deduced from the chemistry of large rivers. *Chemical Geology*, 159(1-4): 3-30.
- Gaillardet, J., Millot, R., Dupre, B., 2003. Chemical denudation rates of the western Canadian orogenic belt: the Stikine terrane. *Chemical Geology*, 201(3-4): 257-279.

- Goldfarb, R.J. et al., 2004. The Late Cretaceous donlin creek gold deposit, southwestern Alaska: Controls on epizonal ore formation. *Economic Geology and the Bulletin of the Society of Economic Geologists*, 99(4): 643-671.
- Goldfarb, R.J., Farmer, G.L., Cieutat, B.A., Meier, A.L., 1997. Major-element, traceelement, and strontium-isotope systematic of natural waters in the Fairbanks Mining District: constraints from local geology. U.S. Geological Survey Professional Paper 1614: 12.
- Harris, N.R., Sisson, V.B., Wright, J.E., Pavlis, T.L., 1996. Evidence for Eocene mafic underplating during fore-arc intrusive activity, eastern Chugach Mountains, Alaska. *Geology*, 24(3): 263-266.
- Hobson, K.A., 1999. Tracing origins and migration of wildlife using stable isotopes: a review. *Oecologia*, 120(3): 314-326.
- Hobson, K.A., Barnett-Johnson, R., Cerling, T.E., 2010. Using Isoscapes to Track Animal Migration. In: West, J.B., Bowen, G.J., Dawson, T.E., Tu, K.P. (Eds.), *Isoscapes: Understanding movement, pattern, and process on Earth through isotope mapping*. Springer Science.
- Hodell, D.A., Quinn, R.L., Brenner, M., Kamenov, G., 2004. Spatial variation of strontium isotopes (Sr-87/Sr-86) in the Maya region: a tool for tracking ancient human migration. *Journal of Archaeological Science*, 31(5): 585-601.
- Hoppe, K.A., Koch, P.L., 2007. Reconstructing the migration patterns of late Pleistocene mammals from northern Florida, USA. *Quaternary Research*, 68(3): 347-352.
- Hoppe, K.A., Koch, P.L., Carlson, R.W., Webb, S.D., 1999. Tracking mammoths and mastodons: Reconstruction of migratory behavior using strontium isotope ratios. *Geology*, 27(5): 439-442.

- Huh, Y., Edmond, J.M., 1999. The fluvial geochemistry of the rivers of Eastern Siberia: III. Tributaries of the Lena and Anabar draining the basement terrain of the Siberian Craton and the Trans-Baikal Highlands. *Geochimica Et Cosmochimica Acta*, 63(7-8): 967-987.
- Ingram, B.L., Weber, P.K., 1999. Salmon origin in California's Sacramento-San Joaquin river system as determined by otolith strontium isotopic composition. *Geology*, 27(9): 851-854.
- Keller, K., Blum, J.D., Kling, G.W., 2007. Geochemistry of soils and streams on surfaces of varying ages in arctic Alaska. *Arctic Antarctic and Alpine Research*, 39(1): 84-98.
- Keller, K., Blum, J.D., Kling, G.W., 2010. Stream geochemistry as an indicator of increasing permafrost thaw depth in an arctic watershed. *Chemical Geology*, 273(1-2): 76-81.
- Kennedy, B.P., Blum, J.D., Folt, C.L., Nislow, K.H., 2000. Using natural strontium isotopic signatures as fish markers: methodology and application. *Canadian Journal of Fisheries and Aquatic Sciences*, 57(11): 2280-2292.
- Kennedy, B.P., Folt, C.L., Blum, J.D., Chamberlain, C.P., 1997. Natural isotope markers in salmon. *Nature*, 387(6635): 766-767.
- Kennedy, B.P., Klaue, A., Blum, J.D., Folt, C.L., Nislow, K.H., 2002. Reconstructing the lives of fish using Sr isotopes in otoliths. *Canadian Journal of Fisheries and Aquatic Sciences*, 59(6): 925-929.
- Koch, P.L. et al., 1992. Sr Isotopic Composition of Hydroxyapatite from Recent and Fossil Salmon - the Record of Lifetime Migration and Diagenesis. *Earth and Planetary Science Letters*, 108(4): 277-287.
- Mackey, G.N., Fernandez, D.P., 2011. High throughput Sr isotope analysis using an automated column chemistry system., American Geophysical Union, San Francisco, California.

- Meybeck, M., 1986. Composition Chimique Naturelle Des Ruisseaux Non Pollués En France. Bulletin De La Société Géologique, 39: 3-77.
- Miller, J.A., 2011. Life history variation in upper Columbia River Chinook salmon (*Oncorhynchus tshawytscha*): a comparison using modern and similar to 500-year-old archaeological otoliths (vol 68, pg 603, 2011). Canadian Journal of Fisheries and Aquatic Sciences, 68(5): 953-953.
- Miller, J.A., Kent, A.J.R., 2009. The determination of maternal run time in juvenile Chinook salmon (*Oncorhynchus tshawytscha*) based on Sr/Ca and Sr-87/Sr-86 within otolith cores. Fisheries Research, 95(2-3): 373-378.
- Miller, M.L. et al., 2007. The restricted Gemuk Group: A Triassic to Lower Cretaceous succession in southwestern Alaska. In: Ridgeway, K.D., Trop, J.M., Glen, J.M.G., O'Neill, J.M. (Eds.), Tectonic Growth of a Collisional Continental Margin: Crustal Evolution of Southern Alaska Geological Society of America, Boulder, CO.
- Millot, R., Gaillardet, J., Dupre, B., Allegre, C.J., 2003. Northern latitude chemical weathering rates: Clues from the Mackenzie River Basin, Canada. Geochimica Et Cosmochimica Acta, 67(7): 1305-1329.
- Moore, T.E., Mull, G., 2013. Geology of the Brooks Range and North Slope. In: Nokleberg, W.J., Fisher, M.A., M. Schmidt, R.A., Nokleberg, W.J., Page, R.A. (Eds.), Alaskan Geological and Geophysical Transect American Geophysical Union, Washington, D. C.
- Muhlfeld, C.C., Thorrold, S.R., McMahon, T.E., Marotz, B., 2012. Estimating westslope cutthroat trout (*Oncorhynchus clarkii lewisi*) movements in a river network using strontium isoscapes (vol 69, pg 906, 2012). Canadian Journal of Fisheries and Aquatic Sciences, 69(6): 1129-1130.

- Nelson, J.L., et al. 2006. Paleozoic tectonic and metallogenetic evolution of pericratonic terranes in Yukon, northern British Columbia and eastern Alaska. In: Colpron, M., Nelson, J.L. (Eds.), *Paleozoic Evolution and Metallogeny of Pericratonic Terranes at the Ancient Pacific Margin of North America, Canadian and Alaskan Cordillera*. Geological Association of Canada, pp. 323-360.
- Newberry, R.J., et al. 1996. Preliminary geologic map of the Fairbanks Mining District, Alaska. In: *Surveys, ADGG*. (Editor). Alaska Division of Geological and Geophysical Surveys Public Data File 96-16, Alaska Division of Geological and Geophysical Surveys Public Data File 96-16, pp. 2.
- Outridge, P.M., Chenery, S.R., Babaluk, J.A., Reist, J.D., 2002. Analysis of geological Sr isotope markers in fish otoliths with subannual resolution using laser ablation-multicollector-ICP-mass spectrometry. *Environmental Geology*, 42(8): 891-899.
- Palmer, M.R., Edmond, J.M., 1992. Controls over the Strontium Isotope Composition of River Water. *Geochimica Et Cosmochimica Acta*, 56(5): 2099-2111.
- Peucker-Ehrenbrink, B., Miller, M.W., 2003. Quantitative bedrock geology of Alaska and Canada. *Geochemistry Geophysics Geosystems*, 4(4):8005.
- Potter, B.A., Irish, J.D., Reuther, J.D., Gelvin-Reymiller, C., Holliday, V.T., 2011. A Terminal Pleistocene Child Cremation and Residential Structure from Eastern Beringia. *Science*, 331(6020): 1058-1062.
- Quade, J., English, N., DeCelles, P.G., 2003. Silicate versus carbonate weathering in the Himalaya: a comparison of the Arun and Seti River watersheds. *Chemical Geology*, 202(3-4): 275-296.

- Radloff, F.G.T., Mucina, L., Bond, W.J., le Roux, P.J., 2010. Strontium isotope analyses of large herbivore habitat use in the Cape Fynbos region of South Africa. *Oecologia*, 164(2): 567-578.
- Sellick, M.J., Kyser, T.K., Wunder, M.B., Chipley, D., Norris, D.R., 2009. Geographic Variation of Strontium and Hydrogen Isotopes in Avian Tissue: Implications for Tracking Migration and Dispersal. *Plos One*, 4(3): e4735.
- Shields, G., Veizer, J., 2002. Precambrian marine carbonate isotope database: Version 1.1. *Geochemistry Geophysics Geosystems*, 3(6): 1525-2027.
- Steiger, R.H., Jager, E., 1977. Subcommittee on Geochronology: Convention on the use of decay constants in Geo- and Cosmochronology. *Earth and Planetary Science Letters*, 36: 359-362.
- Stewart, B.W., Capo, R.C., Chadwick, O.A., 1998. Quantitative strontium isotope models for weathering, pedogenesis and biogeochemical cycling. *Geoderma*, 82(1-3): 173-195.
- Till, A.B., Harris, A.G., Wardlaw, B.R., Mullen, M., 2007. Upper Triassic continental margin strata of the central Alaska Range: Implications for paleogeographic reconstruction, Tectonic Growth of a Collisional Continental Margin: Crustal Evolution of Southern Alaska. Geological Society of America, Boulder, Colorado, pp. 191-205.
- Trop, J.M., Ridgeway, K.D., 2007. Mesozoic and Cenozoic tectonic growth of southern Alaska: A sedimentary basin perspective. In: Ridgeway, K.D., Trop, J.M., Glen, J.M.G, O'Neill, J.M. (Ed.), Tectonic Growth of a Collisional Continental Margin: Crustal Evolution of Southern Alaska. Geological Society of America, Boulder, Colorado, pp. 55-94.
- Wadleigh, M.A., Veizer, J., Brooks, C., 1985. Strontium and Its Isotopes in Canadian Rivers - Fluxes and Global Implications. *Geochimica Et Cosmochimica Acta*, 49(8): 1727-1736.

- Wahrhaftig, C., 1965. Physiographic Divisions of Alaska. U.S. Geological Survey Professional Paper, 482.
- Walther, B.D., Thorrold, S.R., Olney, J.E., 2008. Geochemical signatures in otoliths record natal origins of American shad. *Transactions of the American Fisheries Society*, 137(1): 57-69.
- Wilson, F.H., et al. 2006. Reconnaissance bedrock geologic map for the northern Alaska Peninsula area, southwest Alaska. U.S. Geological Survey Open-File Report, 2006-1303.
- Wilson, F.H., Coonrad, W.L., 2005. The Togiak-Tikchik Complex of southwest Alaska, a replacement for the Gemuk Group: Stratigraphic nomenclature that has outlived its time. In: SIR-2005-5019, U.S.G.S.S.I.R. (Editor).
- Wilson, F.H., et al. 1998. Geologic map of Central (Interior) Alaska. U.S. Geological Survey Open-File Report, 98-133: 86.
- Wilson, F.H., Hults, C.P., Shew, N., Labay, K.A., 2008. Digital data for Geology of the Prince William Sound and Kenai Peninsula region, Alaska. U.S. Geological Survey Open-File Report, 2008-1002.
- Woodhead, J., Swearer, S., Hergta, J., Maasa, R., 2005. *In situ* Sr-isotope analysis of carbonates by LA-MC-ICP-MS: interference corrections, high spatial resolution and an example from otolith studies. *Journal of Analytical Atomic Spectrometry*, 20(1): 22-27.

APPENDIX 1.1

$^{87}\text{Sr}/^{86}\text{Sr}$ ratio analyses

The University of Utah ICPMS laboratory has developed an introduction system to purify Sr for $^{87}\text{Sr}/^{86}\text{Sr}$ ratio analyses of aqueous solutions using an inline chromatographic column packed with a crown ether resin (Eichrom's Sr Resin ®), providing high throughput and

accuracy (Mackey and Fernandez, 2011). Prior to isotopic analyses of water from each river, the Sr concentration was determined using an ICPMS (described below, section 3.3). Isotopic run sequences were ordered starting with samples containing lowest concentrations of Sr to progressively higher concentrations. By not running samples with low concentrations directly after samples with high concentrations, potential memory effects in the column were minimized. Samples with relatively high Sr concentrations were diluted with MilliQ water within a range of 40-290 ppb. No sample in this study required evaporative concentration of Sr content. Each sample and standard analysis was preceded by a rinse and blank analysis (4 M BDH Aristar Plus HNO₃), which act to purge the column of residual Sr present prior to each analysis and apply a blank correction. Prior to analyses, water samples were acidified to 4 M HNO₃. During sample uptake the motive force is a vacuum, which transports a set volume of the 4 M HNO₃ sample into a 2 mL coiled PTFE tube (called the loop), which is upstream of the column. Once the set volume of sample is present in the loop, the motive force switches to a peri-pump and the sample is transferred into a column filled with Sr-specific crown ether resin (Eichrom). At high HNO₃ concentrations (≥ 4 M) the crown ether resin has a much higher affinity for Sr than other alkali and alkali earth metals (e.g. Rb), whereas at low HNO₃ concentrations (0.04 M) Sr is eluted from the resin (Horwitz et al., 1992). Thus the column serves to purify the Sr and minimize the ⁸⁷Rb isobaric interference on ⁸⁷Sr. Following Sr purification, the Sr is eluted from the column using a 0.04 M HNO₃ solution directly into the MC-ICPMS. The net result of the column chromatography is the purification and concentration of Sr, which increases the precision and accuracy of the resulting isotopic analysis.

Hyperbolic mixing line carbonate and silicate end-members (EMs)

We assumed a carbonate end-member based on Phanerozoic marine carbonates, which have fairly well constrained X/Na and $^{87}\text{Sr}/^{86}\text{Sr}$ ratios (Burke et al., 1982; Edmond, 1992; Elderfield and Schultz, 1996). The $^{87}\text{Sr}/^{86}\text{Sr}$ ratios of Phanerozoic carbonate vary between 0.707-0.709 (Shields and Vezier, 2002); we use 0.708.

X/Na ratios of Sil EM1-EM5 are reported in Gaillardet et al. (1999) (and references therein) in a worldwide weathering study and include carbonate, granitoid and basaltic EMs (Table 1.1). The Sil EM1 X/Na ratios estimated a basaltic silicate end-member, derived from Gaillardet (1999) of surface waters originating from pure basaltic terrains, which had higher X/Na (>Sil EM2-5) ratios due to mafic compositions (Gaillardet et al., 1999, and references therein). Sil EM2–EM5 X/Na ratios characterized granitoid silicates, which we assumed to have the same X/Na ratio, but different $^{87}\text{Sr}/^{86}\text{Sr}$ ratios.

$^{87}\text{Sr}/^{86}\text{Sr}$ values for the Silicates EM1-EM5 spanned a large range and were derived from the literature. The basaltic silicate end-member (Sil EM1) has the lowest $^{87}\text{Sr}/^{86}\text{Sr}$ value (0.703), and was a realistic value for young mafic igneous and sedimentary rocks emplaced in a tectonic setting such as southern AK, especially in the Alaskan-Aleutian Range (AAR) in the southwest, where much of the material is likely mantle-derived (Arth, 1994; Cowan, 2003; Harris et al., 1996). The $^{87}\text{Sr}/^{86}\text{Sr}$ value used for Sil EM2 (0.707) was a realistic value for weathering of Mesozoic-age felsic igneous and sedimentary rocks in a tectonic setting such as southern AK. This value is corroborated by $^{87}\text{Sr}/^{86}\text{Sr}$ ratios of intrusive rocks in this region (Arth, 1994), compositions of waters in similar geologic settings, such as the Sierra Nevada Batholith (Barnett-Johnson et al., 2008; Ingram and Weber, 1999), and in a study of rivers draining west from the plutonic rocks of the Western Canadian Cordillera (Gaillardet et al., 1999).

The set of possible radiogenic end-members we tested (Sil EM3, EM4, EM5) derive from Keller et al. (2007) for pure silicate catchments in the eastern Brooks Range (Sil EM3 $^{87}\text{Sr}/^{86}\text{Sr}=0.719$); from groundwaters near Fairbanks, AK (Goldfarb et al., 1997) (Sil EM4 $^{87}\text{Sr}/^{86}\text{Sr}=0.732$), also used by Douglas et al. (2013), which estimated the average composition of silicate weathering in groundwaters near Fairbanks, AK in the Yukon-Tanana Uplands (YTU); and a possible very radiogenic end-member, which was observed in the Eastern Canadian Cordillera by Millot et al. (2003) and used to explain very radiogenic streams in this region (Sil EM5 $^{87}\text{Sr}/^{86}\text{Sr} = 0.78$).

References:

- Arth, J.G., 1994. Isotopic composition of the igneous rocks of Alaska. In: Plafker, G., Berg, H.C. (Ed.), *The Geology of Alaska*. Geological Society of America, The Geology of North America, Boulder, Colorado.
- Barnett-Johnson, R., Pearson, T.E., Ramos, F.C., Grimes, C.B., MacFarlane, R.B., 2008. Tracking natal origins of salmon using isotopes, otoliths, and landscape geology. *Limnology and Oceanography*, 53(4): 1633-1642.
- Burke, W.H., et al. 1982. Variation of seawater $^{87}\text{Sr}/^{86}\text{Sr}$ throughout Phanerozoic time. *Geology*, 10: 516-519.
- Cowan, D.S., 2003. Revisiting the Baranof-Leech River hypothesis for early Tertiary coastwise transport of the Chugach-Prince William terrane. *Earth and Planetary Science Letters*, 213(3-4): 463-475.
- Douglas, T.A., Blum, J.D., Guo, L.D., Keller, K., Gleason, J.D., 2013. Hydrogeochemistry of seasonal flow regimes in the Chena River, a subarctic watershed draining discontinuous

- permafrost in interior Alaska (USA). *Chemical Geology*, 335: 48-62.
- Edmond, J.M., 1992. Himalayan Tectonics, Weathering Processes, and the Strontium Isotope Record in Marine Limestones. *Science*, 258(5088): 1594-1597.
- Elderfield, H., Schultz, A., 1996. Mid-ocean ridge hydrothermal fluxes and the chemical composition of the ocean. *Annual Review of Earth and Planetary Sciences*, 24: 191-224.
- Gaillardet, J., Dupre, B., Louvat, P., Allegre, C.J., 1999. Global silicate weathering and CO₂ consumption rates deduced from the chemistry of large rivers. *Chemical Geology*, 159(1-4): 3-30.
- Goldfarb, R.J., Farmer, G.L., Cieutat, B.A., Meier, A.L., 1997. Major-element, traceelement, and strontium-isotope systematic of natural waters in the Fairbanks Mining District: constraints from local geology. U.S. Geological Survey Professional Paper 1614: 12.
- Harris, N.R., Sisson, V.B., Wright, J.E., Pavlis, T.L., 1996. Evidence for Eocene mafic underplating during fore-arc intrusive activity, eastern Chugach Mountains, Alaska. *Geology*, 24(3): 263-266.
- Horwitz, E.P., Chiarizia, R., Dietz, M.L., 1992. A Novel Strontium-Selective Extraction Chromatographic Resin. *Solvent Extraction and Ion Exchange*, 10(2).
- Ingram, B.L., Weber, P.K., 1999. Salmon origin in California's Sacramento-San Joaquin river system as determined by otolith strontium isotopic composition. *Geology*, 27(9): 851-854.
- Keller, K., Blum, J.D., Kling, G.W., 2007. Geochemistry of soils and streams on surfaces of varying ages in arctic Alaska. *Arctic Antarctic and Alpine Research*, 39(1): 84-98.

Mackey, G.N., Fernandez, D.P. 2011. High throughput Sr isotope analysis using an automated column chemistry system. Abstract V31B-2525 presented at 2011 Fall Meeting, AGU, San Francisco, California., 5-9 Dec.

Millot, R., Gaillardet, J., Dupre, B., Allegre, C.J., 2003. Northern latitude chemical weathering rates: Clues from the Mackenzie River Basin, Canada. *Geochimica Et Cosmochimica Acta*, 67(7): 1305-1329.

Shields, G., Veizer, J., 2002. Precambrian marine carbonate isotope database: Version 1.1. *Geochemistry Geophysics Geosystems*, 3.

CHAPTER 2:

Strontium isotopes in otoliths of a non-migratory fish (slimy sculpin): implications for aquatic provenance studies¹

ABSTRACT

Heterogeneity in $^{87}\text{Sr}/^{86}\text{Sr}$ ratios of river-dissolved strontium (Sr) across geologically diverse environments is a useful tool for investigating provenance, connectivity and movement patterns of various organisms and materials. Evaluation of site-specific $^{87}\text{Sr}/^{86}\text{Sr}$ temporal variability throughout study regions is a prerequisite for ecological provenance research, but the dynamics driving temporal variability are not well understood, or accurately predictable. We used the time-keeping properties of otoliths from non-migratory slimy sculpin (*Cottus cognatus*) to evaluate multi-scale $^{87}\text{Sr}/^{86}\text{Sr}$ temporal variability of river waters throughout the Nushagak River, a large (34,700 km²) watershed in Alaska, USA. Slimy sculpin otoliths incorporated site-specific temporal variation at sub-annual resolution and recorded on the order of 0.0001 changes in the $^{87}\text{Sr}/^{86}\text{Sr}$ ratio. $^{87}\text{Sr}/^{86}\text{Sr}$ profiles of slimy sculpin collected in tributaries and main-stem channels of the upper watershed indicated that these regions were temporally stable, whereas the Lower Nushagak River exhibited some spatio-temporal variability. This study illustrates how the behavioral ecology of a non-migratory organism can be used to evaluate sub-annual $^{87}\text{Sr}/^{86}\text{Sr}$ temporal variability and has broad implications for provenance studies employing this tracer.

¹ Brennan, S.R., Fernandez, D.P., Zimmerman, C.E., Cerling, T.E., Brown, R.J., Wooller, M.J. In review. Strontium isotopes in otoliths of a non-migratory fish (slimy sculpin.): implications for aquatic provenance studies. *Geochimica et Cosmochimica Acta*.

INTRODUCTION

Strontium (Sr) isotope ratios ($^{87}\text{Sr}/^{86}\text{Sr}$) recorded in fish otoliths (the auditory structure of teleost fish) are a useful tool in fish ecology research aiming to decipher natal origins (Barnett-Johnson et al. 2008, Walther et al. 2008, Zimmerman et al. 2013) and movement patterns (Hegg et al. 2013, Kennedy et al. 2002, Miller 2011). Their utility stems from biological, geological and hydrological properties of the $^{87}\text{Sr}/^{86}\text{Sr}$ ratio and the inherent time-keeping properties of otoliths, which incrementally grow via metabolically inert concentric rings of CaCO_3 throughout a fish's life (Campana 1999). $^{87}\text{Sr}/^{86}\text{Sr}$ ratios do not fractionate during formation of biogenic materials (Capo et al. 1998) and their variability across landscapes scales with geologic heterogeneity (Bataille and Bowen 2012). In aquatic ecosystems, Sr dissolved in surface waters is ultimately derived from bedrock, but is moderated by differential chemical weathering rates of rock-minerals within a catchment (Blum and Erel 2003, Horton et al. 1999). Sr in fish otoliths is primarily derived from ambient water (Kalish 1990, Walther and Thorrold 2006), and directly reflects environmental isotopic conditions experienced by individual fish (Barnett-Johnson et al. 2008, Muhlfeld et al. 2012). Thus, otoliths represent unadulterated records of a fish's entire environmental $^{87}\text{Sr}/^{86}\text{Sr}$ history.

To employ $^{87}\text{Sr}/^{86}\text{Sr}$ ratios in provenance or migration studies, baseline data characterizing $^{87}\text{Sr}/^{86}\text{Sr}$ ratios throughout a region of interest is imperative, both with respect to time and space. Sampling campaigns are often limited to spatially explicit 'snap-shots' in time across large geographic regions (Hegg et al. 2013, Ingram and Weber 1999, Walther et al. 2008) making it difficult to fully evaluate site-specific temporal variation throughout a study area. Though some studies document temporal stability in $^{87}\text{Sr}/^{86}\text{Sr}$ ratios on seasonal (Kennedy et al. 2000, Muhlfeld et al. 2012) and inter-annual scales (Barnett-Johnson et al. 2008), temporal

stability is certainly not a rule. The dynamics driving temporal variation are not well understood or accurately predictable, and variability can occur on sub-seasonal (Douglas et al. 2013), seasonal (Douglas et al. 2013, Semhi et al. 2000, Voss et al. 2014), inter-annual (Keller et al. 2010, Walther and Thorrold 2009) and decadal scales (Keller et al. 2010). Additionally, the inherent growth structure of incremental metabolically inert biogenic materials (e.g., otoliths and teeth) and turnover rates of metabolically active tissues (e.g., blood, muscle, and bone) dictate the different time frames and scales being recorded (Hobson et al. 2010), further emphasizing the need to evaluate temporal variability and its influence on $^{87}\text{Sr}/^{86}\text{Sr}$ ratios observed within materials. Thus, evaluating time-dependent variation remains a persistent problem for aquatic provenance studies employing $^{87}\text{Sr}/^{86}\text{Sr}$ ratios and solutions remain elusive.

We approached this problem by using otoliths from slimy sculpin, *Cottus cognatus*, to evaluate site-specific temporal variability of $^{87}\text{Sr}/^{86}\text{Sr}$ ratios in river waters throughout a large (34,700 km²) and remote watershed in southwest Alaska (AK), the Nushagak River. Slimy sculpin have been identified as a useful sentinel species for monitoring temporal changes in freshwater ecosystems, because of their overall sedentary life history, wide distribution and high abundance (Cunjak et al. 2005, Gray et al. 2004, Gray and Munkittrick 2005). They are benthic, non-migratory, small-bodied fish lacking a swim bladder, and generally live for 5 - 7 years (Gray et al. 2004). Previous tagging studies have documented home ranges for freshwater sculpin species to be < 50 m, including slimy sculpin (Morgan and Ringler 1992) and the closely related mottled sculpin, *Cottus bairdii* (Breen et al. 2009, Hill and Grossman 1987, Petty and Grossman 2004). Approximate annual median displacements of slimy sculpin have been reported to be < 20 m (Cunjak et al. 2005, Gray 2003, Schmetterling and Adams 2004). This long-term site fidelity,

which defines slimy sculpin behavioral ecology, makes it a good study organism of site-specific time-dependent environmental variation.

The overall objective of this work was to produce a spatially and temporally robust $^{87}\text{Sr}/^{86}\text{Sr}$ ratio baseline dataset throughout the Nushagak River. We hypothesized that otoliths from slimy sculpin could be used to discern time-dependent site-specific variation in $^{87}\text{Sr}/^{86}\text{Sr}$ ratios of river waters throughout this watershed. The coupling of slimy sculpin behavioral ecology, otolith growth structure, and biogeochemical properties of $^{87}\text{Sr}/^{86}\text{Sr}$ ratios may be useful in evaluating multi-scale temporal variability in rivers and has implications for provenance research, including natal origin and movement pattern studies of fish. For example, development of a robust $^{87}\text{Sr}/^{86}\text{Sr}$ -baseline dataset for the Nushagak River has implications for research and management of Pacific salmon resources in southwest AK.

Study area

The Nushagak River is one of nine major river systems flowing into Bristol Bay, which collectively make up the largest wild sockeye salmon (*Oncorhynchus nerka*) fishery in the world (Schindler et al. 2010). The Nushagak River also produces the third largest Chinook salmon (*O. tshawytscha*) run in Western AK, as well as abundant runs of coho (*O. kisutch*), pink (*O. gorbuscha*) and chum (*O. keta*) salmon (Jones et al. 2013). Because Pacific salmon populations have shown dramatic changes in returns into Western AK rivers in recent periods (ADF&G 2013, Krueger et al. 2009) and salmon population structure is hierarchical, tools need to be developed for accurately identifying natal origins and tracking movement patterns of salmon in Western AK.

Geographically, the Nushagak River watershed is defined by regional geological heterogeneity. Namely, young mafic rocks from the Cenozoic Alaskan-Aleutian Range (AAR) arc dominate rock materials of eastern tributaries (Wilson et al. 2006). Cretaceous meta-sedimentary rocks, in part derived from old continental sources (Goldfarb et al. 2004), underlie central tributaries draining the Nushagak Hills and Taylor Mountains (Wilson et al. 2006). Western tributaries drain the Cretaceous to Paleozoic Togiak-Tikchik complex of the Ahklun Mountain Province (AMP), which is a complex assemblage of oceanic sedimentary deposits derived in part from continental and arc-related materials (Wilson and Coonrad 2005). The geochemical weathering regime is dominated by silicate weathering (Brennan et al. in revision), as such its isotopic end-members are likely to be defined by the older felsic materials of the Nushagak Hills and Togiak-Tikchik complex and the younger mafic rocks of the AAR.

METHODS

Otolith and water collection and preparation

Slimy sculpin (n = 49 total) were trapped at 22 locations in the Nushagak River using minnow traps and a pole-seine (4.6 m long, 3.2 mm mesh size). Locations ranged from headwater tributaries to the lower main-stem river (Figure 2.1). Water samples were taken from every major tributary and from the main-stem river channels upstream and downstream of tributary confluences (n = 95 waters samples). All trapping of slimy sculpin, and almost all water sampling, occurred in the autumn of 2011, 2012 and 2013 (collected under Alaska Department of Fish and Game Fish Resource Permit numbers SF2011-236, SF2012-231, and SF2013-255; and Institutional Animal Care and Use Committee protocol number 178401-11).

Sagittal otoliths were dissected from each individual in the field and stored dry in polypropylene centrifuge tubes until sectioning and isotope analysis. Sectioning and mounting methods were similar to those outlined by Donohoe and Zimmerman (2010). Otoliths from individuals trapped in 2011 were sectioned in the transverse plane. Otolith pairs from each fish captured in 2012 were both sectioned, one in the frontal plane and one in the transverse plane. Due to the inherent morphology of slimy sculpin otoliths (the frontal growth axis is ~ 2 times longer than transverse), sectioning in the frontal plane affords approximately twice the spatial resolution (and therefore temporal resolution). All otoliths collected in 2013 were sectioned in the frontal axis. Prior to isotopic analyses, otoliths were sonicated for five minutes in MilliQ water, rinsed, and dried in a laminar flow hood. All otoliths were aged by counting annuli via a consensus score of two and in general yielded an accuracy of approximately ± 1 year. We considered annuli to be the translucent region discerned in reflected light (Figure 2.2). Distances to annuli were measured using AmScope MT1 software. Fish populations of Subpolar (45° - 70° N) regions accrete opaque regions between May and October months (Beckman and Wilson 1995). As such, we have considered the translucent region of slimy sculpin otoliths to represent winter growth, whereas the opaque region to represent summer and autumn growth. Hereafter, we refer to the translucent and opaque regions as winter and summer, respectively.

Water samples ($n = 95$) were collected upstream of the collector in acid-washed 250 ml low-density polyethylene (LDPE) wide-mouth bottles. Within 48 hours of collection, each sample was filtered through a $0.45 \mu\text{m}$ Luer-lock syringe filter (polypropylene membrane) using a 50 cm^3 polypropylene syringe into a clean acid-washed 125 ml LDPE narrow-mouth bottle. Within a maximum of 16 days of collection, samples were acidified with 2 ml ultra pure

concentrated HNO₃ (BDH Aristar Ultra). To evaluate consistency in field collection methods 11 of these samples were collected as field triplicates.

Water and otolith ⁸⁷Sr/⁸⁶Sr ratio analyses

Water samples were analyzed for ⁸⁷Sr/⁸⁶Sr ratios at the University of Utah, Department of Geology and Geophysics, ICPMS laboratory using multi-collector inductively coupled plasma mass spectrometry (MC-ICPMS) (Thermo Scientific, High Resolution NEPTUNE, Bremen, Germany). The University of Utah laboratory has developed an introduction system to purify Sr for ⁸⁷Sr/⁸⁶Sr ratio analyses of aqueous solutions using an inline chromatographic column packed with a crown ether resin (Eichrom's Sr Resin ®) (Mackey and Fernandez 2011). During analyses reported herein, we determined the ⁸⁷Sr/⁸⁶Sr ratio of the standard reference material SRM987 (NIST; www.nist.gov) (n = 81) to be 0.710297 ± 0.000051 (weighted 2σ standard error (SE)). Precision of field triplicate analyses ranged from ± 0.000046 - 0.00000047 (weighted 2σ SE) (Table 2.1).

⁸⁷Sr/⁸⁶Sr ratios of slimy sculpin otoliths were measured from core to edge of each individual otolith using laser ablation (LA) (193 nm Excimer Laser, Photo Machines) MC-ICPMS at the University of Utah, Department of Geology and Geophysics ICPMS laboratory. LA transects were implemented using a 31.4 μm diameter circle with a pulse rate of 10 Hz, a scan rate of 2 μm/second, and a laser energy of 45 %. Counts per second (cps) of ⁸⁸Sr, ⁸⁷Sr, ⁸⁶Sr, ⁸⁵Rb and ⁸³Kr were measured at the Faraday cups with an integration time of 0.524 seconds, corresponding to one cycle. Setting the integration time to be approximately half of the scan speed was extra insurance against aliasing and also allowed for error estimation along transects.

Prior to each ablation, transect background intensities (V) of each isotope were measured for 120 cycles and the mean was used as a blank correction during sample analyses.

Analytical accuracy of LA data was evaluated by measuring the $^{87}\text{Sr}/^{86}\text{Sr}$ ratio of a modern marine shell during and after each LA run ($n = 7$ runs; 8 to 12 shell analyses/run). LA run-means of shell ratios ranged from 0.70922 - 0.70928 with an average weighted 2σ SE of ± 0.00012 . Consistency between LA versus solution methods was evaluated by digesting the same marine shell using HNO_3 and HF acids and determined the $^{87}\text{Sr}/^{86}\text{Sr}$ ratio using same solution methods described above to be 0.70921 ± 0.000024 (2σ SD), which was indistinguishable from LA data. During solution analysis of the shell the SRM987 $^{87}\text{Sr}/^{86}\text{Sr}$ ratio was 0.710296 ± 0.0000096 (2σ SD), which was consistent with the SRM987 ratio measured during water analyses described above. The solution ratio of marine shell was also determined to be within the accepted range of the modern global marine value for seawater, biogenic and abiogenic carbonates (0.70918 ± 0.00006 2σ SD), a value determined by adjusting to SRM987 = 0.71025 (Faure and Mensing 2005). We therefore applied no standard-correction to otolith data. $^{87}\text{Sr}/^{86}\text{Sr}$ ratios of otoliths and river water samples were corrected for mass bias using an exponential law and for isobaric interference.

Statistical analyses

We used Generalized Additive Models (GAMs) to analyze the $^{87}\text{Sr}/^{86}\text{Sr}$ ratio variation from the core to edge of slimy sculpin otoliths. GAMs are a non-parametric extension of Generalized Linear Models, but do not require an a priori response function (e.g., linear or quadratic) to be known and take the general form:

Equation 1: $y_i = f(x_i) + \varepsilon$,

where y is a response variable, x is a covariate (distance from otolith core), ε is the random error term and $f(x_i)$ is the smooth function. Using the MGCV package in R (<http://cran.r-project.org/>), we fitted thin-plate regression spline functions to the LA data using penalized iteratively re-weighted least squares (P-IRLS) to maximize goodness-of-fit and general cross validation (GCV) methods to minimize over-fitting (e.g., a penalty on ‘wiggleness’) (Wood 2006). P-IRLS and GCV algorithms of GAMs essentially ‘back-fit’ a series of polynomial spline functions, which are additive, to $^{87}\text{Sr}/^{86}\text{Sr}$ LA data (Wood 2006). To guard against prematurely over-penalizing any GAM, we scaled the basis dimension (k) (the maximum effective degrees of freedom (edf) allowable) with the number of data (N) in each profile by $k = 10N^{2/9}$ (Kim and Gu 2004). The edf is related to the number of splines used to fit each GAM (Wood 2006). Additionally, we estimated Bayesian confidence intervals along each $^{87}\text{Sr}/^{86}\text{Sr}$ fitted GAM profile and approximate p-values (Wood 2006). We interpreted only those p-values $\ll 0.05$ (i.e., $p < 0.01$) as significant at the 95 % confidence level, because GAM p-values are inherently approximate and can be as little as half the correct value when the null is true (Wood 2006).

We used logistic regression to investigate if the distance between a sampling site and the nearest isotopically different environment (i.e., a confluence) and age-of-fish were significant predictors of whether we observed $^{87}\text{Sr}/^{86}\text{Sr}$ variation along the growth axis of otoliths. To this end, we executed a targeted supplementary sampling campaign of two adjacent lower river tributaries, Kokwok River and Klutuk Creek, where slimy sculpin were trapped every ~ 0.2 km starting at the confluence with the main stem Nushagak River to ~ 1 km upstream within

respective tributaries. All distances between sampling sites and the nearest isotopically different confluence were measured along main flow paths using waypoints taken by a Global Positioning Device (GPS) and Google Earth. The nearest isotopically different confluence was discerned using locations of the spatially explicit $^{87}\text{Sr}/^{86}\text{Sr}$ water data reported herein. For tributary sites, this distance was always between a sampling site and the confluence of main-stem channel. For sites on main-stem channels this distance was the nearest upstream or downstream isotopically different tributary. We considered two environments to be isotopically different if the difference was > 0.0004 between $^{87}\text{Sr}/^{86}\text{Sr}$ ratios. The binary response for logistic regression was whether the GAM of an individual indicated a significant p-value (i.e., GAM, $p \ll 0.05 = 1$; $p > 0.01 = 0$).

RESULTS

Spatially explicit water $^{87}\text{Sr}/^{86}\text{Sr}$ ratios

$^{87}\text{Sr}/^{86}\text{Sr}$ ratios of 98 river waters from the Nushagak watershed ranged from 0.70425 - 0.70910 (Table 2.1). The isotopic end-members are tributaries of the Alaskan-Aleutian Range (AAR) and the Nushagak Hills/Taylor Mountains (Figure 2.1). The lower Nushagak River exhibits intermediate ratios (autumn samples, 0.70653 - 0.70735), because it is an isotopic mixture of the three major tributaries: the Nuyakuk (0.70786), Upper Nushagak (0.70835) and Mulchatna Rivers (0.70572). At one site in the lower river (near village of New Stuyahok), we measured the $^{87}\text{Sr}/^{86}\text{Sr}$ ratio during each autumn of 2011- 2013 (0.70653 - 0.70662 \pm 0.00005 2σ SD) and one measurement during the spring freshet just after ice-breakup in 2013 (0.70603).

This difference reflects a shift (~ 0.0005) in the $^{87}\text{Sr}/^{86}\text{Sr}$ ratio towards the Mulchatna River ratios during the freshet.

GAMs and $^{87}\text{Sr}/^{86}\text{Sr}$ ratio otolith profiles

We assumed a Gaussian distribution for GAMs and inspection of residuals and normal probability plots indicated that this assumption was reasonable for slimy sculpin LA data. Durbin-Watson tests of some GAM-fitted isotope profiles (i.e., only GAM profiles with $p \ll 0.05$) indicated that autocorrelation was problematic (Durbin-Watson test, $p < 0.05$). However, inspection of diagnostic autocorrelation and partial autocorrelation function (ACF and PACF, respectively) plots indicated no distinct correlation structure and lags indicative of significant autocorrelation at the 95 % confidence level were only slightly significant showing very small correlation coefficients (e.g., < 0.08). As such, we consider any autocorrelation present in ablation transects reported herein to be inconsequential to variances and overall $^{87}\text{Sr}/^{86}\text{Sr}$ patterns found in slimy sculpin otoliths.

Twenty-four of 49 slimy sculpin indicated distance along the otolith growth axis was a significant predictor of $^{87}\text{Sr}/^{86}\text{Sr}$ variation (GAM $p \ll 0.05$), whereas 25 indicated distance along otolith growth axis was not a significant predictor (GAM $p > 0.01$) at the 95 % confidence level (Table 2.2). GAMs with $p > 0.01$ approximated flat linear lines (edf ~ 1), whereas sculpin with $p \ll 0.05$ showed highly variable and irregular $^{87}\text{Sr}/^{86}\text{Sr}$ profiles (edf > 5). GAMs approximating flat lines (GAM $p > 0.01$) were observed in sculpin trapped from tributaries (e.g., sites Ca, St, Kt, Ck, Kw and Kl) and the main channels of the three largest branches of the Nushagak River (e.g., M2, Ny, UN1 and UN2). GAMs with $p \ll 0.05$, showing highly variable $^{87}\text{Sr}/^{86}\text{Sr}$ profiles, were

observed from sculpin trapped in the Lower Nushagak River (sites LN1 and LN2), but also in some tributaries (Table 2.2).

Superimposing the locations of otolith annuli onto LA-MC-ICPMS $^{87}\text{Sr}/^{86}\text{Sr}$ data and fitted GAMs (Figure 2.2) indicated $^{87}\text{Sr}/^{86}\text{Sr}$ variability was resolvable between years and within summer seasons, but not during winter due to attenuated otolith growth during this period. Winter growth periods had mean otolith distances of 50 ± 4 and 36 ± 4 μm (2σ SE) in frontal and transverse sections, respectively (Figure 2.2). Summer growth regions had mean otolith distances of 220 ± 18 and 99 ± 14 μm (2σ SE) in frontal and transverse sections, respectively (Figure 2.2). Additionally, because otolith growth also attenuated as slimy sculpin aged, we observed the temporal (and spatial) resolution of LA-MC-ICPMS data and respective fitted GAMs to decrease within individual sculpin otoliths with increasing age (Figure 2.2).

Both frontal and transverse sectioning methods of the same individuals yielded very similar $^{87}\text{Sr}/^{86}\text{Sr}$ profiles and fitted GAMs (Figure 2.3). Frontal sections, however, yielded GAMs with higher precision (95 % Bayesian confidence intervals are approximately half of transverse, Figure 2.3) and resolution (isotope transitions in frontal section are notably sharper). The results with respect to GAM p-values (Table 2.2) and overall $^{87}\text{Sr}/^{86}\text{Sr}$ life-history patterns however, were identical for both sectioning methods (Figure 2.3).

Tributaries and main-stem river channels upstream of Mulchatna River confluence

At some tributary sites (e.g., M1, St, Ny, Kl and Kw), we observed conflicting $^{87}\text{Sr}/^{86}\text{Sr}$ profiles between individuals trapped from the same site (Figure 2.4), where one slimy sculpin indicated $p \ll 0.05$ and another indicated $p > 0.01$. This result was observed only at trapping

sites that were proximal to nearby confluences or water masses of differing $^{87}\text{Sr}/^{86}\text{Sr}$ composition. Additionally, heterogeneous profiles ($p \ll 0.05$) from tributary sites indicated that deviations from the expected $^{87}\text{Sr}/^{86}\text{Sr}$ ratio of river water at a trapping site were always shifted towards the $^{87}\text{Sr}/^{86}\text{Sr}$ ratio of the nearest neighboring river environment (Figure 2.4).

The distance separating a trapping site and the nearest isotopically different environment was a significant (Distance, $p = 0.007$, Figure 2.5) predictor of the occurrence of slimy sculpin GAM profiles with $p \ll 0.05$ (Table 2.3). Distance was ln-transformed prior to regression, because its distribution was right-skewed. The residual deviance of the logistic regression was 37.3 on 39 degrees of freedom; as such over-dispersion was not problematic. The probability of observing a $p \ll 0.05$ decreased by 0.39 for every km separating a trapping site and an isotopically different water mass. Age was not a significant predictor (logistic regression model including age-of-fish as a predictor, Age + Distance, $p > 0.05$) of the occurrence of slimy sculpin with GAM $p \ll 0.05$ (Table 2.3A). Slimy sculpin trapped in lower river sites were not included in logistic regression, because all but one individual trapped at LN1 and LN2 exhibited heterogeneous $^{87}\text{Sr}/^{86}\text{Sr}$ profiles ($p \ll 0.05$).

Kokwok River and Klutuk Creek exhibited different patterns with regard to the relationship between the distance separating a trapping site and the main Nushagak River channel and the occurrence of slimy sculpin with a GAM $p \ll 0.05$ (Figure 2.3, panel B). In the Kokwok River, all slimy sculpin trapped above site Kw2 (0.35 km above main river confluence) exhibited GAM profiles with $p > 0.01$ (Table 2.2). Contrastingly, in Klutuk Creek we observed some slimy sculpin with GAM $p \ll 0.05$ at sites K11 - K15, which reached up to 1.1 km upstream from confluence with the main-stem Nushagak River (Table 2.2).

Lower Nushagak River

Seven out of 8 slimy sculpin trapped at lower river sites (LN1 and LN2) (n = 4 per site) illustrated variable and irregular $^{87}\text{Sr}/^{86}\text{Sr}$ profiles ($p \ll 0.05$) (Figure 2.6). Inspection of superimposed annuli on isotope profiles indicated that sculpin trapped at the same site reflected asynchronous time-dependent patterns along respective otolith growth axes (Figure 2.6). Thus, the variation we observed in the Lower Nushagak River was at the scale of individuals, as well as between sites. All profiles exhibited $^{87}\text{Sr}/^{86}\text{Sr}$ ratios that vary between the isotopic composition of Mulchatna River and the most downstream point of the Upper Nushagak River (Nush_1_11) before its confluence with the Mulchatna River. Although the majority of each respective profile reflected lower river ratios downstream of this confluence, there were significant excursions towards these two isotopic end-members. Overall, heterogeneity was notably more apparent in sculpin from LN1, whereas sculpin from LN2 did not show the same magnitude or frequency of variation towards these end-member values. Additionally, it was apparent from lower river sites that changes in the 4th decimal of the $^{87}\text{Sr}/^{86}\text{Sr}$ ratio were discernable along the sculpin otolith growth axis. For example, the GAM of sculpin_26_13 trapped at LN2 (Figure 2.6D) showed a distinguishable shift during its 3rd summer of 0.70690 ± 0.00004 to 0.70704 ± 0.00004 (2σ SE), corresponding to a 0.00014 difference.

Individuals with marine influence in their otolith core

Four individuals had $^{87}\text{Sr}/^{86}\text{Sr}$ profiles that indicated Sr within the otolith core had an isotopic composition equivalent to marine waters (Figure 2.6C and Figure 2.8). The accepted global marine $^{87}\text{Sr}/^{86}\text{Sr}$ ratio is 0.70918, as adjusted to SRM987 $^{87}\text{Sr}/^{86}\text{Sr} = 0.71025$ (Faure and Mensing 2005) and 95 % confidence intervals of core values overlap this value (Figure 2.6C and

Figure 2.8⁶). Additionally, the ^{88}Sr intensity (V) within the otolith core is also > 2 times (~ 2.5 V) the intensity of regions distal of the core (~ 1 V) (Figure 2.8), strongly indicative of marine derivation (Kalish 1990, Zimmerman and Reeves 2002).

Autumn water versus overall life-long otolith $^{87}\text{Sr}/^{86}\text{Sr}$ ratios

Autumn water $^{87}\text{Sr}/^{86}\text{Sr}$ ratios were a significant predictor of the overall, long-term isotopic means of individual slimy sculpin otoliths (mean of each fish lifelong isotope profile, 2-7 years), which approximated a 1:1 relationship ($p \ll 0.001$, slope = 0.992, $r^2 = 0.999$) (Figure 2.7, Table 2.4). The regression only incorporated sculpin with $p \ll 0.05$ from tributary and main-stem trapping sites upstream of Mulchatna River confluence with Lower Nushagak River (Figure 2.7). The overall sculpin otolith means from site LN1 plot at higher $^{87}\text{Sr}/^{86}\text{Sr}$ ratios from what is predicted by water ratios at this site. Additionally, sculpin means from LN1 exhibited greater variation than sculpin from LN2. These findings supported results from individual profiles (Figure 2.6), that the downstream lower river site (LN2) was less heterogeneous than the upstream site (LN1).

DISCUSSION

Evaluating temporal variation of $^{87}\text{Sr}/^{86}\text{Sr}$ ratios of river waters throughout a targeted study region is a prerequisite for all studies aiming to use this tracer to discern natal origins or movement patterns of aquatic animals (Elsdon et al. 2008, Hobson et al. 2010). Sampling campaigns limited to singular time-slices are inherently flawed, because i) there may be multi-scale temporal variation occurring within the environment, and ii) how this variation is recorded

into particular biogenic materials used to discern movement patterns and natal sources influences interpretation of $^{87}\text{Sr}/^{86}\text{Sr}$ data. The driving forces of time-dependent variation in $^{87}\text{Sr}/^{86}\text{Sr}$ ratios are not well understood or accurately predictable, and robust evaluation of temporal variation via intensive sampling campaigns is economically prohibitive and logistically impractical. This problem is especially profound in remote Sub-arctic and Arctic regions defined by extreme seasonality, such as the Bristol Bay region of AK, where there are no roads and access is limited to small boats and aircraft. We approached this problem within the Nushagak River watershed by employing the time-keeping properties of otoliths from a non-migratory sedentary fish, the slimy sculpin. Slimy sculpin are often used as indicator species of site-specific variation, because of life-long high site fidelity (Cunjak et al. 2005, Gray et al. 2004, Gray and Munkittrick 2005). Overall, we found that slimy sculpin are a viable organism for evaluating site-specific variation in $^{87}\text{Sr}/^{86}\text{Sr}$ ratios through time.

Elucidating hydrogeochemical temporal variability and micro-movements

Slimy sculpin otoliths were able to determine temporal variability at sub-annual scales and micro-movements at < 1 km spatial scales. We interpret the variation exhibited by some sculpin (those with GAM $p \ll 0.05$) in tributary sites and main river channels upstream of Mulchatna River confluence to be due to behavioral variation in micro-movements (< 1.5 km) of individual sculpin and not to reflect site-specific variation through time. Three lines of evidence support this interpretation. Firstly, the distance separating a trapping site and an isotopically different environment was a strong predictor of whether significant variation (GAM $p \ll 0.05$) was observed along the growth axis of sculpin otoliths. Secondly, all significant shifts observed along sculpin otoliths equilibrated with, or approached, the isotopic composition of proximal

environments. Finally, conflicting results were observed from individuals trapped at the same site (i.e., a flat-line profile alongside a variable profile). As such, we interpret the stable (i.e., flat-line) $^{87}\text{Sr}/^{86}\text{Sr}$ profiles to reflect site-specific time-dependent variation, of which there was no evidence at the sub-annual scale, as recorded along the growth axis of otoliths.

We found movements of slimy sculpin of ~ 1.5 km, a distance much greater than previously reported in tagging studies of both slimy (Cunjak et al. 2005, Schmetterling and Adams 2004) and closely related mottled sculpin (Breen et al. 2009, Hill and Grossman 1987, Petty and Grossman 2004). In tagging studies, the largest movement documented for a freshwater sculpin species was 511 m by the mottled sculpin (Breen et al. 2009). However, these studies were not able to rule out the possibility of larger movements because un-recaptured sculpin may have moved out of respective study areas during observation periods (Breen et al. 2009, Cunjak et al. 2005, Schmetterling and Adams 2004). Additionally, slimy sculpin from Iliamna Lake, AK were hypothesized to migrate on the order of kilometers to sockeye salmon spawning grounds during the 20 day spawning period (Foote and Brown 1998). Our $^{87}\text{Sr}/^{86}\text{Sr}$ life-history profiles for slimy sculpin from the Nushagak River indicated movements that are behaviorally deliberate, occurring in both upstream and downstream directions. For example, slimy sculpin caught in Klutuk Creek indicated variable movement patterns back-and-forth between Klutuk and the Lower Nushagak River, which, depending on trapping site, was a distance ranging from 0.2 - 1.1 km (e.g., Figure 2.2). Our findings highlight the utility of using $^{87}\text{Sr}/^{86}\text{Sr}$ ratios to elucidate small-scale movements of even sedentary fish in isotopically heterogeneous environments.

Sculpin home ranges were different between individuals trapped at the same site (e.g., conflicting results between sculpin caught at same site) and between tributary systems. The latter

was illustrated by Klutuk Creek and Kokwok River (see Figure 2.1), which exhibited different patterns (Table 2.2) with respect to the maximum distance where sculpin indicative of micro-movements between tributaries and the lower river were no longer observed (1.1 and 0.35 km respectively). The Kokwok River is larger, deeper and has a much lower gradient, whereas Klutuk Creek is smaller, shallower and has a higher gradient. Habitat differences could possibly be driving this variability and further investigation is warranted. Another driver of home range variability may be food resource availability as it relates to the spatial distribution in salmon spawning grounds and the temporally pulsed nature of the spawning season (Foote and Brown 1998).

Upstream watershed area and geochemical heterogeneity as drivers of temporal variability

$^{87}\text{Sr}/^{86}\text{Sr}$ ratios in river water

We found that the existence of site-specific temporal variability is related to intra-watershed geography (i.e., the amount of upstream area of a single location) and the corresponding spatial distribution of geochemical heterogeneity. For example, within the Nushagak watershed, we found sub-annual temporal stability in tributaries and main river channels above Mulchatna River confluence (see Figure 2.1). However, we found evidence of complex multi-scale spatio-temporal variability in the lower river. Thus, our results indicate that parameters such as: i) the amount of upstream area contributing to a single downstream point in a river network and ii) the corresponding existence of upstream geochemical heterogeneity can influence site-specific temporal variability in $^{87}\text{Sr}/^{86}\text{Sr}$ ratios.

In the lower river, heterogeneity was asynchronous within and between both sites among individuals and was notably more expressed at the upper river site (LN1) compared to the lower

river site (LN2). We interpret the difference in heterogeneity observed between LN1 and LN2 to imply a relative state of mixing between water originating from Mulchatna River and the Upper Nushagak River, whereby LN1 is less mixed compared to LN2. Our water data support this interpretation. Namely, waters collected at LN1 (~ 0.7065) were less radiogenic than waters collected at LN2 (~ 0.7070), while the only significant contributions of water to the Lower Nushagak River downstream of LN1 had $^{87}\text{Sr}/^{86}\text{Sr}$ ratios of ~ 0.7047 (Kokwok River and Klutuk Creek). Thus, both the lower-river water and sculpin data indicated that water mass fronts originating at the Mulchatna River confluence persists to at least ~ 40 km downstream. However, the water mass fronts were notably more eroded at LN2 versus LN1, as indicated by sculpin data from LN2, suggestive of a relatively mixed environment compared to LN1. The observation of asynchronicity between individuals at sites suggests behavioral variation in the micro-movements between individuals across isotopically distinct water-mass fronts present within the ambient environment. As such, the Lower Nushagak River is characterized by complex multi-scale spatio-temporal heterogeneity originating at the Mulchatna River confluence and persisting via a decreasing gradient to far distances downstream (~ 40 km).

Autumn water $^{87}\text{Sr}/^{86}\text{Sr}$ ratios as a predictor of life-long values observed in otoliths

Overall life-long sculpin otolith $^{87}\text{Sr}/^{86}\text{Sr}$ means from individuals ranging from 2 to 7 years old were accurately predictable using autumn $^{87}\text{Sr}/^{86}\text{Sr}$ water ratios, approaching a 1:1 relationship (Figure 2.7). Contributing to this result was the fact that winter growth rates in otoliths were substantially attenuated relative to the summer (Figures 2 - 4 and 6). Thus, overall computed $^{87}\text{Sr}/^{86}\text{Sr}$ means were weighted towards ambient water conditions characterizing summer and autumn when otoliths were growing ~ 4 times faster. Summer water sampling has

been shown to be a good predictor of $^{87}\text{Sr}/^{86}\text{Sr}$ ratios measured in the first summer growth region of Chinook salmon caught during different years in the California Central Valley (Barnett-Johnson et al. 2008, Ingram and Weber 1999).

Implications for natal origins and movement pattern studies

The extent to which slimy sculpin otoliths (or other fish species) accurately record time-dependent environmental variation changes seasonally and throughout a fish's life, due to otolith growth structure. The potential for integration (or 'blurring') of actual environmental signals was more pronounced in winter (low growth rate regions) versus summer (high growth rate regions) and later in life versus earlier (Figure 2.2 - 2.4 and 2.6). Working in concert with these morphological and physiologically driven time-integrations, sampling parameters such as laser beam size, scan speed and instrument integration time also played into apparent temporal resolution accessible via otoliths. These biological and sampling phenomena illustrate limitations and constraints of the method and should influence research design and hypothesis development for studies using $^{87}\text{Sr}/^{86}\text{Sr}$ ratios in otoliths to study natal origins, rearing and overall movement patterns of fish. For example, when employing LA transects perpendicular to the growth axis, discerning true winter versus summer time signals was markedly difficult, if not improbable using a $\sim 30\ \mu\text{m}$ beam size when winter growth regions were $\sim 50\ \mu\text{m}$ wide (e.g., Figures 2 - 4 and 6). While employing a LA transect parallel to growth axis within a winter region will yield a more accurate $^{87}\text{Sr}/^{86}\text{Sr}$ ratio corresponding to beam width (Hegg et al. 2013), it does not nullify the biological 'blurring' taking place within the otolith and beam width. These are important considerations when a study objective aims to discern over-wintering versus summer rearing grounds, particularly if baseline information hinges on water versus otolith measurements.

However, natal origins studies, particularly of Pacific salmon, often target the first summer growth period after yolk absorption of juvenile salmon (Barnett-Johnson et al. 2008, Hegg et al. 2013, Walther et al. 2008). Because this region was accreted when the fish and otoliths were growing fast, $^{87}\text{Sr}/^{86}\text{Sr}$ measurements in this region accurately reflected ambient environmental variation of this period, which was also ecologically meaningful to the natal origin question. Arguably, for salmon natal origin studies, the most important temporal scale to evaluate in terms of site-specific time-dependent variation in $^{87}\text{Sr}/^{86}\text{Sr}$ ratios is inter-annual variability, particularly of the summer in Subarctic and Arctic regions.

We have demonstrated that temporal variability is accurately evaluated with slimy sculpin otoliths on sub-annual scales. Based on our results from the Nushagak River, we suggest that successive generations of salmon (sockeye, coho and Chinook) produced in tributaries and in the main-stem river channels above Mulchatna River confluence will have consistent $^{87}\text{Sr}/^{86}\text{Sr}$ ratios within their first summer growth region. However, salmon produced in the main-stem river may have ratios falling anywhere between the envelope documented at sites LN1 and LN2, due to multi-scale spatio-temporal heterogeneity characterizing the lower river.

Marine-derived Sr in the core of four individuals

A surprising observation from our study was the potentially marine-derived Sr in the core of four individuals caught at sites LN1, K11 and K12 (Figure 2.6C and Figure 2.8). All individuals analyzed in this study, including these four, showed no indication of marine Sr in regions distal of core. We put forward two hypotheses that could account for this finding.

One hypothesis is that these core signals were maternally derived. Core material can be maternally derived, such as in salmon otoliths, as newly hatched fish use up their yolk (Kalish

1990, Zimmerman and Reeves 2002). If reproductively mature females formed their eggs either in the marine environment (e.g., adult salmon) or primarily using marine derived materials in a freshwater environment (e.g., a diet of spawned salmon eggs), then their eggs could have $^{87}\text{Sr}/^{86}\text{Sr}$ compositions similar to the global marine value (~ 0.70918). The former is highly unlikely, if not impossible, for purely freshwater resident slimy sculpin trapped > 60 km from marine water. Sr enters the blood stream of fishes via two competing pathways, the branchial membrane and intestinal lining (Campana 1999). Otolith Sr is primarily derived from ambient water (Farrell and Campana 1996, Walther and Thorrold 2006), except in core of some fish due to maternal influence, such as salmon (Kalish 1990). Thus, the latter would imply either: i) during egg formation mature female slimy sculpin partitioned diet-derived Sr and ambient-derived Sr into different materials (i.e., diet-Sr into eggs; ambient-Sr into otolith), or ii) during egg formation otolith growth was substantially attenuated such that the marine signal (temporarily composing blood plasma from seasonally available salmon eggs) was not detectable in the otolith. Slimy sculpin have eggs that are only 2.5 - 3 mm in diameter (Morrow 1980). Though relatively large for a small fish, further research is needed to validate whether slimy sculpin eggs are large enough to impart maternal signals into otolith cores of progeny. Further research is also needed to investigate whether mature female slimy sculpin with a marine diet form eggs with marine $^{87}\text{Sr}/^{86}\text{Sr}$ composition.

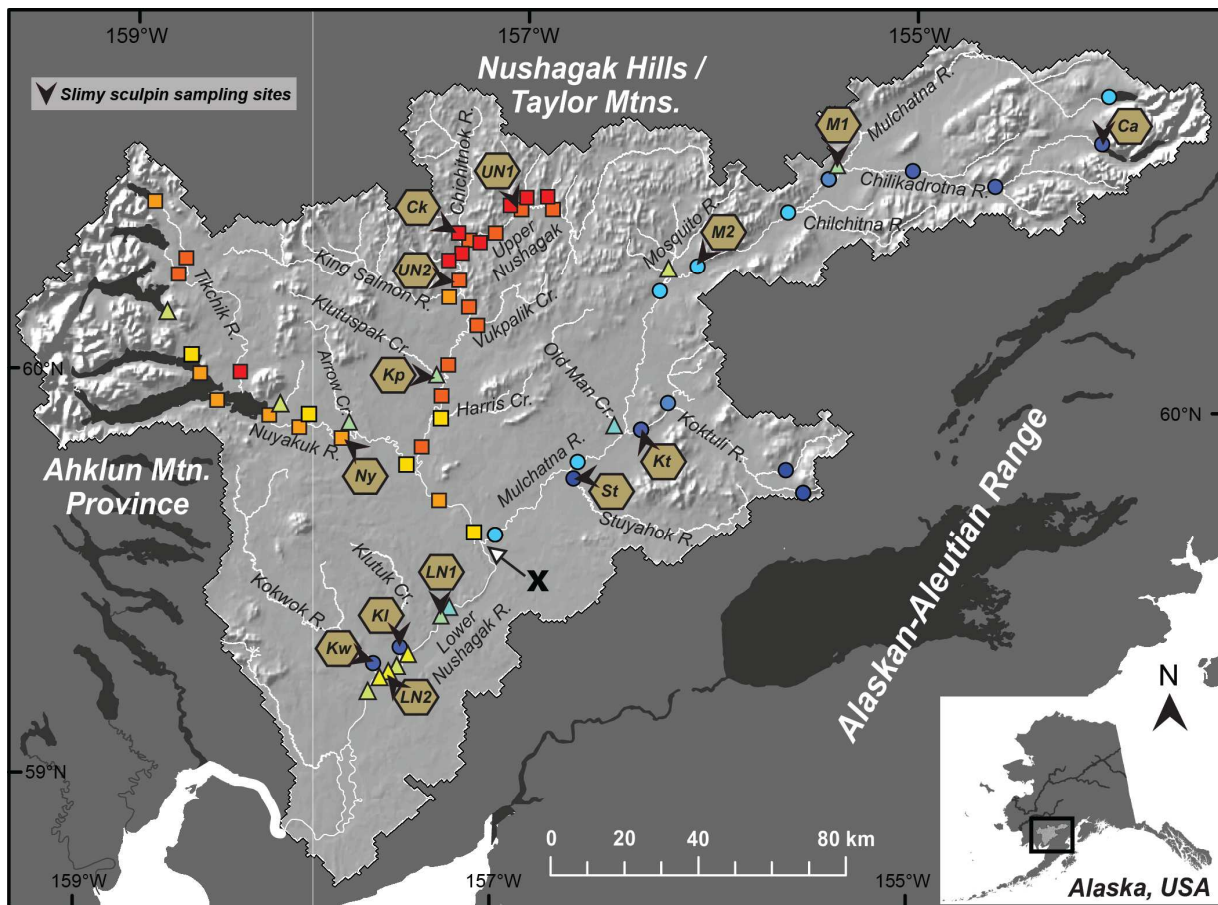
A second hypothesis is that these four individuals were coastrange sculpin (*Cottus aleuticus*). Coastrange sculpin exhibit an amphidromous life history, where hatched larvae are initially planktonic, drift downstream into an estuary, and then migrate back upstream into freshwater after adopting a benthic lifestyle (Brown et al. 1995, Morrow 1980). This hypothesis would require that these four individuals i) drifted as larvae into the estuarine environment

adopting a marine signal in otolith cores, ii) migrated back into freshwater before accreting otolith regions distal of core, and iii) continued migrating back upstream to trapping sites (site K11 and K12 > 60 km, and site LN1 > 78 km from estuary) over the course of their lives (6 - 7 years, Table 2.2). Coastrange sculpin have been found at distances < 80 km from the ocean in other systems and these upstream populations must have been recruited from the lower drainage (Brown et al. 1995). Because lower river trapping sites (K11, K12 and LN1) were within the habitat range where slimy and coastrange sculpin could overlap; and since these two sculpin species are very similar in appearance, further research is warranted.

CONCLUSION

We have demonstrated that otoliths from a non-migratory fish, which exhibits high spatial and temporal residency, can be used to evaluate $^{87}\text{Sr}/^{86}\text{Sr}$ temporal variability throughout large watersheds. Specifically, we showed that temporal variability in the $^{87}\text{Sr}/^{86}\text{Sr}$ ratio in slimy sculpin otoliths could be elucidated on sub-annual time scales and could record changes in the 4th decimal in the $^{87}\text{Sr}/^{86}\text{Sr}$ ratio. To ensure $^{87}\text{Sr}/^{86}\text{Sr}$ ratio otolith profiles are reflective of site-specific temporal variation we recommend trapping sites be > 2 km from confluences. However, even at closer distances (< 1 km), slimy sculpin exhibiting higher site fidelity can yield site-specific information due to variation in behavioral movement patterns between individuals. We also conclude that in addition to the presence of permafrost (Douglas et al. 2013) and glaciers (Anderson et al. 2000) within a watershed, parameters such as upstream area and corresponding upstream geochemical heterogeneity of a single point within a river network influence the existence of site-specific $^{87}\text{Sr}/^{86}\text{Sr}$ temporal variation. Finally, because of the wide geographic distribution and high abundance of slimy sculpin (Morrow 1980), we suggest that this general

research framework is a viable approach to evaluating $^{87}\text{Sr}/^{86}\text{Sr}$ temporal variability across North American watersheds at sub-annual time scales. As such, the findings of this research have broad implications for aquatic provenance studies using this tracer, especially in the remote regions of the Arctic and Subarctic.



River water $^{87}\text{Sr}/^{86}\text{Sr}$ ratios:	●	0.7042 - 0.7046	▲	0.7058 - 0.7062	■	0.7075 - 0.7079
	●	0.7046 - 0.7050	▲	0.7062 - 0.7067	■	0.7079 - 0.7083
	●	0.7050 - 0.7054	▲	0.7067 - 0.7071	■	0.7083 - 0.7087
	●	0.7054 - 0.7058	▲	0.7071 - 0.7075	■	0.7087 - 0.7091

Figure 2.1. Slimy sculpin sampling sites and $^{87}\text{Sr}/^{86}\text{Sr}$ ratios of river waters.

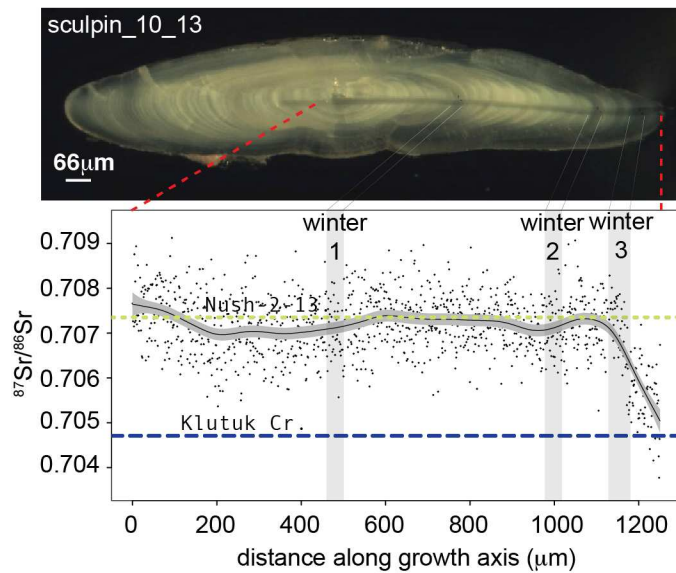


Figure 2.2. An example of a laser ablation transect along the growth axis of slimy sculpin otolith (top image; sculpin_10_13; site = K15) with annuli (vertical gray bars on bottom panel, translucent winter growth regions on top image) superimposed on data. On the otolith image (top panel) the winter region is translucent and the summer region is opaque. Black circles are raw $^{87}\text{Sr}/^{86}\text{Sr}$ ratios, each representing a 0.524 (sec) integration period. The solid black line and gray shading indicate the fitted GAM and 95 % Bayesian confidence intervals. Horizontal dotted lines indicate the $^{87}\text{Sr}/^{86}\text{Sr}$ of water at the trapping site (large blue dotted line) and nearby environment (small green dotted line).

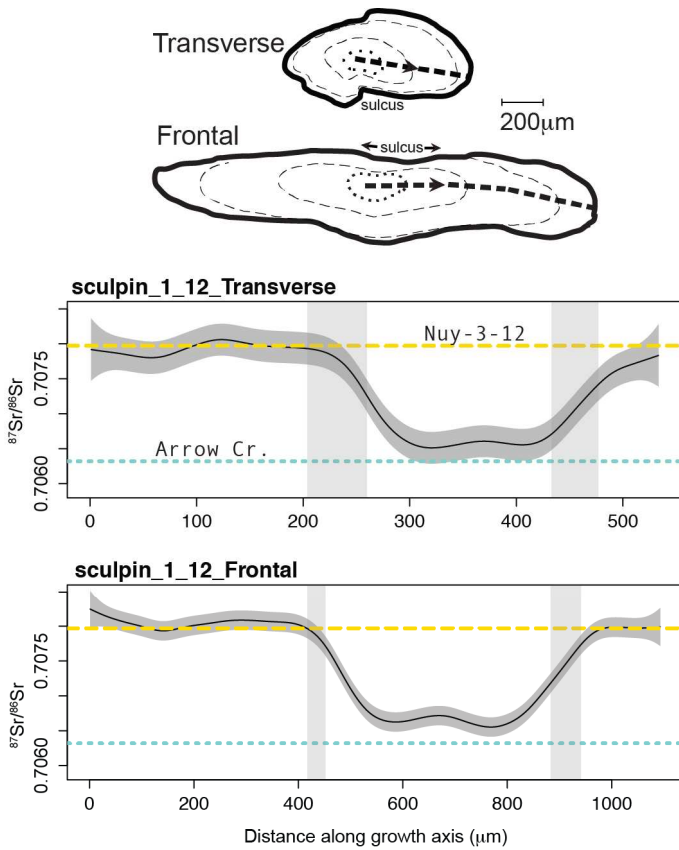


Figure 2.3. An example of a frontal versus transverse section of a slimy sculpin otolith (top images; sculpin_1_12, site = Ny) and respective laser ablation transects (large black dotted lines on images). The solid black line is the fitted GAM and the gray shading is the 95 % Bayesian confidence interval. Vertical gray bars denote the location of annuli (winter growth regions). Horizontal dotted lines indicate the $^{87}\text{Sr}/^{86}\text{Sr}$ of water at a trapping site (large yellow dotted line) and the nearby environments (small blue dotted line).

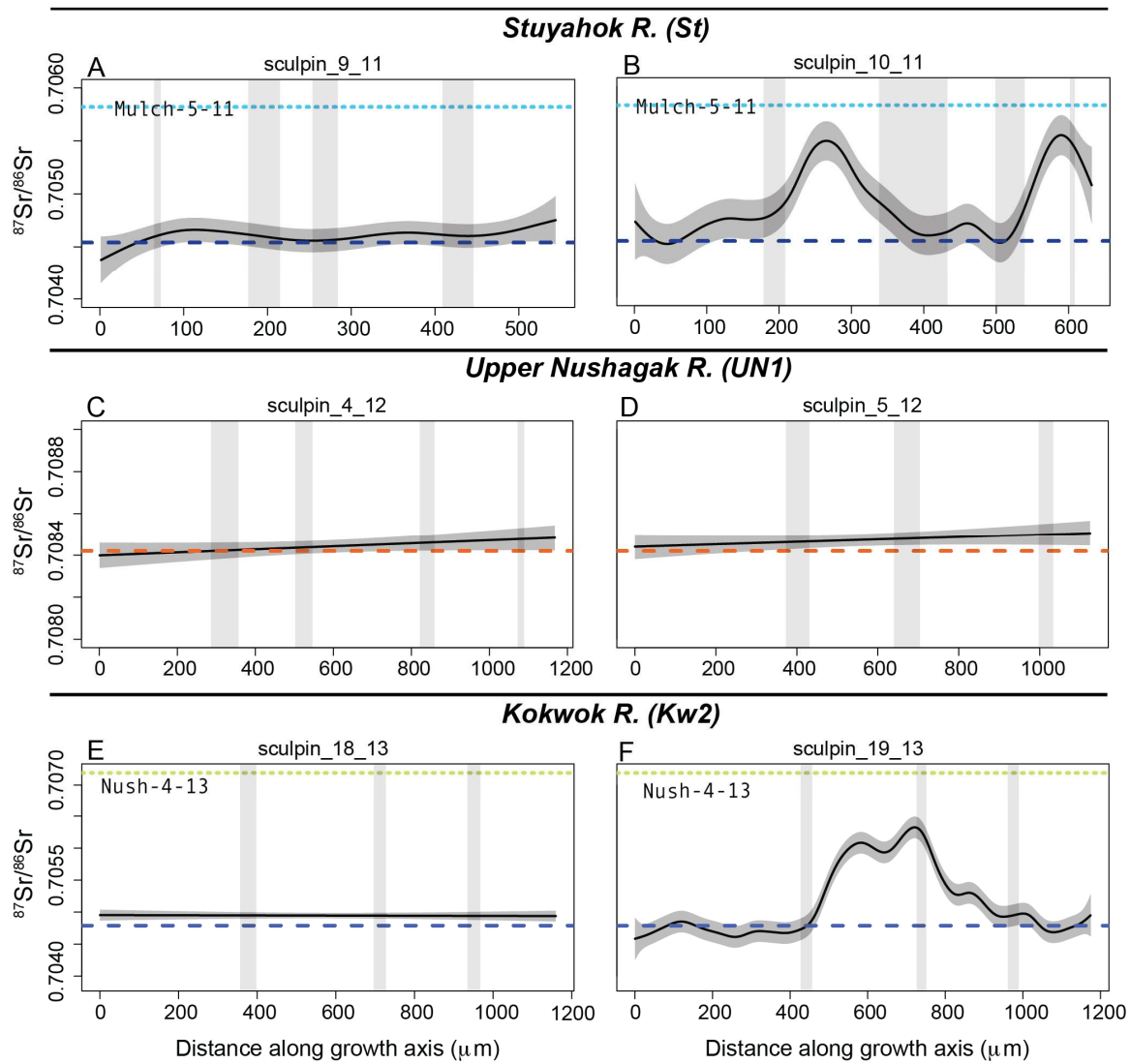


Figure 2.4. Examples of $^{87}\text{Sr}/^{86}\text{Sr}$ ratio profiles of slimy sculpin trapped in tributaries and main-stem river channels upstream of Mulchatna River confluence, including sites St (A and B), UN1 (C and D) and Kw2 (E and F). Sculpin from St and Kw2 are examples where conflicting $^{87}\text{Sr}/^{86}\text{Sr}$ ratio profiles were observed at the same trapping site, whereas sculpin from UN1 both show flat-line profiles. Vertical gray bars denote the location of annuli (winter growth regions). Horizontal dotted lines indicate the $^{87}\text{Sr}/^{86}\text{Sr}$ ratio of water at a trapping site (large dotted line) and the nearby environments (small dotted line). C and D do not have small dotted lines because these individuals exhibited site-fidelity.

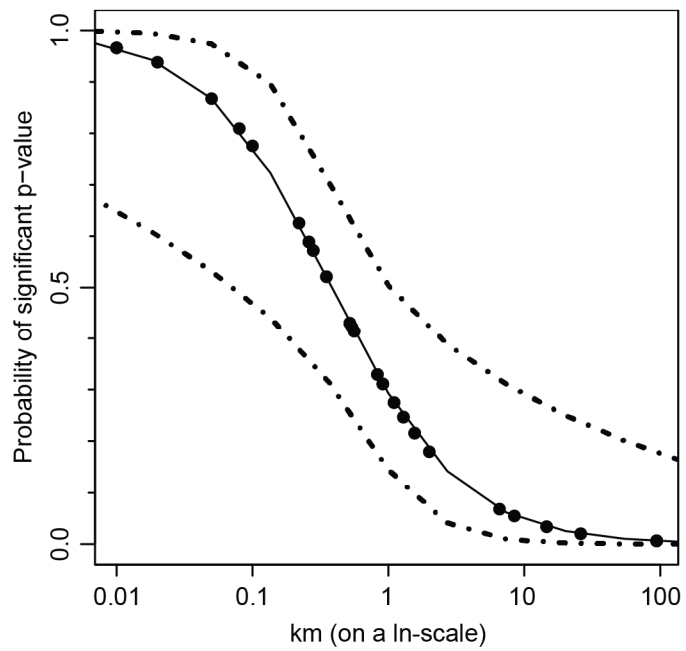


Figure 2.5. A logistic regression used to illustrate the probability of observing a variable $^{87}\text{Sr}/^{86}\text{Sr}$ ratio life-history profile (GAM $p \ll 0.05$) as a function of distance separating trapping site and nearest isotopically different environment. Dotted lines are 95 % confidence intervals of fitted logistic regression model.

Lower Nushagak slimy sculpin

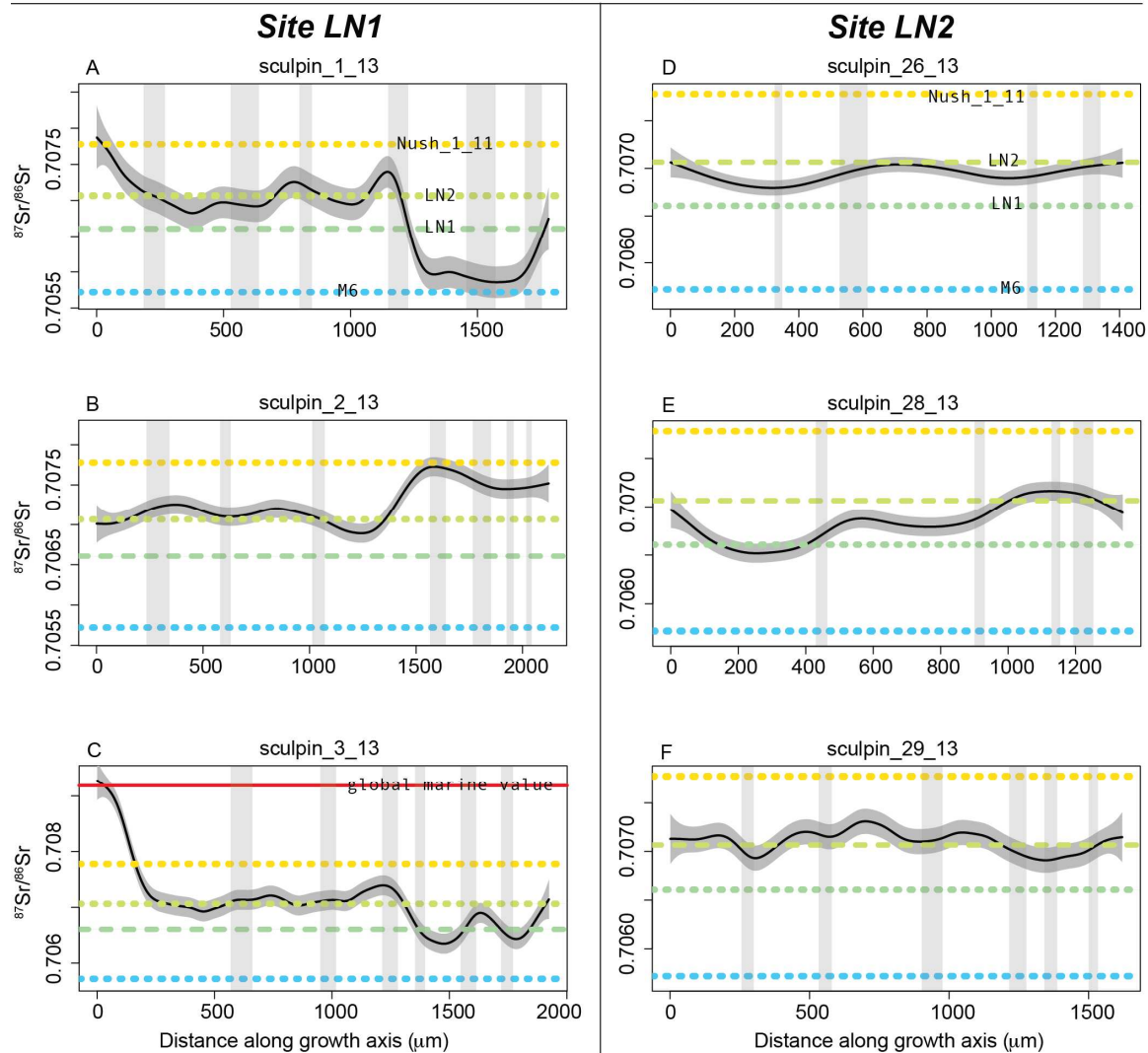


Figure 2.6. Examples of $^{87}\text{Sr}/^{86}\text{Sr}$ ratio profiles of slimy sculpin trapped in the lower river sites, LN1 and LN2. Vertical gray bars denote location of annuli (winter growth regions). Horizontal dotted lines (site names indicated on top panels and colors are consistent in each panel) indicate the $^{87}\text{Sr}/^{86}\text{Sr}$ ratio of water at a trapping site (large dotted line) and nearby environments (small dotted lines). Red line in panel C is global marine value (0.70918).

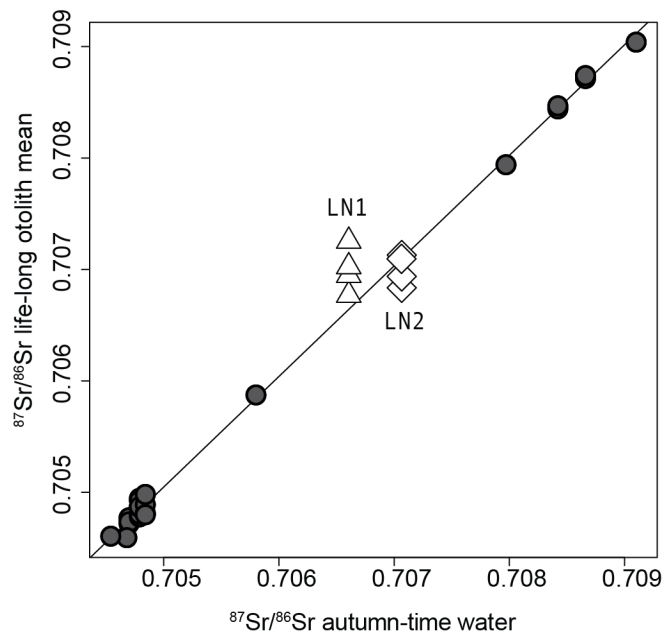


Figure 2.7. Autumn water values used to predict overall, long-term mean $^{87}\text{Sr}/^{86}\text{Sr}$ ratios of otoliths from 2 to 7 year old slimy sculpin. Large residuals from LN1 sculpin (open triangles) illustrate LN1's greater heterogeneity compared to sculpin from LN2 (open squares).

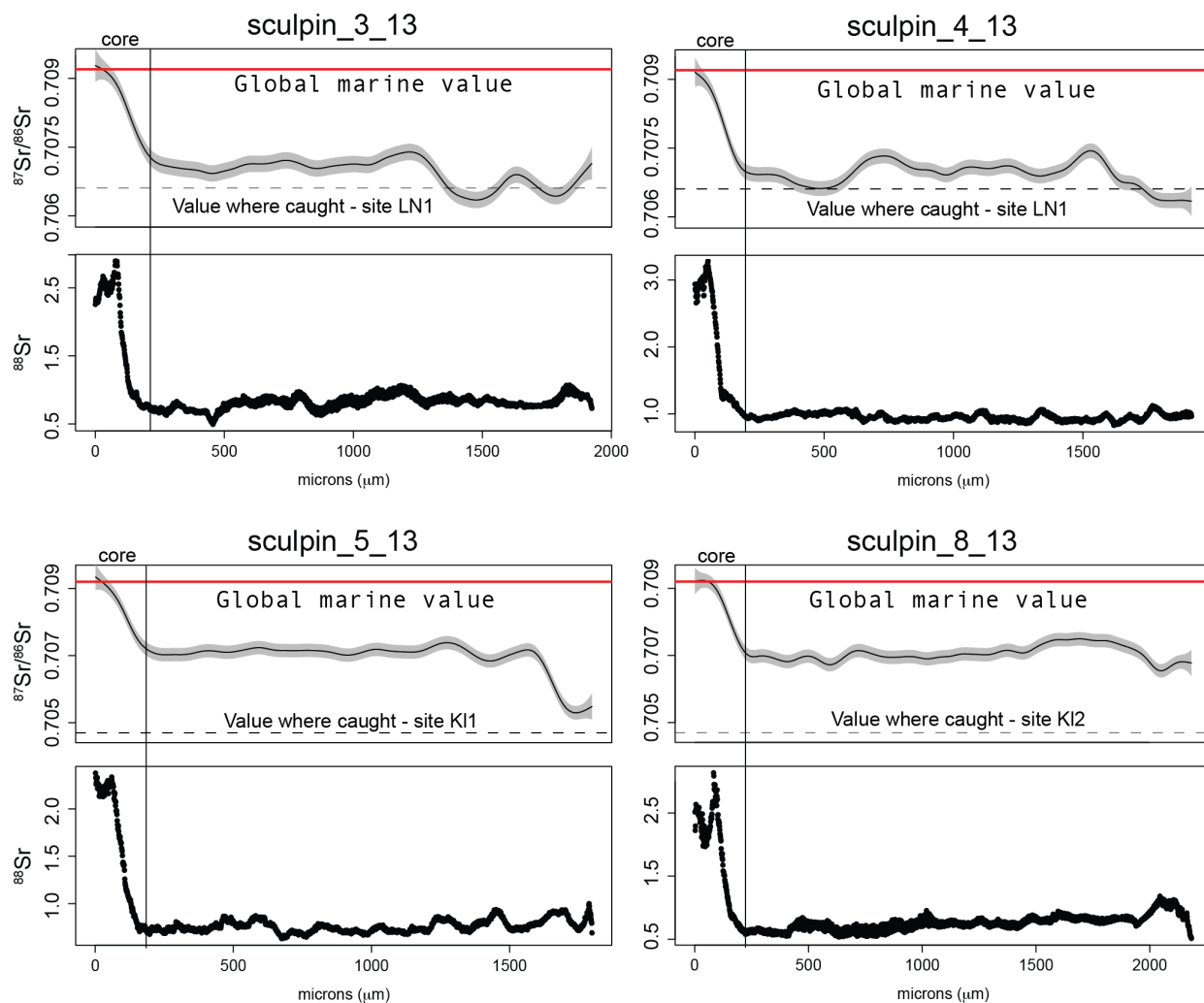


Figure 2.8. $^{87}\text{Sr}/^{86}\text{Sr}$ ratio profiles of four individuals indicating marine Sr in otolith core. Bottom panels are corresponding ^{88}Sr (V) profile of each fish. Horizontal red line is the global marine value (0.70918). Black vertical line denotes the end of the core region.

Table 2.1. Spatially explicit Nushagak River $^{87}\text{Sr}/^{86}\text{Sr}$ water data.

River Name	Collection Date	Latitude	Longitude	$^{87}\text{Sr}/^{86}\text{Sr}$	SE (abs)
South Fork Koktuli ^a	Jun_2011	59.8303	-155.2768	0.704248	0.000046
North Fork Koktuli	Jun_2011	59.8430	-155.7197	0.704284	0.000030
Turquoise Lake	17-Aug-11	60.7817	-154.0108	0.705550	0.000024
Chilikad-1-11	18-Aug-11	60.6648	-154.0458	0.704838	0.000014
Little Mulchatna R.	20-Aug-11	60.5579	-154.5897	0.704618	0.000020
Chilikad-3-11	21-Aug-11	60.5942	-155.0086	0.704970	0.000013
Mulch-1-11	22-Aug-11	60.5945	-155.3970	0.706364	0.000017
Mulch-2-11 ^a	22-Aug-11	60.5708	-155.4367	0.705355	0.000000
Chilichitna R.	23-Aug-11	60.4859	-155.6367	0.705471	0.000019
Mulch-3-11	23-Aug-11	60.3466	-156.0877	0.705804	0.000015
Mosquito R.	24-Aug-11	60.3063	-156.2630	0.706844	0.000015
Old Man Cr.	25-Aug-11	59.9264	-156.4549	0.705935	0.000029
Mulch-4-11 ^a	25-Aug-11	60.2894	-156.2743	0.705801	0.000020
Koktuli R. ^a	26-Aug-11	59.9406	-156.3662	0.704682	0.000028
Swan R.	26-Aug-11	60.0052	-156.2143	0.705018	0.000023
Mulch-5-11	27-Aug-11	59.8377	-156.6755	0.705822	0.000018
Stuyahok R.	28-Aug-11	59.8293	-156.6892	0.704535	0.000032
Nush-1-11	28-Aug-11	59.6421	-157.1228	0.707779	0.000023
Mulch-6-11 ^a	28-Aug-11	59.6695	-157.0532	0.705724	0.000008
Nush-2-11	29-Aug-11	59.4467	-157.3033	0.706531	0.000018
Nishlik Lake	27-Aug-12	60.4408	-158.8398	0.707955	0.000011
Upnuk R.	28-Aug-12	60.2634	-158.6852	0.708418	0.000014
Tik-2-12	28-Aug-12	60.3031	-158.6734	0.708568	0.000011
Tik-3-12	30-Aug-12	60.0321	-158.3510	0.708830	0.000010
Little King Salmon R.	30-Aug-12	59.9286	-158.1735	0.706744	0.000013
Nuy-1-12	30-Aug-12	59.9304	-158.1792	0.708056	0.000011
'Little Cr.'	31-Aug-12	59.9139	-157.9948	0.707672	0.000013
Nuv-2-12 ^a	31-Aug-12	59.9139	-157.9964	0.707987	0.000014
Arrow Cr.	1-Sep-12	59.8965	-157.7958	0.706318	0.000016
Nuy-3-12	1-Sep-12	59.8930	-157.8013	0.707972	0.000011
Nuy-4-12	1-Sep-12	59.8337	-157.4982	0.707859	0.000012
Nush-1-12 ^a	6-Sep-12	60.4869	-156.8522	0.708377	0.000009
'No Name Cr.'	6-Sep-12	60.4910	-156.8860	0.708801	0.000016
Nush-2-12	7-Sep-12	60.4736	-157.0015	0.708637	0.000014
Polly Cr.	7-Sep-12	60.4855	-156.9772	0.708803	0.000019
Fifteen Mile Cr.	8-Sep-12	60.4610	-157.0254	0.709021	0.000019
Nush-3-12	8-Sep-12	60.4737	-157.0015	0.708416	0.000011
Nush-4-12 ^a	8-Sep-12	60.4091	-157.1341	0.708487	0.000003
Lefty Cr.	9-Sep-12	60.4042	-157.2193	0.708730	0.000023

Table 2.1. continued. Spatially explicit Nushagak River $^{87}\text{Sr}/^{86}\text{Sr}$ water data.

River Name	Collection Date	Latitude	Longitude	$^{87}\text{Sr}/^{86}\text{Sr}$	SE (abs)
Chichitnok R. ^a	9-Sep-12	60.3941	-157.2931	0.709101	0.000002
Nush-5-12	9-Sep-12	60.3931	-157.2608	0.708483	0.000010
Nush-7-12	10-Sep-12	60.2710	-157.2841	0.708662	0.000010
Klutapuk Cr.	10-Sep-12	60.3381	-157.3178	0.709049	0.000020
Nush-6-12	10-Sep-12	60.3391	-157.3104	0.708743	0.000021
Nush-8-12	11-Sep-12	60.2212	-157.2332	0.708633	0.000023
Vukpalik Cr.	11-Sep-12	60.1804	-157.2324	0.708585	0.000011
King Salmon R.	11-Sep-12	60.2530	-157.3053	0.708243	0.000024
Nush-11-12	12-Sep-12	59.8698	-157.4221	0.708347	0.000021
Nush-9-12	12-Sep-12	60.0623	-157.3307	0.708526	0.000018
Klutusnak Cr. ^a	12-Sep-12	60.0452	-157.3694	0.706511	0.000040
Harris Cr.	12-Sep-12	59.9445	-157.3966	0.707538	0.000024
Nush-12-12	12-Sep-12	59.7430	-157.3300	0.707952	0.000019
Nush-10-12	12-Sep-12	60.0024	-157.3493	0.708414	0.000021
Nush-13-12 (@Nush-2-11) ^a	13-Sep-12	59.4467	-157.3033	0.706541	0.000031
Nush-15-12	13-Sep-12	59.2679	-157.6490	0.706929	0.000017
Kokwok R.	13-Sep-12	59.3425	-157.6491	0.704770	0.000023
Klutuk Cr.	13-Sep-12	59.3407	-157.4866	0.704712	0.000021
Nush-14-12	13-Sep-12	59.3208	-157.5397	0.707051	0.000022
Nush Spr Freshet (@Nush-2-11) ^a	16-May-13	59.4615	-157.2789	0.706034	0.000016
Head of Allen River	17-May-13	60.1619	-158.7478	0.706969	0.000006
Tikchik Narrows Lodge	17-May-13	59.9625	-158.4777	0.707901	0.000007
Base of Aleen River	17-May-13	60.0610	-158.6321	0.707824	0.000007
Northwest Passage	17-May-13	60.0248	-158.5470	0.708188	0.000007
Nush-1-13 (@Nush-2-11)	15-Aug-13	59.4623	-157.2774	0.706617	0.000008
Klutuk Cr. (@Klutuk2)	16-Aug-13	59.3416	-157.4872	0.704713	0.000008
Nush-2-13	18-Aug-13	59.3407	-157.4847	0.707353	0.000007
Nush-3-13	18-Aug-13	59.2971	-157.5987	0.707193	0.000007
Nush-4-13 ^a	18-Aug-13	59.2989	-157.5780	0.707065	0.000001
Kokwok R. (@Kokwok3)	18-Aug-13	59.3044	-157.5968	0.704793	0.000009

^aField triplicate

Table 2.2. Slimy sculpin trapping site and otolith data.

ID	Date caught	Site ^a	River name	Site description	⁸⁷ Sr/ ⁸⁶ Sr mean ^f	SE	GAM p-value	Distance ^c (km)	size (mm)	Age (yr)
sculpin-1-11	Aug_2011	Ca ^d	Chilikad-1-11	Tributary	0.70481	0.00004	0.259	94.1	110	5
sculpin-2-11	Aug_2011	Ca ^d	Chilikad-1-11	Tributary	0.70489	0.00003	0.375	94.1	76	4
sculpin-3-11	Aug_2011	Ca ^d	Chilikad-1-11	Tributary	0.70480	0.00006	0.253	94.1	76	4
sculpin-4-11	Aug_2011	Ca ^d	Chilikad-1-11	Tributary	0.70498	0.00003	0.183	94.1	91	5
sculpin-5-11	Aug_2011	M1 ^d	Mulch-1-11	Mulchatna main channel	0.70601	0.00003	0.006 *	0.22	85	5
sculpin-6-11	Aug_2011	M1 ^d	Mulch-1-11	Mulchatna main channel	0.70529	0.00003	2.12e-15 **	0.1	75	3
sculpin-7-11	Aug_2011	M2 ^d	Mulch-3-11	Mulchatna main channel	0.70587	0.00002	0.381	8.45	78	3
sculpin-8-11	Aug_2011	Kt ^d	Koktuli	Tributary	0.70459	0.00003	0.229	6.57	-	4
sculpin-9-11	Aug_2011	St ^d	Stuyahok	Tributary	0.70461	0.00003	0.386	0.26	77	4
sculpin-10-11	Aug_2011	St ^d	Stuyahok	Tributary	0.70488	0.00003	<2e-16 **	0.26	85	4
sculpinF-1-12 ^b	Sep_2012	Ny ^d	Nuy-3-12	Nuyakuk main channel	0.70750	0.00003	<2e-16 **	0.56	77	2
sculpinF-2-12 ^b	Sep_2012	Ny ^d	Nuy-3-12	Nuyakuk main channel	0.70794	0.00002	0.238	0.56	80	3
sculpinF-3-12	Sep_2012	Ny ^d	Arrow Cr.	Tributary	0.70777	0.00003	<2e-16 **	0.001	68	4
sculpinF-4-12 ^b	Sep_2012	UN1 ^d	Nush-2-12	UpperNush main channel	0.70844	0.00002	0.112	26	78	4
sculpinF-5-12 ^b	Sep_2012	UN1 ^d	Nush-2-12	UpperNush main channel	0.70847	0.00001	0.093	26	71	3
sculpinF-6-12 ^b	Sep_2012	Ck ^d	Chitchitnok	Tributary	0.70904	0.00002	0.059	2	77	4
sculpinF-7-12	Sep_2012	UN2 ^d	Nush-7-12	UpperNush main channel	0.70871	0.00002	0.324	2	83	4
sculpinF-8-12 ^b	Sep_2012	UN2 ^d	Nush-7-12	UpperNush main channel	0.70874	0.00002	0.127	2	74	3
sculpinF-9-12 ^b	Sep_2012	Kp ^d	Klutuspak	Tributary	0.70725	0.00002	<2e-16 **	0.54	68	3
sculpinF-10-12 ^b	Sep_2012	Kp ^d	Klutuspak	Tributary	0.70709	0.00002	<2e-16 **	0.54	81	5
sculpin-1-13	8/15/13	LN1	Nush-1-13	LowerNush main channel	0.70677	0.00003	<2e-16 **	19.5	91	6
sculpin-2-13	8/15/13	LN1	Nush-1-13	LowerNush main channel	0.70725	0.00002	<2e-16 **	19.5	99	7
sculpin-3-13 ^c	8/15/13	LN1	Nush-1-13	LowerNush main channel	0.70695	0.00002	<2e-16 **	19.5	83	6
sculpin-4-13 ^e	8/15/13	LN1	Nush-1-13	LowerNush main channel	0.70703	0.00002	<2e-16 **	19.5	90	7
sculpin-5-13 ^e	8/16/13	K11	Klutuk	Tributary	0.70697	0.00003	<2e-16 **	0.1	82	6
sculpin-6-13	8/16/13	K11	Klutuk	Tributary	0.70476	0.00001	0.196	0.1	57	3
sculpin-7-13	8/16/13	K12	Klutuk	Tributary	0.70477	0.00001	0.787	0.28	101	7
sculpin-8-13 ^c	8/16/13	K12	Klutuk	Tributary	0.70705	0.00002	<2e-16 **	0.28	85	6
sculpin-9-13	8/16/13	K13	Klutuk	Tributary	0.70705	0.00002	<2e-16 **	0.52	78	3
sculpin-10-13	8/16/13	K13	Klutuk	Tributary	0.70711	0.00002	<2e-16 **	0.52	69	3
sculpin-11-13	8/16/13	K14	Klutuk	Tributary	0.70472	0.00002	0.157	0.83	48	3
sculpin-12-13	8/16/13	K14	Klutuk	Tributary	0.70568	0.00004	<2e-16 **	0.83	65	3
sculpin-13-13	8/16/13	K15	Klutuk	Tributary	0.70473	0.00002	0.319	1.1	59	3
sculpin-14-13	8/16/13	K15	Klutuk	Tributary	0.70597	0.00003	<2e-16 **	1.1	75	4
sculpin-15-13	8/16/13	K11	Klutuk	Tributary	0.70640	0.00002	<2e-16 **	0.1	70	4
sculpin-16-13	8/17/13	Kw1	Kokwok	Tributary	0.70655	0.00003	<2e-16 **	0.01	89	7
sculpin-17-13	8/17/13	Kw1	Kokwok	Tributary	0.70482	0.00002	0.426	0.08	62	5
sculpin-18-13	8/17/13	Kw2	Kokwok	Tributary	0.70495	0.00002	0.838	0.35	65	3

Table 2.2. continued. Slimy sculpin trapping site and otolith data.

ID	Date caught	Site ^a	River name	Site description	⁸⁷ Sr/ ⁸⁶ Sr mean ^f	SE	GAM p-value	Distance ^c (km)	size (mm)	Age (yr)
sculpin-19-13	8/17/13	Kw2	Kokwok	Tributary	0.70514	0.00003	<2e-16 **	0.35	53	3
sculpin-20-13	8/17/13	Kw3	Kokwok	Tributary	0.70487	0.00002	0.976	0.91	62	4
sculpin-21-13	8/17/13	Kw3	Kokwok	Tributary	0.70478	0.00002	0.735	0.91	66	5
sculpin-22-13	8/17/13	Kw4	Kokwok	Tributary	0.70480	0.00002	0.336	1.29	64	5
sculpin-23-13	8/17/13	Kw4	Kokwok	Tributary	0.70486	0.00002	0.030	1.29	65	5
sculpin-24-13	8/17/13	Kw5	Kokwok	Tributary	0.70493	0.00002	0.105	1.56	60	3
sculpin-25-13	8/17/13	Kw5	Kokwok	Tributary	0.70487	0.00002	0.414	1.56	67	5
sculpin-26-13	8/17/13	LN2	Nush-4-13	LowerNush main channel	0.70694	0.00002	<0.001 **	1.32	72	4
sculpin-27-13	8/17/13	LN2	Nush-4-13	LowerNush main channel	0.70713	0.00002	0.099	1.32	91	6
sculpin-28-13	8/17/13	LN2	Nush-4-13	LowerNush main channel	0.70684	0.00002	<2e-16 **	1.32	70	4
sculpin-29-13	8/17/13	LN2	Nush-4-13	LowerNush main channel	0.70710	0.00002	0.002 *	1.32	84	5

^acorresponds to Figure 1

^bFrontal (F) sections also sectioned in transverse plane

^cdistance between trapping site and nearest isotopic change

^dsites which are upstream of Mulchatna River confluence

^eindividuals with marine core signal

^flife-long mean of individual

* significant at 95% confidence level (see text for description)

** significant at <99% confidence level

Table 2.3. Logistic regression results for model with distance (km separating two isotopically different areas) and age-of-fish as predictors (A) and model with only distance as predictor (B). See text for detailed description of distance. Bold values indicate p-values of regression coefficients and AIC values.

A) Model with distance and age-of-fish as predictors

Coefficients:

	Estimate	Std. Error	z value	Pr(> z)
(Intercept)	0.3985	1.3981	0.285	0.77562
logkm	-1.0445	0.3797	-2.751	0.00594
age	-0.3589	0.357	-1.005	0.31479

Null deviance: 54.846 on 40 degrees of freedom

Residual deviance: 36.271 on 38 degrees of freedom

AIC: 42.271

B) Model with only distance as predictor

Coefficients:

	Estimate	Std. Error	z value	Pr(> z)
(Intercept)	-0.9482	0.4593	-2.065	0.03897
logkm	-0.9523	0.3542	-2.689	0.00717

Null deviance: 54.846 on 40 degrees of freedom

Residual deviance: 37.327 on 39 degrees of freedom

AIC: 41.327

Table 2.4. Linear regression results of autumn water versus life-long slimy sculpin otolith mean $^{87}\text{Sr}/^{86}\text{Sr}$ ratio. Bold values indicate the slope, p-value of the slope, and r^2 .

Coefficients:				
	Estimate	Std. Error	t value	Pr(> t)
(Intercept)	0.005389	0.005345	1.008	0.324
Slope	0.992423	0.007575	131.02	<2e-16
Residual standard error:	6.11E-05			
F-statistic:	1.72E+04			
r^2	0.9986			
on 23 degrees of freedom				

REFERENCES

- ADF&G, C.R.T. 2013. Chinook salmon stock assessment and research plan, 2013. **Special Publication No. 13-01.**
- Anderson, S.P., Drever, J.I., Frost, C.D., and Holden, P. 2000. Chemical weathering in the foreland of a retreating glacier. *Geochim Cosmochim Acta* **64**(7): 1173-1189.
- Barnett-Johnson, R., Pearson, T.E., Ramos, F.C., Grimes, C.B., and MacFarlane, R.B. 2008. Tracking natal origins of salmon using isotopes, otoliths, and landscape geology. *Limnol Oceanogr* **53**(4): 1633-1642.
- Bataille, C.P., and Bowen, G.J. 2012. Mapping Sr-87/Sr-86 variations in bedrock and water for large scale provenance studies. *Chem Geol* **304**: 39-52.
- Beckman, D.W., and Wilson, C.A. 1995. Seasonal timing of opaque zone formation in fish otoliths. *In Recent Developments in Fish Otolith Research. Edited by D.H. Secor, J.M. Dean and S.E. Campana.* University of South Carolina Press, Columbia, South Carolina. pp. 27-43.
- Blum, J.D., and Erel, Y. 2003. Radiogenic Isotopes in Weathering and Hydrology. *In Treatise on Geochemistry. Edited by J.I. Drever, Executive Editors: H.D. Holland and K.K. Turekian.* Elsevier. pp. 365-392.
- Breen, M.J., Ruetz, C.R., Thompson, K.J., and Kohler, S.L. 2009. Movements of mottled sculpins (*Cottus bairdii*) in a Michigan stream: how restricted are they? *Can J Fish Aquat Sci* **66**(1): 31-41.
- Brennan, S.R. et al. in revision. Strontium isotope variation and carbonate versus silicate weathering in rivers from across Alaska: implications for provenance studies. *Chemical Geology.*

- Brown, L.R., Matern, S.A., and Moyle, P.B. 1995. Comparative Ecology of Prickly Sculpin, *Cottus-Asper*, and Coastrange Sculpin, *C-Aleuticus*, in the Eel River, California. *Environ Biol Fish* **42**(4): 329-343.
- Campana, S.E. 1999. Chemistry and composition of fish otoliths: pathways, mechanisms and applications. *Mar Ecol Prog Ser* **188**: 263-297.
- Capo, R.C., Stewart, B.W., and Chadwick, O.A. 1998. Strontium isotopes as tracers of ecosystem processes: theory and methods. *Geoderma* **82**(1-3): 197-225.
- Cunjak, R.A., Roussel, J.M., Gray, M.A., Dietrich, J.P., Cartwright, D.F., Munkittrick, K.R., and Jardine, T.D. 2005. Using stable isotope analysis with telemetry or mark-recapture data to identify fish movement and foraging. *Oecologia* **144**(4): 636-646.
- Donohoe, C.J., and Zimmerman, C.E. 2010. A method of mounting multiple otoliths for beam-based microchemical analyses. *Environ Biol Fish* **89**(3-4): 473-477.
- Douglas, T.A., Blum, J.D., Guo, L.D., Keller, K., and Gleason, J.D. 2013. Hydrogeochemistry of seasonal flow regimes in the Chena River, a subarctic watershed draining discontinuous permafrost in interior Alaska (USA). *Chem Geol* **335**: 48-62.
- Elsdon, T.S., Wells, B.K., Campana, S.E., Gillanders, B.M., Jones, C.M., Limburg, K.E., Secor, D.H., Thorrold, S.R., and Walther, B.D. 2008. Otolith chemistry to describe movements and life-history parameters of fishes: Hypotheses, assumptions, limitations and inferences. *Oceanogr Mar Biol* **46**: 297-330.
- Farrell, J., and Campana, S.E. 1996. Regulation of calcium and strontium deposition on the otoliths of juvenile tilapia, *Oreochromis niloticus*. *Comp Biochem Phys A* **115**(2): 103-109.

- Faure, G., and Mensing, T.M. 2005. *Isotopes Principles and Applications*. Wiley, Hoboken, New Jersey.
- Foote, C.J., and Brown, G.S. 1998. Ecological relationship between freshwater sculpins (genus *Cottus*) and beach-spawning sockeye salmon (*Oncorhynchus nerka*) in Iliamna Lake, Alaska. *Can J Fish Aquat Sci* **55**(6): 1524-1533.
- Goldfarb, R.J., Ayuso, R., Miller, M.L., Ebert, S.W., Marsh, E.E., Petsel, S.A., Miller, L.D., Bradley, D., Johnson, C., and McClelland, W. 2004. The Late Cretaceous donlin creek gold deposit, southwestern Alaska: Controls on epizonal ore formation. *Econ Geol Bull Soc* **99**(4): 643-671.
- Gray, M.A. 2003. Assessing non-point source pollution in agricultural regions of the upper St. John River basin using the slimy sculpin (*Cottus cognatus*). Doctoral dissertation. University of New Brunswick.
- Gray, M.A., Cunjak, R.A., and Munkittrick, K.R. 2004. Site fidelity of slimy sculpin (*Cottus cognatus*): insights from stable carbon and nitrogen analysis. *Can J Fish Aquat Sci* **61**(9): 1717-1722.
- Gray, M.A., and Munkittrick, K.R. 2005. An effects-based assessment of slimy sculpin (*Cottus cognatus*) populations in agricultural regions of northwestern New Brunswick. *Water Qual Res J Can* **40**(1): 16-27.
- Hegg, J.C., Kennedy, B.P., Chittaro, P.M., and Zabel, R.W. 2013. Spatial structuring of an evolving life-history strategy under altered environmental conditions. *Oecologia* **172**(4): 1017-1029.
- Hill, J., and Grossman, G.D. 1987. Home Range Estimates for 3 North-American Stream Fishes. *Copeia*(2): 376-380.

- Hobson, K.A., Barnett-Johnson, R., and Cerling, T.E. 2010. Using Isoscapes to Track Animal Migration. *In* *Isoscapes: Understanding movement, pattern, and process on Earth through isotope mapping*. Edited by J.B. West, G.J. Bowen, T.E. Dawson and K.P. Tu. Springer Science.
- Horton, T.W., Chamberlain, C.P., Fantle, M., and Blum, J.D. 1999. Chemical weathering and lithologic controls of water chemistry in a high-elevation river system: Clark's Fork of the Yellowstone River, Wyoming and Montana. *Water Resour Res* **35**(5): 1643-1655.
- Ingram, B.L., and Weber, P.K. 1999. Salmon origin in California's Sacramento-San Joaquin river system as determined by otolith strontium isotopic composition. *Geology* **27**(9): 851-854.
- Jones, M., Sands, T., Morstad, S., Salomone, P., Buck, G., West, F., Brasil, C., and Krieg, T. 2013. 2012 Bristol Bay Area Annual Management Report. Alaska Department of Fish and Game, Fishery Management Report No. 13-20.
- Kalish, J.M. 1990. Use of Otolith Microchemistry to Distinguish the Progeny of Sympatric Anadromous and Non-Anadromous Salmonids. *Fishery Bulletin* **88**(4): 657-666.
- Keller, K., Blum, J.D., and Kling, G.W. 2010. Stream geochemistry as an indicator of increasing permafrost thaw depth in an arctic watershed. *Chem Geol* **273**(1-2): 76-81.
- Kennedy, B.P., Blum, J.D., Folt, C.L., and Nislow, K.H. 2000. Using natural strontium isotopic signatures as fish markers: methodology and application. *Can J Fish Aquat Sci* **57**(11): 2280-2292.
- Kennedy, B.P., Klaue, A., Blum, J.D., Folt, C.L., and Nislow, K.H. 2002. Reconstructing the lives of fish using Sr isotopes in otoliths. *Can J Fish Aquat Sci* **59**(6): 925-929.
- Kim, Y.J., and Gu, C. 2004. Smoothing spline Gaussian regression: more scalable computation via efficient approximation. *J Roy Stat Soc B* **66**: 337-356.

- Krueger, C.C., Zimmerman, C.E., and American Fisheries Society. 2009. Pacific salmon : ecology and management of western Alaska's populations. *In* American Fisheries Society symposium 70. American Fisheries Society, Bethesda, MD.
- Mackey, G.N., and Fernandez, D.P. 2011. High throughput Sr isotope analysis using an automated column chemistry system. Abstract V31B-2525 presented at 2011 Fall Meeting AGU, San Francisco, California, 5-9 Dec.
- Miller, J.A. 2011. Life history variation in upper Columbia River Chinook salmon (*Oncorhynchus tshawytscha*): a comparison using modern and similar to 500-year-old archaeological otoliths (vol 68, pg 603, 2011). *Can J Fish Aquat Sci* **68**(5): 953-953.
- Morgan, C.R., and Ringler, N.H. 1992. Experimental Manipulation of Sculpin (*Cottus-Cognatus*) Populations in a Small Stream. *J Freshwater Ecol* **7**(2): 227-232.
- Morrow, J.E. 1980. *The Freshwater Fishes of Alaska*. Alaska Northwest Publishing Company, Anchorage, Alaska.
- Muhlfeld, C.C., Thorrold, S.R., McMahon, T.E., and Marotz, B. 2012. Estimating westslope cutthroat trout (*Oncorhynchus clarkii lewisi*) movements in a river network using strontium isoscapes (vol 69, pg 906, 2012). *Can J Fish Aquat Sci* **69**(6): 1129-1130.
- Petty, J.T., and Grossman, G.D. 2004. Restricted movement by mottled sculpin (*pisces* : *cottidae*) in a southern Appalachian stream. *Freshwater Biol* **49**(5): 631-645.
- Schindler, D.E., Hilborn, R., Chasco, B., Boatright, C.P., Quinn, T.P., Rogers, L.A., and Webster, M.S. 2010. Population diversity and the portfolio effect in an exploited species. *Nature* **465**(7298): 609-612.
- Schmetterling, D.A., and Adams, S.B. 2004. Summer movements within the fish community of a small Montane stream. *N Am J Fish Manage* **24**(4): 1163-1172.

- Semhi, K., Clauer, N., and Probst, J.L. 2000. Strontium isotope compositions of river waters as records of lithology-dependent mass transfers: the Garonne river and its tributaries (SW France). *Chem Geol* **168**(3-4): 173-193.
- Voss, B.M., Peucker-Ehrenbrink, B., Eglinton, T.I., Fiske, G., Wang, Z.A., Hoering, K.A., Montlucon, D.B., LeCroy, C., Pal, S., Marsh, S., Gillies, S.L., Janmaat, A., Bennett, M., Downey, B., Fanslau, J., Fraser, H., Macklam-Harron, G., Martinec, M., and Wiebe, B. 2014. Tracing river chemistry in space and time: Dissolved inorganic constituents of the Fraser River, Canada. *Geochim Cosmochim Acta* **124**: 283-308.
- Walther, B.D., and Thorrold, S.R. 2006. Water, not food, contributes the majority of strontium and barium deposited in the otoliths of a marine fish. *Mar Ecol Prog Ser* **311**: 125-130.
- Walther, B.D., and Thorrold, S.R. 2009. Inter-annual variability in isotope and elemental ratios recorded in otoliths of an anadromous fish. *J Geochem Explor* **102**(3): 181-186.
- Walther, B.D., Thorrold, S.R., and Olney, J.E. 2008. Geochemical signatures in otoliths record natal origins of American shad. *Transactions of the American Fisheries Society* **137**(1): 57-69.
- Wilson, F.H., Blodgett, R.B., Blomé, C.D., Mohadjer, S., Preller, C.C., Klimasauskas, E.P., Gamble, B.M., and Coonrad, W.L. 2006. Reconnaissance bedrock geologic map for the northern Alaska Peninsula area, southwest Alaska. U.S. Geological Survey Open-File Report **2006-1303**.
- Wilson, F.H., and Coonrad, W.L. 2005. The Togiak-Tikchik Complex of southwest Alaska, a replacement for the Gemuk Group: Stratigraphic nomenclature that has outlived its time: U.S. Geological Survey Scientific Investigations Report 2005-5019.

Wood, S.N. 2006. Generalized additive models : an introduction with R. Chapman & Hall/CRC, Boca Raton, FL.

Zimmerman, C.E., and Reeves, G.H. 2002. Identification of steelhead and resident rainbow trout progeny in the deschutes river, oregon, revealed with otolith microchemistry. Transactions of the American Fisheries Society **131**(5): 986-993.

Zimmerman, C.E., Swanson, H.K., Volk, E.C., and Kent, A.J.R. 2013. Species and life history affect the utility of otolith chemical composition for determining natal stream of origin for pacific salmon. Transactions of the American Fisheries Society **142**(5): 1370-1380.

CHAPTER 3:

Strontium isotopes provide new tool for fine-scale biodiversity conservation of Pacific salmon¹

ABSTRACT

Over a decade of research has shown that the biodiversity characterizing wild Pacific salmon (*Oncorhynchus* spp.) populations in the Bristol Bay region of Alaska imparts resiliency to environmental change and temporal stability to the region's overall productivity and dependent human systems. This body of research has motivated the development of tools to monitor biodiversity and the potential impacts from perturbations, such as climate change, mineral development, and commercial fisheries. Accurate methods exist for monitoring broad-scale population structure (e.g., watershed-specific populations) of sockeye salmon (*O. nerka*) harvests. However, the ability to apportion group membership of harvests to fine-scale population structure (e.g., stream-specific populations) is minimal, and no tools currently exist to discern mixed stock harvests of Chinook (*O. tshawytscha*) and coho (*O. kisutch*) salmon. We used the naturally occurring variation in $^{87}\text{Sr}/^{86}\text{Sr}$ ratios within the Nushagak River (one of the nine major watersheds flowing into Bristol Bay, which collectively make up the largest wild sockeye salmon fishery in the world) to discern natal origins and freshwater movement patterns of Chinook salmon (n = 255) harvested during the commercial sockeye salmon fishery. We found that three regions of the Nushagak River produced > 70% of the incidental catch of adult Chinook salmon. Additionally, we were able to identify differences in movement patterns and

¹ Brennan, S.R., Zimmerman, C.E., Fernandez, D.P., Cerling, T.E., McPhee, M.V., Wooller, M.J. In review. Strontium isotopes provide new tool for fine-scale biodiversity conservation of Pacific salmon. Proceedings of the National Academy of Sciences.

habitat use during freshwater residence. This study demonstrated that $^{87}\text{Sr}/^{86}\text{Sr}$ ratios within geologically heterogeneous regions can be used to discern fine-scale population structure of harvests from fisheries and provides a new way of monitoring the biodiversity of Nushagak River salmon populations.

INTRODUCTION

A challenging issue in the management, conservation, and research of Pacific salmon (*Oncorhynchus* spp.) is tracking their responses to perturbations across the multiple scales of population structure that characterize these species (1). In the Bristol Bay region of Alaska (AK), the largest producer of wild sockeye salmon, *O. nerka*, in the world, three relevant perturbations to Pacific salmon populations include climate change (2), proposed mineral development (3), and commercial fisheries (4). These perturbations generally come in the form of changes to oceanic and freshwater habitat conditions (the former two), or over-fishing of distinct populations (the latter). Over a decade of research within the Bristol Bay region, primarily on sockeye salmon (4-6), has demonstrated how the inherent biodiversity of Pacific salmon populations imparts resiliency to environmental perturbations, lending temporal stability to their overall productivity and the human systems (e.g., subsistence and commercial fisheries) dependent upon such productivity. This biodiversity is primarily due to precise homing of adults to their natal sites and resultant locally adapted populations. Thus, salmon population structure is hierarchical with a strong geographic component, whereby both fine-scale (e.g., stream specific) and broad-scale (e.g., watershed-specific) levels contribute to the regions overall biodiversity (7). Due to the ecosystem services and economic value provided by these salmon populations (5, 8), as well as

their high exploitation rates (9), there has been considerable effort invested into developing tools to track and monitor the biodiversity of this region.

One of the most accurate ways to determine how biodiversity influences fisheries and overall regional productivity is by using genetic differentiation (i.e., variation in single nucleotide polymorphisms [SNPs] and microsatellite DNA) among populations to apportion mixed stock fishery harvests to respective contributing watersheds (i.e., mixed stock analysis [MSA]) (10). In the Bristol Bay region, these analyses contribute to accurate estimations of stock productivity (10). Currently, baseline datasets only exist for sockeye salmon (7, 10) although research is underway to develop a genetic baseline for Chinook salmon (*O. tshawytscha*) (11-13). However, even after a large-scale RAD-sequencing SNP discovery effort, Bristol Bay Chinook salmon are still indistinguishable from those of the lower Kuskokwim River (11). No genetic baseline information exists for coho salmon (*O. kisutch*). Using SNPs and microsatellite DNA analyses, nine genetically distinct reporting groups of sockeye salmon can be discerned from mixed stock harvests, which correspond to the nine major watersheds draining into Bristol Bay (7, 10). Although these genetic techniques have been effective at discerning the broad-scale population structure of harvests from Bristol Bay (10, 14), determining group membership of harvests to the fine-scale structure has been more difficult (7) and remains largely untested. Within many of the watersheds fine-scale genetic structure does exist (7, 10, 14), but there are statistical costs to employing it in MSAs (15) and within some watersheds the structure is considerably shallow (14). One example is the Nushagak River, where all sockeye salmon populations from this large watershed are combined into one reporting group (7, 10). At the finer level of genetic structure, the Tikchik Lakes system appears to be distinct, but SNPs and microsatellite DNA analyses both indicate that the Nushagak River is quite homogeneous (7, 10,

14). Although management is currently focused on apportioning harvests to the major watersheds of Bristol Bay, harvests in each district, including the Nushagak River, can be a mixture of tens to hundreds of locally adapted populations (5). This level of biodiversity has been recognized as an important aspect of sustainable fisheries (5), and questions remain as to how it responds to environmental perturbations, including fisheries, mineral development, and climate change. Thus, tools are needed to determine finer levels of population structure in mixed stock fishery harvests.

Recent research has demonstrated that geographic heterogeneity in strontium (Sr) isotope ($^{87}\text{Sr}/^{86}\text{Sr}$) ratios throughout freshwater habitats is also a valuable tool for tracking natal origins and movement patterns of fishes, including salmon (16-21). The utility of $^{87}\text{Sr}/^{86}\text{Sr}$ ratios stems from the conservative nature of the $^{87}\text{Sr}/^{86}\text{Sr}$ ratio during physical and biological processes and the inherent time-keeping properties of fish otoliths, which grow incrementally via metabolically inert concentric rings of CaCO_3 throughout a fish's life (22). $^{87}\text{Sr}/^{86}\text{Sr}$ ratios of biogenic materials directly reflect the isotopic composition of their sources (23) and their variability across landscapes scales with geologic heterogeneity (24). Thus, variation in $^{87}\text{Sr}/^{86}\text{Sr}$ ratios exists at multiple spatial scales, including regional (e.g., among watersheds) and local scales (e.g., within watersheds) (Brennan et al., in review). In aquatic ecosystems, Sr dissolved in surface waters is ultimately derived from bedrock, but its isotopic composition is moderated by differential chemical weathering rates of rock-minerals within a catchment (25, 26). Sr within fish otoliths is primarily (~ 88%), derived from ambient water whereas the remainder is derived from diet (27, 28). As such, Sr incorporated into the CaCO_3 of otoliths reflects the environmental isotopic conditions experienced by individual fish via a 1:1 relationship (16, 18). Otoliths, thus, represent unadulterated records of a fish's entire environmental $^{87}\text{Sr}/^{86}\text{Sr}$ history.

In this study we used $^{87}\text{Sr}/^{86}\text{Sr}$ ratios to discern the natal river of origin of Nushagak River Chinook salmon incidentally caught during a three-day fishing period of the commercial sockeye salmon fishery, which also corresponded to the peak of the Chinook salmon run (29). We hypothesized that within-watershed $^{87}\text{Sr}/^{86}\text{Sr}$ variation would allow us to apportion this mixed stock harvest to geographically and geologically distinct sub-basins within the catchment (30). The Nushagak River is one of the nine major river systems flowing into Bristol Bay and is a major contributor to the sockeye salmon fishery. It also produces the third largest wild Chinook salmon run in Western AK, which ranks it as one of the largest Chinook salmon runs in the world (31). Additionally, it produces abundant runs of wild coho, pink (*O. gorbuscha*) and chum (*O. keta*) salmon (9). We recently established that geologic heterogeneity within the Nushagak River gives rise to strong geographic patterns in $^{87}\text{Sr}/^{86}\text{Sr}$ ratios of river waters (Brennan et al., in review). We have also demonstrated that site-specific $^{87}\text{Sr}/^{86}\text{Sr}$ ratios throughout the Nushagak River are temporally stable at sub-annual time scales, particularly during the summer and autumn months (Brennan et al., in review). In this current study we focused on Chinook salmon because: i) no methods for discerning this species stock composition within this watershed currently exist; ii) its annual bycatch during the sockeye fishery in the Nushagak district is often > 10,000 individuals (9, 29); iii) juveniles from Subarctic populations spend one full year in the freshwater environment before out-migration to sea (32) and, thus, adopt accurate $^{87}\text{Sr}/^{86}\text{Sr}$ ratios from their natal habitats (20); and iv) Chinook salmon populations have shown dramatic changes across AK in the last decade and tools are needed to accurately discern their fine-scale population structure (31, 33).

Our overall objective was to discern the natal origins and movement patterns of Nushagak River Chinook salmon using $^{87}\text{Sr}/^{86}\text{Sr}$ ratios in otoliths. To do this we constructed a

baseline discriminant function analysis (DFA) model using water data from throughout the Nushagak River (Brennan et al., in review). We then validated the performance of the model to accurately classify natal origins of Chinook salmon by using otolith samples of known origin. Finally, we used the model to conduct an $^{87}\text{Sr}/^{86}\text{Sr}$ -based MSA of incidentally caught Chinook salmon during the 2011 commercial sockeye salmon fishery in Nushagak Bay. In addition, we evaluated the relative differences in freshwater movement patterns of both incidentally caught adults and juvenile Chinook salmon of known origin within the Nushagak River.

RESULTS

Training the baseline DFA model

We grouped water data into seven Strontium Isotopic Groups (SIGs) (Figure 1 and 2A) based on similarity in both $^{87}\text{Sr}/^{86}\text{Sr}$ ratios and geography. Some SIGs encompassed geographically separated tributaries (e.g., the Tikchik and Upper Nushagak Rivers, Figure 1). However, because they were isotopically similar they were determined to be within the same SIG. SIGs met the necessary assumptions of homogeneity of variances for a linear DFA (Levene's test, $p = 0.57$). The regression of water versus otolith $^{87}\text{Sr}/^{86}\text{Sr}$ ratios (measured parallel to growth axis, see SI text) yielded a slope of 0.983 ± 0.017 (2σ SE) and a coefficient of determination (r^2) of 0.99, which approximated a 1:1 relationship (Figure 2B). This result demonstrated the validity of using water data to build the DFA model. Several individuals had very different $^{87}\text{Sr}/^{86}\text{Sr}$ ratios ($\gg 2\sigma$ SD) (Figure 2B, Dataset S1) than the ambient environment in which they were captured. Their ratios, however, were similar to proximal environments to their respective trapping sites. These individuals most likely moved into respective trapping

areas just prior to being captured (e.g., Brennan et al., in review). As such, we excluded them from the regression and also the DFA during our validation tests (described in detail below).

$^{87}\text{Sr}/^{86}\text{Sr}$ life history profiles of juvenile Chinook salmon

$^{87}\text{Sr}/^{86}\text{Sr}$ life history profiles (measured perpendicular to growth axis, see SI text) of juvenile Chinook salmon revealed that some individuals (20% of total sub-sample) moved between isotopically different freshwater environments (Dataset S2). At the sites where we observed obvious outliers in our regression (e.g., sites St, Kl, and Ny1) (Figure 2B) we also observed life histories of individuals indicative of movements between isotopically different, but proximal, habitats. This also corroborated their exclusion from the regression and DFA based on the evidence ($^{87}\text{Sr}/^{86}\text{Sr}$ otolith ratios) that some individuals did not originate from the trapping area. For example, the only juveniles captured in tributaries of the lower Nushagak River (i.e., Klutuk Creek, site Kl, $n = 2$) had natal origin ratios similar to the lower Nushagak River, but rearing ratios similar to Klutuk Creek. There were also examples of juveniles moving between SIGs 6 and 7; SIGs 1 and 2; SIGs 3 and 2; and SIGs 4 and 5. Additionally, between 89 and 93% of the Sr present within the otolith cores of juvenile Chinook salmon was derived from marine sources (see SI text and Figure S1A). The proportion of marine-derived Sr in juvenile Chinook otoliths consistently approached 0% at a distance $\sim 250 \mu\text{m}$ from primordia (e.g., Figure S1B).

Validating baseline DFA model

The two independent validation tests we conducted of our DFA model yielded overall classification accuracies of 90% and 88% for known origin juvenile Chinook salmon ($n = 153$)

and slimy sculpin ($n = 33$), respectively (Table S1). SIG specific classification rates (G_{cr}) ranged from 0.6 - 1.0 for juvenile Chinook salmon (Table S1A) and 0.5 - 1.0 for slimy sculpin (Table S1B). We defined G_{cr} as the proportion of correctly classified individuals into each SIG, where $G_{cr} < 1$ indicates that a proportion of individuals were misclassified into the said SIG. Despite the minor number of misclassifications between SIGs during these tests the overall accuracies of the DFA model were high ($\sim 90\%$).

Mixed Stock Analysis (MSA)

Of the 255 adult Chinook salmon analyzed in this study, our DFA model predicted a total of 71% originated from three of the SIGs: SIG 1 (22%), SIG 2 (22%), and SIG 6 (27%) (Figure 3A). The next largest contributors were SIGs 3 (10%) and 5 (11%); SIG 4 contributed the smallest proportion (4%) (Figure 3A). The DFA model predicted natal origins of 89% ($n = 228$) of all adult Chinook salmon with posterior probabilities $> 80\%$ for SIG membership. Natal origin predictions with probabilities $> 70\%$ for group membership composed 94% ($n = 239$) of the total sample. Our MSA results for the overall proportions of SIG membership only slightly changed (Table S2) when we set a probability threshold for group membership of $> 80\%$ or $> 70\%$ probability. Thus, we believe our overall MSA results were 90% accurate, as suggested by our independent classification tests of known origin samples and an examination of the posterior probabilities of SIG membership from the DFA.

During the three-day fishing period, the proportion of individuals from respective SIGs changed and exhibited a geographic pattern in terms of day-specific MSAs (Figure 3B). For example, the proportion of fish from SIGs 1 and 2 increased steadily over the three-day period (e.g., by $\sim 13\%$). Correspondingly, SIGs 5, 6, and 7 appeared to decrease (e.g., SIG 6 by $\sim 8\%$).

Geographically, these respective groups of SIGs represent the two primary upper watershed areas of the Nushagak (e.g., the Mulchatna River and the Upper Nushagak River, respectively) (Figure 1).

Movement patterns

In addition to predicting natal origins, we also inferred freshwater movement patterns of all adult Chinook salmon (Figure 4 and Table S3A). Generally, we observed four different types of $^{87}\text{Sr}/^{86}\text{Sr}$ life history patterns during freshwater residence. Firstly, individuals indicating site fidelity (no apparent change in $^{87}\text{Sr}/^{86}\text{Sr}$ ratios) during freshwater residence composed 72% of our sample of 255 Chinook salmon. Secondly, 7% showed profiles indicative of rearing in a different $^{87}\text{Sr}/^{86}\text{Sr}$ environment than their natal origin. Thirdly, 17% originated and reared in the same $^{87}\text{Sr}/^{86}\text{Sr}$ environment, but showed short forays towards lower river ratios (the migration corridor through which all upstream fish must swim). Finally, 4% of the individuals, who reared in a different environment, showed a foray just before their migration to the sea. Movements toward lower river $^{87}\text{Sr}/^{86}\text{Sr}$ ratios generally occurred over an otolith distance of $< 100 \mu\text{m}$ and were located just before migration to the ocean. Thus, they often never fully equilibrated with lower river ratios (e.g., Figure 4). Of the individuals that were indicative of having reared in a different $^{87}\text{Sr}/^{86}\text{Sr}$ environment than their natal origin ($n = 26$ total), approximately half ($n = 14$) had $^{87}\text{Sr}/^{86}\text{Sr}$ ratios during the rearing stage that were classified into different SIGs than their natal origin. Using both natal origin and rearing area DFA predictions (Table S3B), we inferred actual migration routes of these individuals providing further insight into their natal origins and freshwater habitat use (see Discussion below and SI text). The remaining individuals showed

changes in the $^{87}\text{Sr}/^{86}\text{Sr}$ ratio (ranging from 0.00011 to 0.00044), but the DFA predicted both the natal origin and rearing signals to be within the same SIG.

DISCUSSION

The results from this study demonstrated that $^{87}\text{Sr}/^{86}\text{Sr}$ ratios recorded in otoliths of Chinook salmon could be used to discern natal origins and freshwater movement patterns of individuals caught during a commercial fishery. Four key features of our study made these results possible. Firstly, we used a robust baseline dataset of river water $^{87}\text{Sr}/^{86}\text{Sr}$ ratios representative of all potential natal sources within the Nushagak River, which has been evaluated with respect to both spatial and temporal variability (Brennan et al., in review). Secondly, we demonstrated that $^{87}\text{Sr}/^{86}\text{Sr}$ ratios of ambient water correspond to otolith ratios of juveniles collected at the same sampling site via a 1:1 relationship ($r^2 = 0.99$). We also showed how fish movements between proximal, but isotopically distinct environments; can affect the observed relationship between ambient water and otolith $^{87}\text{Sr}/^{86}\text{Sr}$ ratios within individual sites. Thirdly, we performed two independent tests of the accuracy of this baseline dataset to predict natal origins of Chinook salmon using known origin samples of juvenile Chinook salmon and slimy sculpin (yielding 90% and 88% correct classification accuracies, respectively). Finally, current management practices deliberately restrict the commercial sockeye salmon fishery to take place within the natural boundaries of the Nushagak Bay, such that the fishery targets primarily fish ultimately bound for Nushagak Bay watersheds (10). Because the Nushagak River Chinook salmon run is so large (> 100,000) compared to the small runs of proximal watersheds within Nushagak Bay (e.g., the largest of which is likely the Muklung River within the upper Wood River system, ~ 400 total) (34), incidentally caught Chinook salmon within Nushagak Bay were

assumed to be bound for the Nushagak River. Thus, our baseline model was representative of all potential natal sources of the mixed stock incidental catch of Chinook salmon.

Building baseline $^{87}\text{Sr}/^{86}\text{Sr}$ datasets using water data

The regression of $^{87}\text{Sr}/^{86}\text{Sr}$ ratios in water versus otoliths from known origin juvenile Chinook salmon demonstrated that otoliths strongly approximate ambient water ratios (Figure 2B) and justified using water data to train the DFA model. The same relationship (slope = 0.99 and $r^2 = 0.99$) in the same watershed was also determined using lifelong (2 - 7 years) mean otolith $^{87}\text{Sr}/^{86}\text{Sr}$ ratios from known origin slimy sculpin (Brennan et al., in review). Thus, water-sampling campaigns, particularly in the autumn, appear to be accurate proxies for otolith variation throughout study regions. However, multi-scale temporal variability is an important characteristic to evaluate, especially in regions defined by extreme seasonality such as the Subarctic (35) and Arctic (36). Arguably, inter-annual variation during autumn is the most important time-scale to evaluate (Brennan et al., in review), because natal origin studies of salmon target the first year of growth within the otolith (16), which reflects the autumn ambient water environment. Additionally, our results from $^{87}\text{Sr}/^{86}\text{Sr}$ life-history profiles of juvenile Chinook salmon (Dataset S2) illustrated that some individuals did not originate from the site in which they were trapped. We also observed this in the data generated by measuring parallel to the growth axis proximal to the otolith edge (e.g., the outliers in Figure 2B, see SI text). These results illustrated the connectivity between freshwater habitats from the perspective of juvenile Chinook salmon. Thus, ‘known origin’ juveniles, as determined by location of trapping site, can be misleading and suggests that otolith data should be compared to water data when building a $^{87}\text{Sr}/^{86}\text{Sr}$ baseline, especially if the baseline hinges primarily on otolith data.

Insights from misclassifications of known origin fish

Though our validation tests of known origin juvenile Chinook salmon and slimy sculpin were ~ 90% accurate, the misclassifications provided insight into where additional water sampling within the study region would further constrain the Nushagak River SIGs. At one site on the Mulchatna River (site M1, within SIG 3), four fish captured were misclassified with > 80% probability into SIG 2 (which also happens to encompass the main-stem channel of the Mulchatna River). Waters at site M1 showed relatively high $^{87}\text{Sr}/^{86}\text{Sr}$ ratios compared to the rest of the main-stem channel (Brennan et al., in review). Thus, these fish may have moved from either proximal downstream or upstream areas characterized by lower $^{87}\text{Sr}/^{86}\text{Sr}$ ratios more akin to SIG 2. Only slimy sculpin from the lower Nushagak River sites (Brennan et al., in review) were misclassified. Six of the eight individuals were classified into SIG 4; and all juvenile Chinook salmon captured in the lower river (site LN2) were correctly classified into SIG 4. Though some spatio-temporal heterogeneity characterized the lower main-stem river (Brennan et al., in review), these results suggested that most fish from the lower Nushagak River (from areas encompassed by SIG 3 and 4, Figure 1) exhibit $^{87}\text{Sr}/^{86}\text{Sr}$ ratios more akin to the range defined by SIG 4.

Movement patterns elucidated via otolith microchemistry

One of the unique features of otolith microchemistry is that it is able to yield useful life-history information for individual fish (17, 18, 37). Because we measured the $^{87}\text{Sr}/^{86}\text{Sr}$ ratio from the otolith core into marine regions of each adult Chinook salmon, we were able to infer relative

differences in movement patterns during freshwater residence. Our interpretation of these transects was limited by two main aspects of the general method: inherent otolith growth structure (e.g., otolith growth is not constant throughout the year or over the life of a fish) and beam-based sampling methods (e.g., the beam size and scan speed of laser ablation (LA) transect). More specifically, our ability to resolve and observe $^{87}\text{Sr}/^{86}\text{Sr}$ changes experienced by individuals depended on i) the magnitude of the actual $^{87}\text{Sr}/^{86}\text{Sr}$ change between environments (e.g., shifts need to be on the order of 0.0001), ii) how long the change persisted during the freshwater residence of a fish (both with respect to real-time and otolith distance), and iii) how large the LA beam diameter was relative to this change as reflected in the otolith (Brennan et al., in review). Thus, our interpretations of movement patterns of Chinook salmon were relative to the dataset as a whole and did not reflect absolute real-time migration reconstructions (e.g., as with a physical tracking device).

However, by using $^{87}\text{Sr}/^{86}\text{Sr}$ profiles we were able to infer movement patterns, relative habitat use, and refine the natal origin predictions of some adult Chinook salmon (Table S3). For example, three individuals originating from areas within SIG 1 had rearing signals from within SIG 2 (e.g., Figure 4 and Table S3B). Given our knowledge of the $^{87}\text{Sr}/^{86}\text{Sr}$ geographic patterns throughout the Nushagak River (Brennan et al., in review), it is probable that these fish originated from the eastern tributaries of the Mulchatna River draining the Alaskan-Aleutian Range (AAR), and then reared in the Mulchatna River for some time before migrating to the ocean. This additional rearing area information refined the natal origin prediction of these fish to the AAR tributaries, which distinguishes them from the isotopically similar lower Nushagak River tributaries (e.g., Kokwok River and Klutuk River) (Figure 1 and Table S3B). Of the SIG 1 fish that exhibited site-fidelity during freshwater residence, $^{87}\text{Sr}/^{86}\text{Sr}$ ratios were not able to

discern this within-SIG 1 natal origin difference. These results suggest differences in movement patterns and habitat use between AAR-Chinook salmon (e.g. site fidelity within the AAR tributaries versus utilization of the Mulchatna River). Across the entire dataset, we observed only 11% of individuals to have reared in a different $^{87}\text{Sr}/^{86}\text{Sr}$ environment than their natal origin (half of which had rearing signals from a different SIG than their natal origin) (Table S3A). Similarly, if we examined the entire adult Chinook salmon dataset ($n = 255$), we observed relative differences in the utilization of the lower Nushagak River main-stem channel (the corridor through which all fish must swim via their migration to the ocean). Of the entire sample, 21% of the individuals indicated short ($< 100 \mu\text{m}$ in otolith) $^{87}\text{Sr}/^{86}\text{Sr}$ forays towards the lower river ratios, whereas the remaining majority did not (Table S3A). Qualitatively, these results suggest differential habitat use among individuals.

MSA using Strontium Isotopic Groups (SIGs)

In this study we apportioned a mixed stock of incidentally harvested Chinook salmon in Nushagak Bay to 7 SIGs within the Nushagak River watershed. Our collections of Chinook salmon in 2011 occurred during the periods of largest bycatch from the commercial sockeye salmon fishery in the Nushagak District and escapement into the Nushagak River (29). The total run of Nushagak River Chinook salmon in 2011 was 107,989, with a total bycatch of 29,811 (half of which occurred on June 26th - the official opening of the fishery) (29). Our collections also included catches from multiple gear types (drift and set gillnets), boats, and days. As such, we believe our MSA results reported herein to be a reasonable estimate of the composition (i.e., the fine-scale population structure as determined via SIGs) of the Nushagak River Chinook salmon runs in 2011, though we were unable to assess the beginning and end of the run.

As a comparison, all Nushagak River sockeye salmon (the only species in the region with a comprehensive genetic baseline) are combined into one reporting group based on, genetic population structure, statistical considerations, and stakeholder interests (7, 10, 14). Although sockeye salmon of the Tikchik Lakes appear genetically distinguishable, the rest of the Nushagak River exhibits quite homogeneous genetic structure (7, 10, 14). MSAs, which employ genetic data of harvested sockeye salmon during commercial fisheries, have been very useful for discerning broad-scale population structure between the major Bristol Bay watersheds (10) and have contributed significantly to the sustainable management of this fishery (4). Genetic MSAs have been able to provide more accurate estimates of watershed-specific total annual recruitment (10) and inform in-season management decisions (14). These estimates provide the framework for setting escapement goals and effective management under the sustained-yield principle (10). However, genetic baselines have not determined group membership of harvests to the fine-scale population structure (e.g., within a watershed) in many of these large watersheds, including the Nushagak River (10, 14). Thus, genetically based MSA results from the commercial sockeye salmon fishery have been largely limited to apportioning harvests to the broad-scale population structure of the Bristol Bay region. Although recent important work using SNPs of closely related populations of Chinook salmon across Western Alaska increased genetically distinguishable reporting groups from one to three in this expansive region, Chinook salmon from Bristol Bay (which includes populations from the Nushagak River) are still indistinguishable from those from the lower Kuskokwim River (11).

SIGs within the Nushagak River watershed provided increased resolution (by a factor of ~ 7) into the fine-scale population structure (i.e., sub-basin level) of the mixed stock incidental catch of Chinook salmon. However, $^{87}\text{Sr}/^{86}\text{Sr}$ information accessed via otoliths is not a direct

insight into population structure. It is inherently indirect, and is more of a proxy for population structure, because it is purely based on environmental differences between habitats, not genotype differences. Arguably, it is a reliable proxy for Pacific salmon population structure because i) strong geographic relationships (e.g., watershed- and stream-specific populations) define salmon population structure (30), and ii) geologic heterogeneity driving $^{87}\text{Sr}/^{86}\text{Sr}$ variation also has a strong geographic relationship.

There are some other additional caveats that are worthy of consideration. For example, the utility of $^{87}\text{Sr}/^{86}\text{Sr}$ ratios for certain species is diminished because of short freshwater residence times of some salmon species (e.g., chum and pink salmon) (20). However, the relatively long freshwater residence times (> 1 year) of Chinook, sockeye, and coho salmon make these species good candidates for $^{87}\text{Sr}/^{86}\text{Sr}$ -based MSAs. Additionally, because the utility of $^{87}\text{Sr}/^{86}\text{Sr}$ ratios scales with geologic heterogeneity, $^{87}\text{Sr}/^{86}\text{Sr}$ ratios will be less useful in regions of relatively homogenous geology. Finally, as we discovered in the Nushagak River, geographically distant areas can exhibit similar $^{87}\text{Sr}/^{86}\text{Sr}$ ratios (e.g., the AAR and the lower Nushagak River tributaries). By using multiple tracers within otoliths sometimes this issue can be resolved (19). Additionally, by coupling genetic with otolith microchemistry tags (38), a hierarchical approach to the mixed stock harvest problem (i.e., discerning broad-scale structure via genetic tags and fine-scale structure via otolith tags) may be a promising research and management linkage.

Implications for biodiversity conservation

In the last decade it has become well established that the biodiversity of Bristol Bay salmon populations significantly influences their resiliency to environmental perturbations and

enhances temporal stability of their regional productivity (4). The importance of this phenomenon has been recognized at the level of both broad-scale (4) and fine-scale (5) population structure. In ecology (as in economics) this phenomenon has been referred to as the portfolio effect (5, 8), whereby a diversification of contributing populations (or assets) imparts stability to overall productivity, and thus, fisheries (or financial portfolios). For example, Schindler, *et al.* (5) showed that if Bristol Bay sockeye salmon were instead one homogenous population (compared to hundreds), inter-annual variability in runs would be 2.2 times greater and would lead to complete fishery closures 10 times the current frequency (currently 1 closure per 100 years). Thus, there have been large efforts in the region to develop tools to conserve the regions biodiversity (10). Our ability to measure changes in the relative productivity at the level of fine-scale population structure has been limited by our ability to apportion fishery harvests to this level of biodiversity. Genetic methods have been able to assign catches to the broad-scale population structure (7, 10), which also provide a robust framework for tracking responses to perturbations (e.g., mineral development, climate change, and commercial fisheries) at the broad-scale level (2, 4). However, genetic techniques have not generally discerned group membership of fishery harvests to the fine-scale population structure. Within the Nushagak River we have demonstrated that variation in $^{87}\text{Sr}/^{86}\text{Sr}$ ratios throughout this catchment (as recorded in otoliths of fish) can discern group membership to the fine-scale population structure (i.e., 7 different SIGs, which corresponds to different geographic areas). We were able to determine natal origins with ~ 90% accuracy for Chinook salmon incidentally harvested during the commercial sockeye fishery and determined that in 2011 three SIGs produced > 70% of the catch in approximately equal proportions. Further, due to the conservative nature of the $^{87}\text{Sr}/^{86}\text{Sr}$ tracer with respect to

physical and biological processes, this tool is also applicable to both sockeye and coho salmon populations within the Nushagak River.

METHODS SUMMARY

Sampling, analytical, and statistical procedures are described in detail in the SI text. Briefly, $^{87}\text{Sr}/^{86}\text{Sr}$ ratios of otoliths were measured using laser ablation (LA) multi-collector inductively coupled plasma mass spectrometry (MC-ICPMS). Otoliths from juvenile Chinook salmon were measured parallel to growth axis $\sim 50 \mu\text{m}$ proximal to edge; a subset of these were also measured perpendicular to growth axis from core to edge (i.e., life-history profiles). Otoliths from adults were measured perpendicular to the growth axis from the core through the freshwater region and into the marine region. We used linear DFA to classify adult Chinook salmon to SIGs. We trained the DFA using a river water dataset from the Nushagak River (Brennan et al., in review) and conducted two validation tests of the DFA using known origin juvenile Chinook salmon and slimy sculpin.

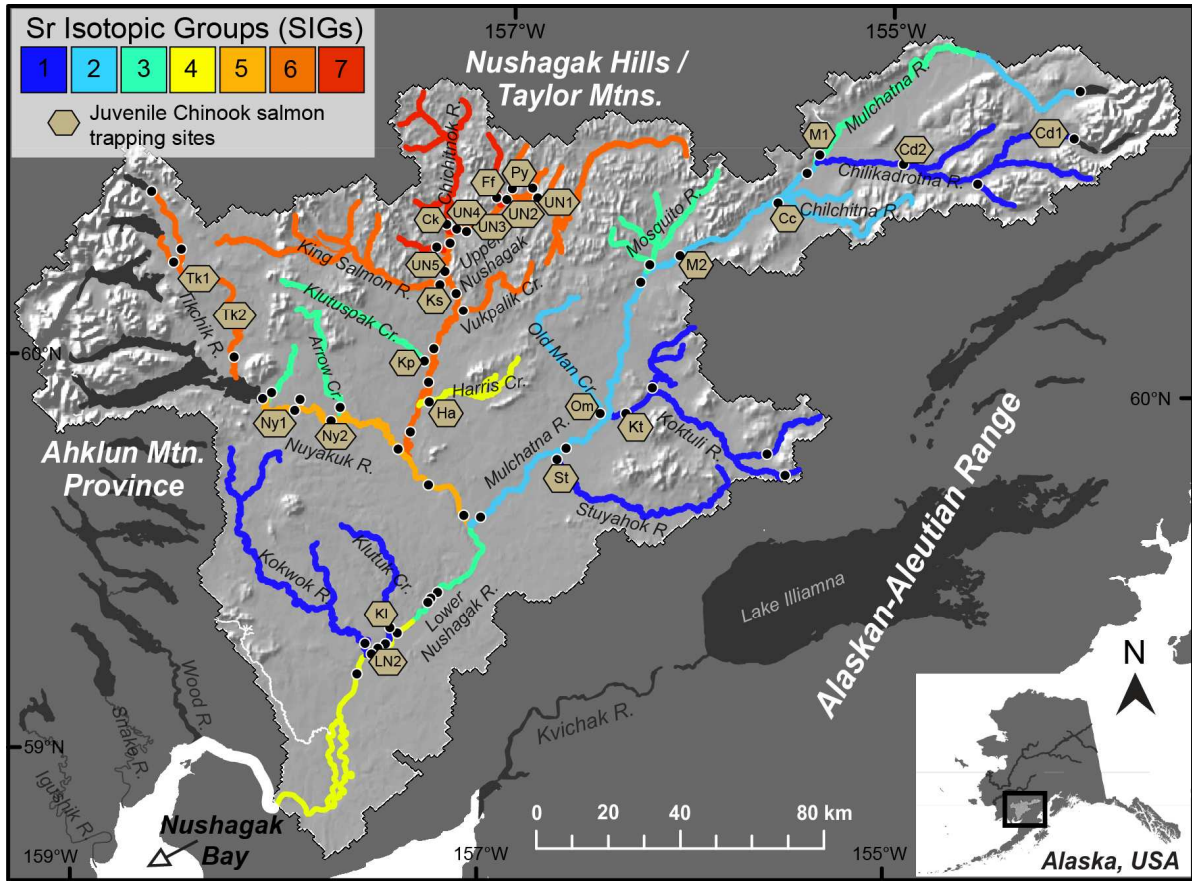


Figure 3.1. Map of the Nushagak River, Strontium Isotopic Groups (SIGs), and sampling sites for juvenile Chinook salmon and waters (black-filled circles) from Brennan et al., (in review).

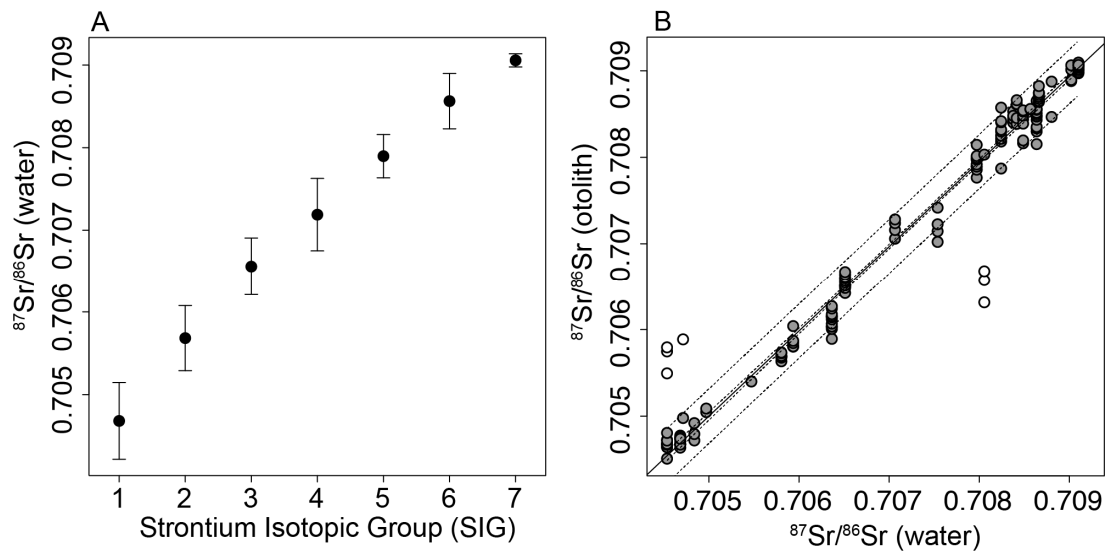


Figure 2.2. SIG $^{87}\text{Sr}/^{86}\text{Sr}$ ratios. A) SIGs determined via water $^{87}\text{Sr}/^{86}\text{Sr}$ ratios (mean $\pm 2\sigma$ SD) from Brennan et al., (in review), and B) the regression of juvenile Chinook salmon and water $^{87}\text{Sr}/^{86}\text{Sr}$ ratios. Lines indicate confidence intervals (2σ SE) and tolerance intervals (2σ SD) of regression. Black-filled circles were the data used for the regression; open circles were considered outliers (see text).

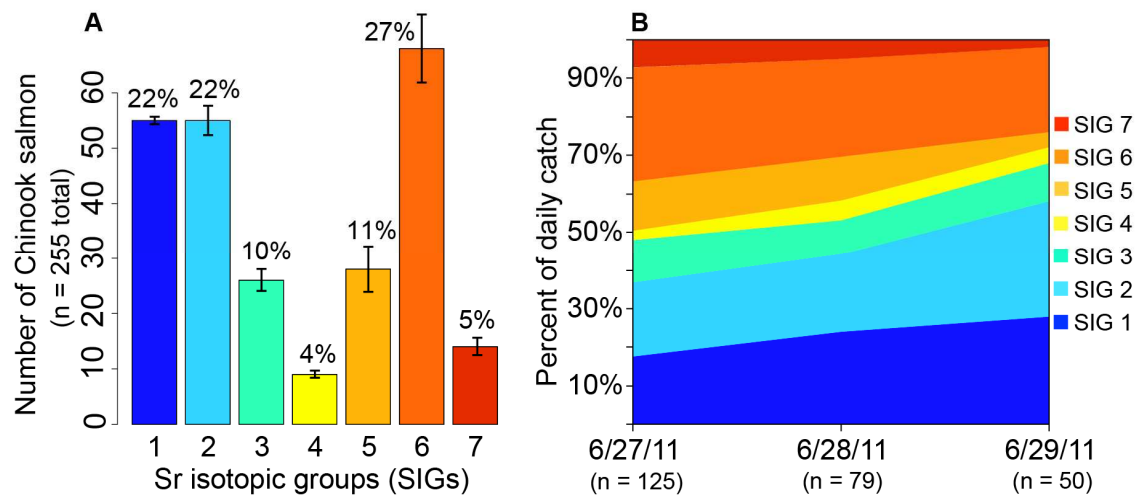


Figure 3.3. Mixed Stock Analysis (MSA). A) Proportion of each SIG in the incidental catch of adult Chinook salmon in Nushagak Bay in 2011. B) Day-specific proportions of each SIG during the three-day fishing period.

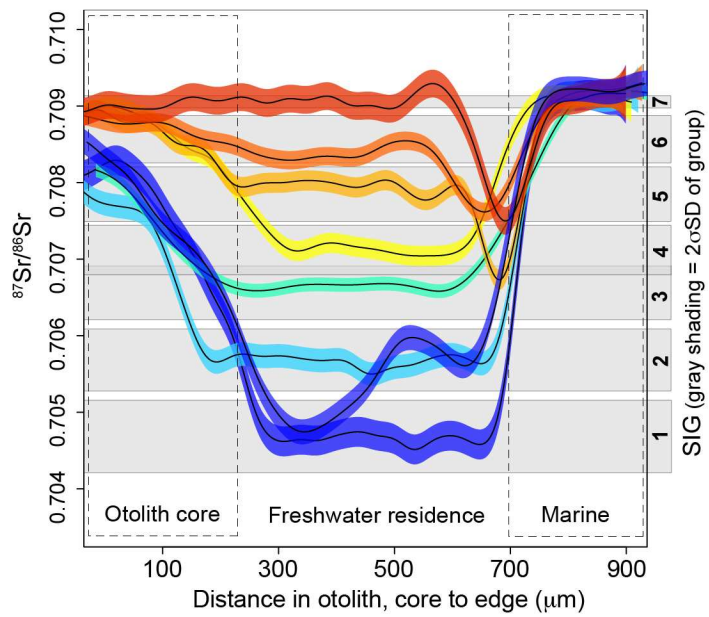


Figure 3.4. $^{87}\text{Sr}/^{86}\text{Sr}$ life history profiles from each SIG of adult Chinook salmon. Colors of profiles correspond to Figure 1. Also shown is an adult, who originated from SIG 1, but reared in SIG 2.

REFERENCES

1. McPhee MV, *et al.* (2009) A Hierarchical Framework to Identify Influences on Pacific Salmon Population Abundance and Structure in the Arctic-Yukon-Kuskokwim Region. *American Fisheries Society Symposium* 70:1177-1198.
2. Schindler DE, *et al.* (2008) Climate Change, Ecosystem Impacts, and Management for Pacific Salmon. *Fisheries* 33(10):502-506.
3. EPA US (2014) An Assessment of Potential Mining Impacts on Salmon Ecosystems of Bristol Bay, Alaska (Final Report). *Environmental Protection Agency, Washington, DC* EPA 910-R-14-001A-C, ES.
4. Hilborn R, Quinn TP, Schindler DE, & Rogers DE (2003) Biocomplexity and fisheries sustainability. *P Natl Acad Sci USA* 100(11):6564-6568.
5. Schindler DE, *et al.* (2010) Population diversity and the portfolio effect in an exploited species. *Nature* 465(7298):609-612.
6. Rogers LA, *et al.* (2013) Centennial-scale fluctuations and regional complexity characterize Pacific salmon population dynamics over the past five centuries. *P Natl Acad Sci USA* 110(5):1750-1755.
7. Habicht C, Seeb LW, & Seeb JE (2007) Genetic and ecological divergence defines population structure of sockeye salmon populations returning to Bristol Bay, Alaska, and provides a tool for admixture analysis. *T Am Fish Soc* 136(1):82-94.
8. Figge F (2004) Bio-folio: applying portfolio theory to biodiversity. *Biodivers Conserv* 13(4):827-849.
9. Jones M, *et al.* (2013) 2012 Bristol Bay Area Annual Management Report. Alaska Department of Fish and Game, Fishery Management Report No. 13-20.

10. Dann TH, *et al.* (2009) Genetic Stock Composition of the Commercial Harvest of Sockeye Salmon in Bristol Bay, Alaska, 2006-2008. *Alaska Department of Fish and Game, Anchorage Fishery Manuscript Series No. 09-06.*
11. Larson WA, Seeb JE, Pascal CE, Templin WD, & Seeb LW (2014) Single-nucleotide polymorphisms (SNPs) identified through genotyping-by-sequencing improve genetic stock identification of Chinook salmon (*Oncorhynchus tshawytscha*) from western Alaska. *Can J Fish Aquat Sci* 71(5):698-708.
12. Everett MV & Seeb JE (2014) Detection and mapping of QTL for temperature tolerance and body size in Chinook salmon (*Oncorhynchus tshawytscha*) using genotyping by sequencing. *Evol Appl* 7(4):480-492.
13. Larson WA, *et al.* (2014) Genotyping by sequencing resolves shallow population structure to inform conservation of Chinook salmon (*Oncorhynchus tshawytscha*). *Evol Appl* 7(3):355-369.
14. Dann TH, Habicht C, Baker TT, & Seeb JE (2013) Exploiting genetic diversity to balance conservation and harvest of migratory salmon. *Can J Fish Aquat Sci* 70(5):785-793.
15. Wood CC, Mckinnell S, Mulligan TJ, & Fournier DA (1987) Stock Identification with the Maximum-Likelihood Mixture Model - Sensitivity Analysis and Application to Complex Problems. *Can J Fish Aquat Sci* 44(4):866-881.
16. Barnett-Johnson R, Pearson TE, Ramos FC, Grimes CB, & MacFarlane RB (2008) Tracking natal origins of salmon using isotopes, otoliths, and landscape geology. *Limnol Oceanogr* 53(4):1633-1642.

17. Hegg JC, Kennedy BP, Chittaro PM, & Zabel RW (2013) Spatial structuring of an evolving life-history strategy under altered environmental conditions. *Oecologia* 172(4):1017-1029.
18. Muhlfeld CC, Thorrold SR, McMahon TE, & Marotz B (2012) Estimating westslope cutthroat trout (*Oncorhynchus clarkii lewisi*) movements in a river network using strontium isoscapes (vol 69, pg 906, 2012). *Can J Fish Aquat Sci* 69(6):1129-1130.
19. Walther BD, Thorrold SR, & Olney JE (2008) Geochemical signatures in otoliths record natal origins of American shad. *T Am Fish Soc* 137(1):57-69.
20. Zimmerman CE, Swanson HK, Volk EC, & Kent AJR (2013) Species and life history affect the utility of otolith chemical composition for determining natal stream of origin for pacific salmon. *T Am Fish Soc* 142(5):1370-1380.
21. Kennedy BP, Folt CL, Blum JD, & Chamberlain CP (1997) Natural isotope markers in salmon. *Nature* 387(6635):766-767.
22. Campana SE (1999) Chemistry and composition of fish otoliths: pathways, mechanisms and applications. *Mar Ecol Prog Ser* 188:263-297.
23. Capo RC, Stewart BW, & Chadwick OA (1998) Strontium isotopes as tracers of ecosystem processes: theory and methods. *Geoderma* 82(1-3):197-225.
24. Bataille CP & Bowen GJ (2012) Mapping Sr-87/Sr-86 variations in bedrock and water for large scale provenance studies. *Chem Geol* 304:39-52.
25. Blum JD & Erel Y (2003) Radiogenic isotopes in weathering and hydrology. *Treatise on Geochemistry*, eds Drever JI, Executive Editors: Holland HD, & Turekian KK (Elsevier), pp 365-392.

26. Horton TW, Chamberlain CP, Fantle M, & Blum JD (1999) Chemical weathering and lithologic controls of water chemistry in a high-elevation river system: Clark's Fork of the Yellowstone River, Wyoming and Montana. *Water Resour Res* 35(5):1643-1655.
27. Walther BD & Thorrold SR (2006) Water, not food, contributes the majority of strontium and barium deposited in the otoliths of a marine fish. *Mar Ecol Prog Ser* 311:125-130.
28. Kalish JM (1990) Use of otolith microchemistry to distinguish the progeny of sympatric anadromous and non-anadromous salmonids. *Fishery Bulletin* 88(4):657-666.
29. Jones M, *et al.* (2011) 2011 Bristol Bay Area Annual Management Report. *Alaska Department of Fish and Game* Fishery Management Report No. 12-21.
30. Neville HM, Isaak DJ, Dunham JB, Thurow RF, & Rieman BE (2006) Fine-scale natal homing and localized movement as shaped by sex and spawning habitat in Chinook salmon: insights from spatial autocorrelation analysis of individual genotypes. *Mol Ecol* 15(14):4589-4602.
31. ADF&G CRT (2013) Chinook salmon stock assessment and research plan, 2013. Special Publication No. 13-01.
32. Taylor EB (1990) Environmental Correlates of Life-History Variation in Juvenile Chinook Salmon, *Oncorhynchus-Tshawytscha* (Walbaum). *J Fish Biol* 37(1):1-17.
33. Krueger CC, Zimmerman CE, & American Fisheries Society. (2009) Pacific salmon : ecology and management of western Alaska's populations. *In* American Fisheries Society Symposium 70 (American Fisheries Society, Bethesda, MD).
34. Dye J (2002) Surveys of the Chinook Sport Fisheries of the Muklung and Upper Wood Rivers, Alaska, 2000. *Alaska Department of Fish and Game* Fishery Data Series No. 02-27.

35. Douglas TA, Blum JD, Guo LD, Keller K, & Gleason JD (2013) Hydrogeochemistry of seasonal flow regimes in the Chena River, a subarctic watershed draining discontinuous permafrost in interior Alaska (USA). *Chem Geol* 335:48-62.
36. Keller K, Blum JD, & Kling GW (2010) Stream geochemistry as an indicator of increasing permafrost thaw depth in an arctic watershed. *Chem Geol* 273(1-2):76-81.
37. Kennedy BP, Klaue A, Blum JD, Folt CL, & Nislow KH (2002) Reconstructing the lives of fish using Sr isotopes in otoliths. *Can J Fish Aquat Sci* 59(6):925-929.
38. Barnett-Johnson R, Teel DJ, & Casillas E (2010) Genetic and otolith isotopic markers identify salmon populations in the Columbia River at broad and fine geographic scales. *Environ Biol Fish* 89(3-4):533-546.

APPENDIX 3.1

METHODS

Otolith collections

Juvenile salmon (n = 153 total) were captured using minnow traps in the autumns of 2011, 2012, and 2013 at 24 locations throughout the Nushagak River watershed (Figure 3.1). Sagittal otoliths were dissected in the field and stored dry in polypropylene tubes until sectioning and analysis. Trapping locations included all of the major tributaries and main river channels of the primary branches of the Nushagak River (e.g., Mulchatna, Nuyakuk, Upper Nushagak, and Lower Nushagak Rivers) (Figure 3.1). We previously generated water $^{87}\text{Sr}/^{86}\text{Sr}$ ratios corresponding to these trapping sites, in addition to many more sites (n = 95 total) (black-filled circles, Figure 3.1) (Brennan et al., in review). Otoliths were collected from adult Chinook

salmon (n = 255 total) incidentally caught during the 2011 commercial sockeye salmon fishery conducted in the Nushagak Fishing District. Collections occurred during a three-day period in late June (June 27th – 29th, 2011) during the peak of the Chinook salmon run (1), and included catches from different gear types (i.e., both set and drift gillnets) and multiple boats. Fish were collected under Alaska Department of Fish and Game Fish Resource Permit numbers SF2011-236, SF2012-231, and SF2013-255; and Institutional Animal Care and Use Committee protocol number 178401-11.

⁸⁷Sr/⁸⁶Sr ratio analyses of otoliths

⁸⁷Sr/⁸⁶Sr ratios of otoliths were measured using laser ablation (LA) (193 nm Excimer Laser, Photo Machines) multi-collector inductively coupled plasma mass spectrometry (MC-ICPMS) (Thermo Scientific, High Resolution NEPTUNE, Bremen, Germany) at the University of Utah, Department of Geology and Geophysics ICPMS laboratory. Sectioning and mounting methods followed those outlined by Donohoe and Zimmerman (2). Juveniles were sectioned in the sagittal plane, whereas adults were sectioned in the transverse plane. Prior to isotopic analyses, otoliths were sonicated for five minutes in MilliQ water, rinsed, and dried in a laminar flow hood. LA transects were implemented using a 31.4 µm diameter circle for juveniles and a 53.1 µm circle for adults with a pulse rate of 10 Hz, a scan rate of 2 µm/second, and a laser energy of 45%. Counts per second (cps) of ⁸⁸Sr, ⁸⁷Sr, ⁸⁶Sr, ⁸⁵Rb and ⁸³Kr were measured at the Faraday cups with an integration time of 0.524 seconds, corresponding to one cycle. Prior to each ablation transect background intensities (V) of each isotope were measured for 120 cycles and the mean was used as a blank correction during sample analyses. Analytical accuracy of LA

data was evaluated by measuring the $^{87}\text{Sr}/^{86}\text{Sr}$ ratio of a modern marine shell during and after each LA run ($n = 10$ runs; 9 to 12 shell analyses/run). LA run-means of shell ratios ranged from 0.70922 - 0.70925 with an average weighted 2σ standard error (SE) of ± 0.00002 , which is consistent with our MC-ICPMS solution analyses of the same shell (Brennan et al., in review) and the global marine value (0.70918 ± 0.00006 2σ standard deviation (SD)) (3). We therefore applied no standard-correction to otolith data. $^{87}\text{Sr}/^{86}\text{Sr}$ ratios of otoliths samples were corrected for mass bias using an exponential law and for isobaric interference.

Adult Chinook salmon otoliths were measured perpendicular to growth axis and each transect encompassed the core, entire freshwater residence, and migration into the marine environment. We determined the natal origin, rearing area (if different from natal origin), and overall freshwater movement pattern. We considered freshwater residence within each otolith to be the region between the distal extent of the core ($\sim 250 \mu\text{m}$ from primordia) and the distal extent of the 1st annulus (i.e., before marine migration). Specifically, we determined the freshwater residence portion of each transect by inspecting i) the $^{87}\text{Sr}/^{86}\text{Sr}$ ratio profile, ii) the corresponding ^{88}Sr intensity (V) profile, and iii) superimposing transects on respective otolith images (taken in reflected light). For each otolith $^{87}\text{Sr}/^{86}\text{Sr}$ life history profile we fitted a Generalized Additive Model (GAM) using the MGCV package in R (<http://cran.r-project.org/>), which uses penalized iteratively re-weighted least squares (P-IRLS) to maximize goodness-of-fit and general cross validation (GCV) methods to minimize over-fitting of each $^{87}\text{Sr}/^{86}\text{Sr}$ profile (4). We also calculated Bayesian 95% confidence intervals along each transect, which allowed us to inspect if and where changes in the $^{87}\text{Sr}/^{86}\text{Sr}$ ratio occurred (4). P-IRLS and GCV algorithms of GAMs essentially ‘back-fit’ a series of polynomial spline functions, which are additive, to $^{87}\text{Sr}/^{86}\text{Sr}$ LA data (4). To guard against prematurely over-penalizing any GAM, we scaled the

basis dimension (k) (the maximum effective degrees of freedom [edf] allowable) with the number of data (N) in each profile by $k = 10N^{2/9}$ (5). The edf is related to the number of splines used to fit each GAM (4). If there was no change in the $^{87}\text{Sr}/^{86}\text{Sr}$ ratio during freshwater residence we determined the natal origin to be represented by the entire freshwater residence period. If, however, there was a change during freshwater residence, we determined the natal origin to be between the distal extent of the core and the inflection point of the first $^{87}\text{Sr}/^{86}\text{Sr}$ change. The rearing signal was determined to be between the end of the natal origin signal and the migration to ocean.

$^{87}\text{Sr}/^{86}\text{Sr}$ ratios of all juvenile Chinook salmon otoliths were measured ~ 50 - 80 μm from the edge of the otolith and parallel to growth axis for 200 μm . This region was targeted because we assumed it to be representative of the ambient environment experienced by each individual just prior to being captured. It was also sufficiently distal of the maternally influenced otolith core region (6, 7). Additionally, to investigate if juvenile salmon captured at a particular site also originated at that site (i.e., the freshwater movements before being captured), we performed additional LA transects perpendicular to growth axis from the otolith core to the edge on a random sub-sample from each trapping site (n = 3 individuals per site). Because we measured from the core to the edge of each otolith of these sub-sampled juveniles we also computed an $^{87}\text{Sr}/^{86}\text{Sr}$ ratio for the core (the middle ~ 100 μm), a natal origin signal, and a rearing signal (if indicative of movement). Using these former two ratios we calculated a $^{87}\text{Sr}/^{86}\text{Sr}$ mass-balance for Sr within the otolith core between marine-derived and freshwater-derived sources of Sr assuming a two end-member mixing model defined by the equation below:

$$\text{Equation 1: } ^{87}\text{Sr}/^{86}\text{Sr}_{\text{core}} = ^{87}\text{Sr}/^{86}\text{Sr}_{\text{marine}} (P) + ^{87}\text{Sr}/^{86}\text{Sr}_{\text{natal}} (1 - P)$$

Where P is the proportion of Sr derived from marine sources via the egg, $^{87}\text{Sr}/^{86}\text{Sr}_{\text{core}}$ is the measured ratio in the otolith core, $^{87}\text{Sr}/^{86}\text{Sr}_{\text{natal}}$ is the measured ratio from the natal origin otolith region, and $^{87}\text{Sr}/^{86}\text{Sr}_{\text{marine}}$ is the global marine value (0.70918).

Classification statistics

We used discriminant function analysis (DFA) to predict natal origins and freshwater movement patterns of adult Chinook salmon caught in Nushagak Bay using the MASS package in R (<http://cran.r-project.org/>). We trained the DFA using a river water dataset ($n = 95$) of the Nushagak River watershed (Brennan et al., in review). To demonstrate that using water data to train the DFA model was appropriate, we conducted a regression of ambient water versus otolith $^{87}\text{Sr}/^{86}\text{Sr}$ ratios. Because water $^{87}\text{Sr}/^{86}\text{Sr}$ ratios exhibited a strong geographic pattern throughout the Nushagak River (Brennan et al., in review), we determined Sr Isotopic Groups (SIGs) for the DFA based on similarity in both $^{87}\text{Sr}/^{86}\text{Sr}$ ratios and geography (Figure 3.1 and Figure 3.2A). In the DFA, each SIG was given equal a priori probabilities (i.e., $1/7$). To validate DFA model, we conducted two independent tests of model accuracy using measurements of otoliths from known origin i) juvenile Chinook salmon (reported here) and ii) slimy sculpin indicative of site-specific temporal variation (see Brennan et al., in review). We then used the DFA model to predict natal origins and movement patterns of adult Chinook salmon ($n = 255$) incidentally caught during the 2011 commercial sockeye salmon fishery. For each unknown individual, posterior probabilities of SIG membership computed by DFA (i.e., SIGs 1 – 7) sum to 1 and individuals were assigned to the SIG with the highest probability of SIG membership. To calculate uncertainty for each SIG proportion computed by DFA (Figure 3.3A and Table A3.2) we used the mean maximum

posterior probability of all individuals within a said SIG. Whereby, the uncertainty of a SIG was its error rate (i.e. $1 - P_{\max}$, where P_{\max} is the mean maximum posterior probability of SIG membership).

RESULTS AND DISCUSSION

Mass-balance calculation of Sr sources within the otolith core

The mass-balance calculation of Sr sources within the otolith core (Equation 1) of the sub-sampled juvenile Chinook salmon indicated that between 89 and 93% of the Sr present within the core is derived from marine sources (Figure A3.1A). The uncertainty associated with this mass-balance estimate decreased (i.e., from $\pm 24\%$ to $\pm 1\%$, 1σ SD) as the difference between natal freshwater ratios and the global marine value (0.70918) increased (Figure A3.1A). This estimate was consistent across all trapping sites, and thus, all geographic regions of the Nushagak River watershed (Dataset 2 in Supplemental Materials). The proportion of marine-derived Sr in juvenile Chinook otoliths consistently approached 0% at a distance $\sim 250 \mu\text{m}$ from primordia (e.g., Figure A3.1B), which also verified our guidelines for determining the freshwater residence period in adult otoliths.

Additional discussion of a minor number of perplexing life history profiles

Inferred movement patterns of a few individual adult Chinook salmon were perplexing and suggested additional water sampling in some regions would help constrain SIGs. For example, five fish had natal origins within SIG 4, but apparently reared within SIG 2 ($n = 2$) and SIG 5 ($n = 3$) (Table A3.3B). Based on rearing signals, likely rearing areas for these fish were

the Mulchatna and Nuyakuk Rivers, respectively. In the former case, it seems probable that these fish originated from western tributaries flowing into the main-stem channel of the Mulchatna River (e.g., Mosquito River). However, the water measurement from the lower Mosquito River (Brennan et al., in review) was within SIG 3, not SIG 4. The upper reaches of the Mosquito River drain rocks that are geologically more akin to $^{87}\text{Sr}/^{86}\text{Sr}$ ratios defining SIGs 4, 5, or possibly even 6 (8). Thus, higher $^{87}\text{Sr}/^{86}\text{Sr}$ ratios may exist in the upper parts of this sub-drainage. In the latter case, it is possible that these fish originated from tributaries flowing into the Nuyakuk River; or that they originated in Harris Creek and reared in main-stem Nushagak River channel between the confluences of the Mulchatna and Nuyakuk Rivers (Figure 3.1). The fact that all of these individuals indicated to have reared in respective main-stem channels, but indicated to originate from $^{87}\text{Sr}/^{86}\text{Sr}$ environments within SIG 4 suggests that additional water sampling within these respective regions would help constrain our SIGs. However, this ancillary rearing area information drew us to conclude that the individuals who reared in the Mulchatna River ($n = 2$) actually belonged to SIG 3 (e.g., the Mosquito River) (Table A3.3B). Though further water sampling in these regions would be helpful in resolving the life history patterns of these five fish, because only a small number of fish presented perplexing movement histories, we did not consider our overall MSA results to be affected.

MSA results and potential habitat amount

Our MSA results appeared to scale with metrics of potential habitat amount (e.g., stream length and basin area within each SIG) (Figure A3.2 and Table A3.4). To investigate the relationship between potential habitat amount and respective proportions of fishery harvest, we compared MSA results to i) total stream length as estimated by the Anadromous Waters

Catalogue (AWC) (<https://www.adfg.alaska.gov/sf/SARR/AWC/>), ii) total stream length as estimated by the National Hydrography Dataset (NHD) (<http://nhd.usgs.gov>), and iii) total basin area as estimated by the NHD. The AWC is likely an underestimate of the potential habitat, whereas stream length and area determined via the NHD are likely to be overestimates. However, the proportion of harvests in 2011 of Chinook salmon indicated to scale positively with each estimate of habitat amount (Figure A3.2). In other AK watersheds (i.e., the Copper River), habitat productivity (as measured via rearing juvenile Chinook salmon) was patchy (9). Whereby, relatively small proportions of stream reaches provided disproportionate amounts of suitable rearing habitat for juvenile Chinook salmon. The proportional nature of our MSA results relative to SIG habitat amount estimates may suggest that the patchy nature of viable rearing habitat for juvenile Chinook salmon may operate at smaller scales than defined by the SIGs (i.e., the ratios of viable to unviable habitat for each SIG are similar). Though these results are suggestive, further investigation is warranted, including water sampling to further constrain SIGs.

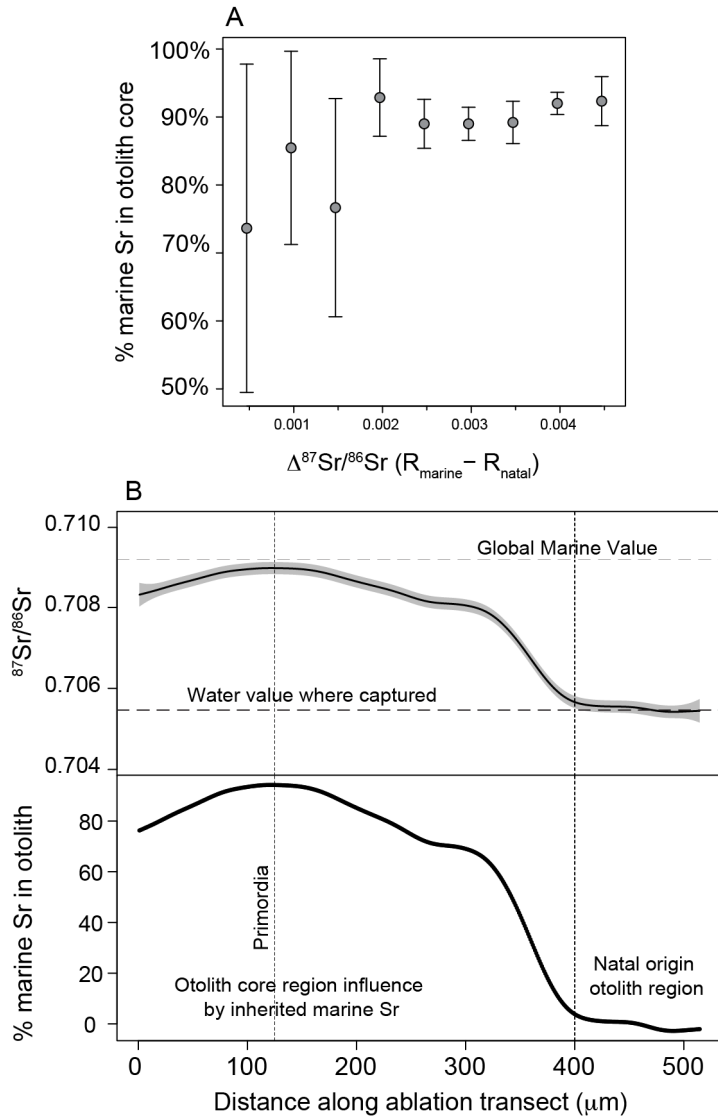


Figure A3.1. Marine-derived Sr in otolith cores. A) The proportion of marine-derived Sr within the otolith core of known origin juvenile Chinook salmon. Shown relative to $\Delta^{87}\text{Sr}/^{86}\text{Sr} = ^{87}\text{Sr}/^{86}\text{Sr}_{\text{marine}} - ^{87}\text{Sr}/^{86}\text{Sr}_{\text{natal}}$. B) An example of a juvenile $^{87}\text{Sr}/^{86}\text{Sr}$ life history (top panel) and the proportion of inherited marine-derived Sr (bottom panel) along the growth axis of its otolith. Bottom panel of B uses the mass-balance equation (see SI text) to calculate the proportion of marine-derived Sr along the growth axis of the otolith, from the core to edge.

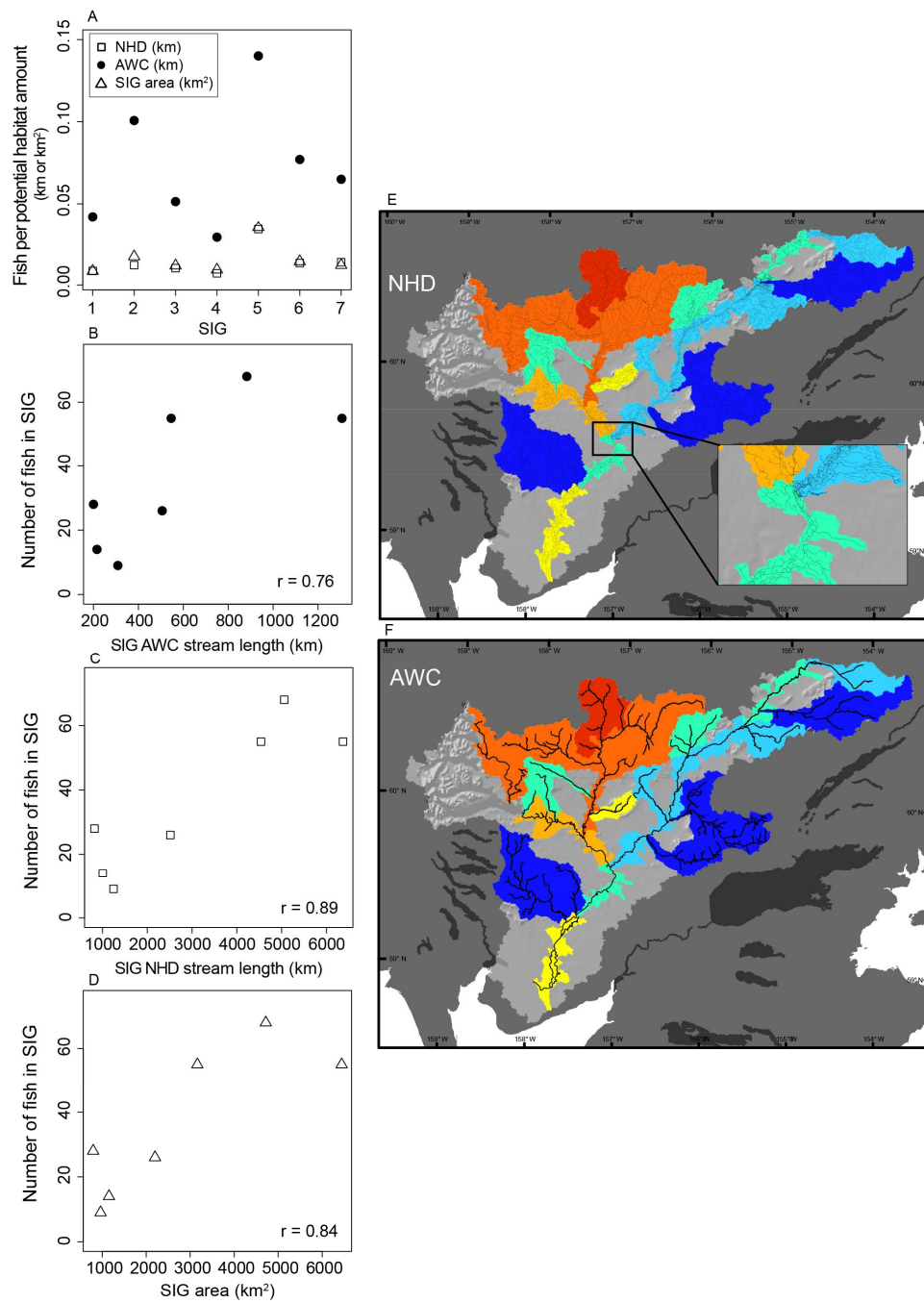


Figure A3.2. SIG proportions and habitat quantity. Scatter plots (A-D) of the number of fish in each SIG versus estimates of potential habitat amount within each SIG. Correlation coefficients (r) for each relationship are also shown. Maps of the potential habitat amounts for each SIG from NHD (E) and AWC (F) datasets.

Table A3.1. Classification tables of known origin samples, (A) juvenile Chinook salmon and (B) slimy sculpin. Numbers along diagonal indicate correct classifications; numbers off diagonal indicate incorrect classification. G_{cr} is the group-specific classification rate (see text for details).

A		Predicted SIG membership						
		1	2	3	4	5	6	7
Known Origin SIG	1	25						
	2		13	6				
	3			17				
	4				8			
	5					9	6	
	6						45	
	7						2	15
G_{cr}		100%	68%	100%	100%	60%	100%	88%
Total		90%						

B		Predicted SIG membership						
		1	2	3	4	5	6	7
Known Origin SIG	1	18						
	2		1					
	3			1	1			
	4			3	3			
	5					1		
	6						4	
	7							1
G_{cr}		100%	100%	50%	50%	100%	100%	100%
Total		88%						

Table A3.2. Posterior probability thresholds for SIG membership (i.e., no threshold, > 80%, and > 70%). A comparison of how MSA results change when posterior probability thresholds are used (e.g., when only those individuals with a group membership probability > than said threshold are assigned into an SIG).

SIG catch proportion	SIG	Probability threshold			SIG mean	SIG error
		None	>80%	>70%	P_{\max}^1	rate ²
	1	55	54	55	0.99	0.01
	2	55	50	53	0.95	0.05
	3	26	21	22	0.92	0.07
	4	9	9	9	0.93	0.07
	5	28	20	23	0.85	0.13
	6	68	62	65	0.91	0.08
	7	14	11	12	0.89	0.10

¹mean maximum probability of SIG membership for each SIG

²1 - P_{\max} , see SI text

Table A3.3. Movement patterns of adult Chinook salmon. (A) Overall movement patterns observed in total catch. (B) Summary of all individuals indicative to have reared in a different ⁸⁷Sr/⁸⁶Sr-environment than their natal origin, and inferred freshwater movement patterns from these individuals.

A	Site fidelity	Different rearing area	Lower river migration blip	Both
# of individuals	184	17	44	10
% of total catch	72.2%	6.7%	17.3%	3.9%

B	Predicted by DFA				Inferred freshwater movements		
	ID	Natal SIG	P	Rearing SIG	P	Natal Origin	Rearing Area
	NBK12	5	0.91	5	1.00	within SIG 5	within SIG 5
	NBK16	6	0.74	7	0.96	SIG 6 (e.g., Upper Nushagak R.)	SIG 7 (e.g., Chichitnok R.)
	NBK28	4	0.99	4	0.99	within SIG 4	within SIG 4
	NBK38	6	0.96	6	0.96	within SIG 6	within SIG 6
	NBK82	1	1.00	2	1.00	SIG 1 (e.g., AAR tributaries)	SIG 2 (e.g., Mulchatna R.)
	NBK89	6	0.81	6	0.93	within SIG 6	within SIG 6
	NBK94	7	0.61	6	0.80	SIG 7 (e.g., Chichitnok R.)	SIG 6 (e.g., Upper Nushagak R.)
	NBK103	3	0.99	3	1.00	within SIG 3	within SIG 3
	NBK113	3	1.00	2	0.90	SIG 3 (e.g., Mosquito R.)	SIG 2 (e.g., Mulchatna R.)
	NBK114	2	0.82	2	1.00	within SIG 2	within SIG 2
	NBK123	1	1.00	1	0.93	within SIG 1	within SIG 1
	NBK131	4	0.99	5	0.87	SIG 4 (e.g. Nuyakuk R. tributaries)	SIG 5 (e.g., Nuyakuk R.)
	NBK135	1	1.00	2	1.00	SIG 1 (e.g., AAR tributaries)	SIG 2 (e.g., Mulchatna R.)
	NBK136	7	0.99	6	0.68	SIG 7 (e.g., Chichitnok R.)	SIG 6 (e.g., Upper Nushagak R.)
	NBK156	4	0.99	5	0.97	SIG 4 (e.g. Nuyakuk R. tributaries)	SIG 5 (e.g., Nuyakuk R.)
	NBK157**	5	0.67	7	0.98	**SIG 6 (e.g., Upper Nushagak R.)	SIG 7 (e.g., Chichitnok R.)
	NBK184	1	1.00	2	0.99	SIG 1 (e.g., AAR tributaries)	SIG 2 (e.g., Mulchatna R.)
	NBK190	6	0.83	7	1.00	SIG 6 (e.g., Upper Nushagak R.)	SIG 7 (e.g., Chichitnok R.)
	NBK192	1	1.00	1	1.00	within SIG 1	within SIG 1
	NBK215	4	1.00	5	0.80	SIG 4 (e.g. Nuyakuk R. tributaries)	SIG 5 (e.g., Nuyakuk R.)
	NBK217	1	1.00	1	1.00	within SIG 1	within SIG 1
	NBK222	1	1.00	1	0.78	within SIG 1	within SIG 1
	NBK226	6	0.94	6	0.97	within SIG 6	within SIG 6
	NBK232	1	1.00	1	1.00	within SIG 1	within SIG 1
	NBK237B**	4	0.97	2	0.97	**SIG 3 (e.g., Mosquito R.)	SIG 2 (e.g., Mulchatna R.)
	NBK247**	4	0.53	2	0.88	**SIG 3 (e.g., Mosquito R.)	SIG 2 (e.g., Mulchatna R.)

**individuals who had their natal origin (SIG) updated based on freshwater movement information

Table A3.4. Summary of potential habitat amounts within each SIG relative to number of adult Chinook salmon predicted into each SIG.

SIG	n fish in SIG	AWC (km)	fish/km	NHD_all (km)	fish/km	NHD/AWC	area (km²)	fish/km²
1	55	1306.6	0.042	6369.2	0.009	4.9	6442.7	0.0085
2	55	545.9	0.101	4537.6	0.012	8.3	3163.4	0.0174
3	26	506.0	0.051	2515.9	0.010	5.0	2200.2	0.0118
4	9	308.4	0.029	1247.1	0.007	4.0	963.0	0.0093
5	28	199.9	0.140	820.9	0.034	4.1	794.9	0.0352
6	68	882.9	0.077	5056.9	0.013	5.7	4718.6	0.0144
7	14	215.4	0.065	1005.9	0.014	4.7	1154.5	0.0121

REFERENCES

1. Jones M, *et al.* (2011) 2011 Bristol Bay Area Annual Management Report. *Alaska Department of Fish and Game* Fishery Management Report No. 12-21.
2. Donohoe CJ & Zimmerman CE (2010) A method of mounting multiple otoliths for beam-based microchemical analyses. *Environ Biol Fish* 89(3-4):473-477.
3. Faure G & Mensing TM (2005) *Isotopes Principles and Applications* (Wiley, Hoboken, New Jersey) Third Edition Ed.
4. Wood SN (2006) *Generalized additive models : an introduction with R* (Chapman & Hall/CRC, Boca Raton, FL) pp xvii, 391 p.
5. Kim YJ & Gu C (2004) Smoothing spline Gaussian regression: more scalable computation via efficient approximation. *J Roy Stat Soc B* 66:337-356.
6. Kalish JM (1990) Use of Otolith Microchemistry to Distinguish the Progeny of Sympatric Anadromous and Non-Anadromous Salmonids. *Fishery Bulletin* 88(4):657-666.
7. Zimmerman CE & Reeves GH (2002) Identification of steelhead and resident rainbow trout progeny in the deschutes river, oregon, revealed with otolith microchemistry. *Transactions of the American Fisheries Society* 131(5):986-993.
8. Wilson FH, *et al.* (2006) Reconnaissance bedrock geologic map for the northern Alaska Peninsula area, southwest Alaska. *U.S. Geological Survey Open-File Report* 2006-1303.
9. Bidlack AL, Benda LE, Miewald T, Reeves GH, & McMahan G (2014) Identifying suitable habitat for chinook salmon across a large, glaciated watershed. *Transactions of the American Fisheries Society* 143:689–699.

GENERAL CONCLUSIONS

Alaska is geographically vast, geologically diverse, and home to a large variety of migratory animals making $^{87}\text{Sr}/^{86}\text{Sr}$ ratios a valuable tool for ecological provenance research across the state. In this dissertation, I demonstrated the use of $^{87}\text{Sr}/^{86}\text{Sr}$ ratios for tracking Pacific salmon (*Oncorhynchus* spp.) migrations in the Nushagak River, a geologically diverse watershed and one that produces some of the largest wild salmon runs in the world. This research also contributes to a statewide understanding of Alaska's overall $^{87}\text{Sr}/^{86}\text{Sr}$ heterogeneity and the regional weathering patterns influencing $^{87}\text{Sr}/^{86}\text{Sr}$ ratios in rivers. By using the behavioral ecology of a non-migratory fish (the slimy sculpin, *Cottus cognatus*) and its otoliths, I showed that site-specific temporal variation in $^{87}\text{Sr}/^{86}\text{Sr}$ ratios of rivers could be evaluated at sub-annual time scales. This particular approach to the persistent problem of site-specific temporal variability in provenance research proved to be an effective solution, especially in a remote region, such as the Nushagak River.

$^{87}\text{Sr}/^{86}\text{Sr}$ ratios varied at multiple spatial scales in Alaska (i.e., regional and local scales) and there were regional patterns between silicate and carbonate weathering influencing $^{87}\text{Sr}/^{86}\text{Sr}$ ratios observed in rivers. At the regional scale, decreasing north-south and east-west gradients characterized the general $^{87}\text{Sr}/^{86}\text{Sr}$ patterns in Alaska. The north-south gradient was especially abrupt across the Denali Fault reflecting the Mesozoic growth of southern Alaska along this mega-suture zone via accretion of exotic island arcs along the North American continent (Trop and Ridgeway 2007). The east-west gradient was not as abrupt and reflected Alaska's western growth from the Precambrian to the Cenozoic along the Precambrian North American miogeocline (Colpron et al. 2007). Though silicate weathering was important across Alaska,

carbonate weathering is more influential in high relief basins north of the Denali Fault and in south-central Alaska than it is in lowland basins north of the fault and southwestern Alaska.

By using otoliths from slimy sculpin collected throughout the Nushagak River, I was able to evaluate temporal variability in river waters at sub-annual scales and changes in the 4th decimal in $^{87}\text{Sr}/^{86}\text{Sr}$ ratios. As a testament to the sensitivity of this method, it also showed micro-movements (< 1 km) of this non-migratory fish (e.g., between tributary and main-stem channel habitats) and illustrated variability in the home ranges between individuals collected at the same site and between tributary systems. Overall, by analyzing slimy sculpin otoliths, I determined that $^{87}\text{Sr}/^{86}\text{Sr}$ ratios of tributaries and main-stem channels above the Mulchatna River confluence were temporally stable, whereas the Lower Nushagak River main-stem channel was characterized by some spatio-temporal heterogeneity.

Using the spatially and temporally robust baseline data set of the Nushagak River I established, I subsequently determined the natal origins and movement patterns of Chinook salmon incidentally harvested during a mixed stock fishery in Nushagak Bay. $^{87}\text{Sr}/^{86}\text{Sr}$ ratios were able to predict the natal origins of Chinook salmon with 90% accuracy into seven different Strontium Isotopic Groups (SIGs). The $^{87}\text{Sr}/^{86}\text{Sr}$ -based mixed stock analysis (MSA) showed that > 70% of the incidental harvest originated from three of the seven SIGs, generally corresponding to the upper parts of the watershed. Compared to genetically based MSAs, which distinguish Nushagak River sockeye salmon as one genetic stock (Dann et al. 2009, Habicht et al. 2007), this was a significant improvement (~ 7 fold) in distinguishing group membership of mixed stock harvests in Nushagak Bay. These findings, and the overall research framework I have established in the Nushagak River, have important implications for the effective conservation of salmon

biodiversity in this region, and elsewhere where geologic heterogeneity is a characteristic of salmon habitat.

I have shown that the naturally occurring variations in $^{87}\text{Sr}/^{86}\text{Sr}$ ratios throughout Alaska are an important tracer for tracking, not only the provenance and movements of Pacific salmon, but also have the potential to track the provenance and movement patterns of other organisms as well. Many animals have Ca-rich, and therefore Sr-rich, biogenic tissues, which grow incrementally throughout their lives (e.g., teeth). Robust maps, like the ones I have shown herein and process oriented predictive models, which have been validated using my baseline data (Bataille et al., in revision), provide necessary baseline information to utilize these biogenic ‘records’ to reconstruct animal movements. To further build on this research I suggest three general future research directions. Firstly, though data from Chapter 1 were used to validate a state-wide predictive model of bioavailable $^{87}\text{Sr}/^{86}\text{Sr}$ heterogeneity, some data holes exist throughout Alaska and further advances could be made via targeted sampling campaigns in areas of high uncertainty identified by these modeling efforts (Bataille et al., in revision) and where few measurements have been made (e.g., Seward Peninsula). Additionally, by using empirical $^{87}\text{Sr}/^{86}\text{Sr}$ data with recent geo-statistical advances for mapping passive particles (e.g., Sr^{2+}) in stream networks (Peterson et al. 2013), even more accurate $^{87}\text{Sr}/^{86}\text{Sr}$ maps of rivers are potentially achievable. Secondly, in the context of Pacific salmon provenance, by coupling $^{87}\text{Sr}/^{86}\text{Sr}$ and genetic methods (Barnett-Johnson et al. 2010) a hierarchical approach to the mixed stock harvest problem (i.e., discerning broad-scale structure via genetic tags and fine-scale structure via otolith tags) is a promising area of research and has implications for linkage to fisheries management. Because $^{87}\text{Sr}/^{86}\text{Sr}$ ratios can identify natal origins of salmon at the sub-basin level of population structure in geologically diverse watersheds, they provide a framework

to test a variety of hypotheses and questions regarding time-dependent patterns (i.e., inter-annual) and intra-watershed productivity. For example, what is the time-dependent variability of salmon habitat productivity at the sub-basin level? What is the nature and magnitude of impacts from climate change, mineral development, and fisheries on productivity at the sub-basin level of population structure and also biodiversity? Finally, because of Alaska's vast geography and multitude of past and modern migratory animals, the field of research of using $^{87}\text{Sr}/^{86}\text{Sr}$ -based information to address long standing questions in regard to the migratory behavior and overall movement patterns of these organisms is wide open. One important example is unraveling the migrations of the ancient megafauna (Mann et al. 2013) and human populations (Potter et al. 2011) of Arctic Alaska and the ice-free corridor composing Beringia (the largely unglaciated region lying between the Lena River in the west and the McKenzie River in the east) during the last glaciation.

REFERENCES

- Arth, J.G. 1994. Isotopic composition of the igneous rocks of Alaska. *In* The Geology of Alaska. Edited by G. Plafker, Berg, H.C. Geological Society of America, The Geology of North America, Boulder, Colorado.
- Barnett-Johnson, R., Pearson, T.E., Ramos, F.C., Grimes, C.B., and MacFarlane, R.B. 2008. Tracking natal origins of salmon using isotopes, otoliths, and landscape geology. *Limnol Oceanogr* **53**(4): 1633-1642.
- Barnett-Johnson, R., Ramos, F.C., Grimes, C.B., and MacFarlane, R.B. 2005. Validation of Sr isotopes in otoliths by laser ablation multicollector inductively coupled plasma mass

- spectrometry (LA-MC-ICPMS): opening avenues in fisheries science applications. *Can J Fish Aquat Sci* **62**(11): 2425-2430.
- Barnett-Johnson, R., Teel, D.J., and Casillas, E. 2010. Genetic and otolith isotopic markers identify salmon populations in the Columbia River at broad and fine geographic scales. *Environ Biol Fish* **89**(3-4): 533-546.
- Bataille, C.P., et al. in revision. A geostatistical framework to predict strontium isotope variations in Alaska Rivers. *Chemical Geology*.
- Bataille, C.P., and Bowen, G.J. 2012. Mapping Sr-87/Sr-86 variations in bedrock and water for large scale provenance studies. *Chem Geol* **304**: 39-52.
- Bataille, C.P., Laffoon, J., and Bowen, G.J. 2013. Mapping multiple source effects on the strontium isotopic signatures of ecosystems from the circum-Caribbean region. *Ecosphere* **3**(12).
- Britton, K., Grimes, V., Dau, J., and Richards, M.P. 2009. Reconstructing faunal migrations using intra-tooth sampling and strontium and oxygen isotope analyses: a case study of modern caribou (*Rangifer tarandus granti*). *J Archaeol Sci* **36**(5): 1163-1172.
- Capo, R.C., Stewart, B.W., and Chadwick, O.A. 1998. Strontium isotopes as tracers of ecosystem processes: theory and methods. *Geoderma* **82**(1-3): 197-225.
- Colpron, M., Nelson, J.L., and Murphy, D.C. 2007. Northern Cordilleran terranes and their interactions through time. *GSA Today* **17**(4/5).
- Copeland, S.R., Sponheimer, M., de Ruiter, D.J., Lee-Thorp, J.A., Codron, D., le Roux, P.J., Grimes, V., and Richards, M.P. 2011. Strontium isotope evidence for landscape use by early hominins. *Nature* **474**(7349): 76-U100.

- Dann, T.H., Habicht, C., Jasper, J.R., Hoyt, H.A., Barclay, A.W., Templin, W.D., Baker, T.T., West, F.W., and Fair, L.F. 2009. Genetic Stock Composition of the Commercial Harvest of Sockeye Salmon in Bristol Bay, Alaska, 2006-2008. Alaska Department of Fish and Game, Anchorage **Fishery Manuscript Series No. 09-06**.
- Ehrlich, S., Gavrieli, I., Dor, L.B., and Halicz, L. 2001. Direct high-precision measurements of the Sr-87/Sr-86 isotope ratio in natural water, carbonates and related materials by multiple collector inductively coupled plasma mass spectrometry (MC-ICP-MS). *J Anal Atom Spectrom* **16**(12): 1389-1392.
- Elsdon, T.S., Wells, B.K., Campana, S.E., Gillanders, B.M., Jones, C.M., Limburg, K.E., Secor, D.H., Thorrold, S.R., and Walther, B.D. 2008. Otolith chemistry to describe movements and life-history parameters of fishes: Hypotheses, assumptions, limitations and inferences. *Oceanogr Mar Biol* **46**: 297-+.
- EPA, U.S. 2014. An Assessment of Potential Mining Impacts on Salmon Ecosystems of Bristol Bay, Alaska (Final Report). Environmental Protection Agency, Washington, DC **EPA 910-R-14-001A-C, ES**.
- Goldfarb, R.J., Farmer, G.L., Cieutat, B.A., and Meier, A.L. 1997. Major-element, trace element, and strontium-isotope systematic of natural waters in the Fairbanks Mining District: constraints from local geology. U.S. Geological Survey Professional Paper **1614**: 12.
- Habicht, C., Seeb, L.W., and Seeb, J.E. 2007. Genetic and ecological divergence defines population structure of sockeye salmon populations returning to Bristol Bay, Alaska, and provides a tool for admixture analysis. *Transactions of the American Fisheries Society* **136**(1): 82-94.

- Hilborn, R., Quinn, T.P., Schindler, D.E., and Rogers, D.E. 2003. Biocomplexity and fisheries sustainability. *P Natl Acad Sci USA* **100**(11): 6564-6568.
- Hobson, K.A., Barnett-Johnson, R., and Cerling, T.E. 2010. Using Isoscapes to Track Animal Migration. *In Isoscapes: Understanding movement, pattern, and process on Earth through isotope mapping. Edited by J.B. West, G.J. Bowen, T.E. Dawson and K.P. Tu. Springer Science.*
- Keller, K., Blum, J.D., and Kling, G.W. 2007. Geochemistry of soils and streams on surfaces of varying ages in arctic Alaska. *Arct Antarct Alp Res* **39**(1): 84-98.
- Koch, P.L., Halliday, A.N., Walter, L.M., Stearley, R.F., Huston, T.J., and Smith, G.R. 1992. Sr Isotopic Composition of Hydroxyapatite from Recent and Fossil Salmon - the Record of Lifetime Migration and Diagenesis. *Earth Planet Sc Lett* **108**(4): 277-287.
- Mann, D.H., Groves, P., Kunz, M.L., Reanier, R.E., and Gaglioti, B.V. 2013. Ice-age megafauna in Arctic Alaska: extinction, invasion, survival. *Quaternary Sci Rev* **70**: 91-108.
- Peterson, E.E., Ver Hoef, J.M., Isaak, D.J., Falke, J.A., Fortin, M.J., Jordan, C.E., McNyset, K., Monestiez, P., Ruesch, A.S., Sengupta, A., Som, N., Steel, E.A., Theobald, D.M., Torgersen, C.E., and Wenger, S.J. 2013. Modelling dendritic ecological networks in space: an integrated network perspective. *Ecol Lett* **16**(5): 707-719.
- Potter, B.A., Irish, J.D., Reuther, J.D., Gelvin-Reymiller, C., and Holliday, V.T. 2011. A Terminal Pleistocene Child Cremation and Residential Structure from Eastern Beringia. *Science* **331**(6020): 1058-1062.
- Schindler, D.E., Augerot, X., Fleishman, E., Mantua, N.J., Riddell, B., Ruckelshaus, M., Seeb, J., and Webster, M. 2008. Climate Change, Ecosystem Impacts, and Management for Pacific Salmon. *Fisheries* **33**(10): 502-506.

- Schindler, D.E., Hilborn, R., Chasco, B., Boatright, C.P., Quinn, T.P., Rogers, L.A., and Webster, M.S. 2010. Population diversity and the portfolio effect in an exploited species. *Nature* **465**(7298): 609-612.
- Trop, J.M., and Ridgeway, K.D. 2007. Mesozoic and Cenozoic tectonic growth of southern Alaska: A sedimentary basin perspective. *In* Tectonic Growth of a Collisional Continental Margin: Crustal Evolution of Southern Alaska. *Edited by* K.D. Ridgeway, Trop, J.M., Glen, J.M.G, and O'Neill. Geological Society of America, Boulder, Colorado. pp. 55-94.
- Woodhead, J., Swearer, S., Hergta, J., and Maasa, R. 2005. In situ Sr-isotope analysis of carbonates by LA-MC-ICP-MS: interference corrections, high spatial resolution and an example from otolith studies. *J Anal Atom Spectrom* **20**(1): 22-27.